

1169

U.S./SPAIN JOINT SOLAR PROGRAM
ANNUAL REPORT

October 1980

Prepared by:

Murrey D. Goldberg
International Division
Solar Energy Research Institute

U.S./SPAIN JOINT SOLAR PROGRAM
ANNUAL REPORT

October 1980

Prepared by:

Murrey D. Goldberg
International Division
Solar Energy Research Institute

This report contains the documentation for solar-related research and development projects carried out under Program Supplement Agreement No. 3 of the Treaty of Friendship and Cooperation between the United States and Spain. All programmatic activities under the Supplemental Agreement are authorized by the United States-Spanish Joint Committee for Scientific and Technical Cooperation. United States representation on the Joint Committee is under the Assistant Secretary for Oceans and International Environmental and Scientific Affairs of the Department of State. The Department of State has requested the Department of Energy to provide management and oversight for all of the solar-related projects, and the Department of Energy (DOE) has assigned this responsibility to the International Division of the Solar Energy Research Institute (SERI).

The five projects included in this program include:

- Project P-3025 - CESA 1: Testing and Evaluation of Solar Energy Collector Systems
- Project P-3051 - Wind Energy Utilization Program
- Project P-3020 - Cooperative Program in Solar Energy
- Project P-3008 - Illuminated Solar Cells on Both Sides of a New Design
- Project P-3014 - Methane Production from Anaerobic Breakdown of Urban Solid Waste.

Each of these projects was generated by a Spanish Investigator who then identified a U.S. scientific counterpart to provide any technical support required to achieve the goals of the project. Treaty funds were provided to both the Spanish and the U.S. investigators to carry out joint activities, with the Spanish Government providing additional funds, where necessary, to supplement the joint effort. The funding for Project P-3025 was provided by State to DOE and then directly to the Sandia National Laboratories. The funding for Projects P-3051 and P-3020 was provided by State to DOE and then to SERI to subcontract for the required work. Finally, funding for Projects P-3008 and P-3014 was provided directly to the U.S. investigators by the Joint Committee.

Each of the projects has had a quite different history. The nature of the required support, the level of effort required, and the time of start-up has varied considerably among them. The Joint Committee has required each of the project teams to provide the Committee with a joint annual progress

report and a joint proposal requesting continued funding in the next program cycle. These joint reports and proposals were submitted at various levels of detail and some only in Spanish. Each project did request continued funding.

This report brings together the available documentation in English which defines progress made in the first year of work and proposals for future work. Due to the different project histories, the documentation is quite different for each project, some relating only to the U.S. work and some to the work of both parties. Following is a brief summary of each project. The individual documents then follow as a set of attachments.

Project P - 3025: CESA-1 Central Receiver System

The Centro de Estudios de la Energia (CEE, Center for Energy Studies) Juan Temboury is designing, constructing and testing a 1 MWe solar central receiver system (CESA-1), using a water/steam cycle. The U.S. technical support is being provided by the Sandia National Laboratories, Livermore (SNLL) Alan C. Skinrod, A.F. Baker. As detailed in the Annual Status Letter (Attachment I), the support effort has been concentrated on the following tasks:

1. Overall project objectives, design and schedule
2. Receiver design assistance
3. HELIOS code cooperation
4. MIRVAL code confirmation
5. Heliostat test plans
6. Heliostat alignment
7. Heliostat controls

Much progress has been made in the design phase of all components of the CESA-1 system, and the facility at Almeria, where the system will be constructed, is in place. The CEE/SNLL collaboration has gone exceptionally well. The project has been funded for the next cycle, both the joint effort by the Joint Committee and the supplemental work by the Spanish government.

~~A financial summary chart for the \$235,000 provided to SNLL is included~~
in the Annual Status Letter.

Attachment I - SNLL Annual Status Letter

Project P-3051: Wind Energy Utilization Program

This project has been unique within the program in that the Spanish investigators, the Instituto Nacional de Tecnica Aeroespacial (INTA) [Carlos Sanchez Tarifa] have performed much work but have formalized no request for U.S. support funding. Thus this has not truly been a joint project. INTA has designed a 100kWe wind turbine, similar to the U.S. Mod-0 model, and has selected a site for construction near Tarifa, at the southern-most tip of Spain. Though several discussions were held between INTA staff and SERI staff looking toward providing support for this design effort, no scope of required effort was provided by INTA. As such, the \$60,000 available for the U.S. effort remains unused at SERI. The Joint Committee has provided no additional funding for the next cycle, but the Spanish government will continue the effort, with plans to call on the support funds when required.

Attachment /None/

Project P-3020: Cooperative Program in Solar Energy

For the Instituto Nacional de Industria (INI, National Industrial Institute), The Gas y Electricidad, S.A. [Feliciano Fuster Jaume] proposed this project, which had three objectives:

1. A study of the possibility of introducing solar energy for thermal processes of up to 100° C in Spain.
2. A study of the development of solar system components, based on fixed non-concentrating solar collectors, in Spain and implementation of demonstration installations.
3. An energy and economic analysis of heat pumps, in comparison with other heat-producing systems, including solar energy.

The U.S. support for this project was supplied by the Franklin Research Center (FRC) [Harold Lorsch] which performed the following set of tasks:

1. Review of energy and economic data for Spain.
2. Review of Spanish meteorological data and proposed solar radiation model.
3. Review of Spanish demographic data.
4. Cost/performance model evaluation.
5. Evaluation of solar market potential in Spain.
6. Identification and analysis of barriers.
7. Training of Spanish engineers in economic and technical analysis and in solar design.
8. Assessment of heat pump applications.

The work done by FRC is summarized in a Technical Status Report (Attachment II), dated September 80. Since the contract to FRC (for \$138,000) was not let by SERI until February 80, the FRC work was accelerated in order to catch up with the INI work which began some months before. As of 3 November 80, \$80,288 was billed against the contract. In addition to the Technical Status Report, the FRC output is contained in a set of working documents deposited at SERI but not reproduced in this report. The titles of these reports are:

Cost Performance Evaluation
Solar Energy in Spain - Market Potential
Solar Energy in Spain - Demonstration Plan
Heat Pump Feasibility Study

The proposal for second phase funding of this project has been translated from the Spanish and is presented in Attachment III.

Attachment II - FRC Technical Status Report
Attachment III - Proposal for Renewal of Funding

Project P-3008: Two-Sided Solar Cells

This project was initiated as a continuation of work initiated at the Universidad Politecnica de Madrid [Antonio Lopez Luque] by the Spanish principal investigator and his colleagues on the development of bifacial silicon solar cells. The U.S. support was provided by the Department of Electrical Engineering, University of Florida [J.G. Fossum, F.A. Lindholm, A. Neugroschel]. The first-year work of the Spanish group accomplished the following three tasks:

1. Theoretical analysis of the n^+pp^+ structure for bifacial illumination.
2. Technological procedures for fabrication at low cost of such cells.
3. Simultaneous measurement of surface recombination velocity and diffusion length of minority carriers at the base.

The U.S. team, during the same period, accomplished the following three tasks:

1. Description of physics of the back-surface-field solar cell.
2. Development of techniques to measure carrier lifetimes and diffusion lengths and effective surface recombination velocities.
3. Identification of the physical mechanisms occurring in bifacial cells.

The work carried out by the U.S. team is described in the Annual Progress Report (Attachment IV), dated April 80 and entitled "Further Development of Two-Sided Solar Cells." The request for renewal for second cycle funding is included as Attachment V, and a brief evaluation of this renewal request, by the SERI Photovoltaic Division, is contained in Attachment VI.

Attachment IV - Annual Progress Report, University of Florida

Attachment V - Request for Renewal

Attachment VI - Request for Renewal Evaluation

Project P-3014: Methane Production from Anaerobic Breakdown of Urban Solid Waste

This project was initiated to explore the potential for methane fuel production from typical urban solid waste generated in Spain. The Madrid-based company, ADARO [Rafael Fernandez Aller], which is involved, among other things, in recovering materials from waste products, developed this project and requested the University of Illinois [John T. Pfeffer] to provide support consulting. The budget for U.S. support was \$10,000.

The work of the first year of effort under this project is described in the Scientific Report, provided by Dr. Pfeffer and appended as Attachment VII. Of the \$10,000 available, approximately \$7,200 have been expended. As noted in the Scientific Report, the scope of the project has been expanded to include resources beyond urban solid waste.

Attachment VII - Scientific Report

SPANISH CESA-1 PROJECT

**Central
Receiver
Technical
Assistance**

**ANNUAL STATUS LETTER
(Project III-P-3025)**

JUNE 1979 - JULY 1980

PREPARED BY:
A. F. BAKER
LARGE POWER SYSTEMS DIVISION
SANDIA LABORATORIES, LIVERMORE, CA



APPROVED BY:
ALAN C. SKINROD
LARGE POWER SYSTEMS DIVISION
SANDIA LABORATORIES, LIVERMORE, CA.

Spanish CESA-1 Project III-P-3025

The work described in this Annual Status Letter was funded by the United States-Spanish Joint Committee for Scientific and Technological Cooperation under the auspices of the Program Supplementary Agreement No. 3 of the Treaty of Friendship and Cooperation between the United States of America and Spain. At the request of the Solar Energy Research Institute and with the approval of the Department of Energy, Sandia National Laboratories, Livermore has provided technical assistance in areas unique to solar energy applications for a 1.0 MWe water/steam solar central receiver project being built by the Spanish in Almeria, Spain. Centro de Estudios de la Energia (CEE) is responsible for design and construction of the project.

The technical assistance that Sandia has provided CEE during the budget year of June 1979 thru July 1980 has been in support of the following tasks:

1. Overall project objectives, design, and schedule
2. Receiver design assistance
3. HELIOS code cooperation
4. MIRVAL code conformation
5. Heliostat test plans
6. Heliostat alignment
7. Heliostat controls

The work that Sandia was requested to perform in each of these tasks was based on the information and data provided by CEE. To the extent that the data was available Sandia completed its support in each task. As additional data becomes available during the next budget year Sandia will continue to support CEE in similar tasks as set forth in the current project budget plan. No major problems were encountered in the past year which would cause the project not to be successful.

Details of the work done by Sandia can be found in Appendix 1 which contains bi-monthly progress letters published during the June 1979 - July 1980 budget year.

A financial summary of the June 1979 - July 1980 budget year is shown in figure 1. There was no equipment purchased by Sandia in support of Project III-P-3025.

U.S. DEPARTMENT OF ENERGY

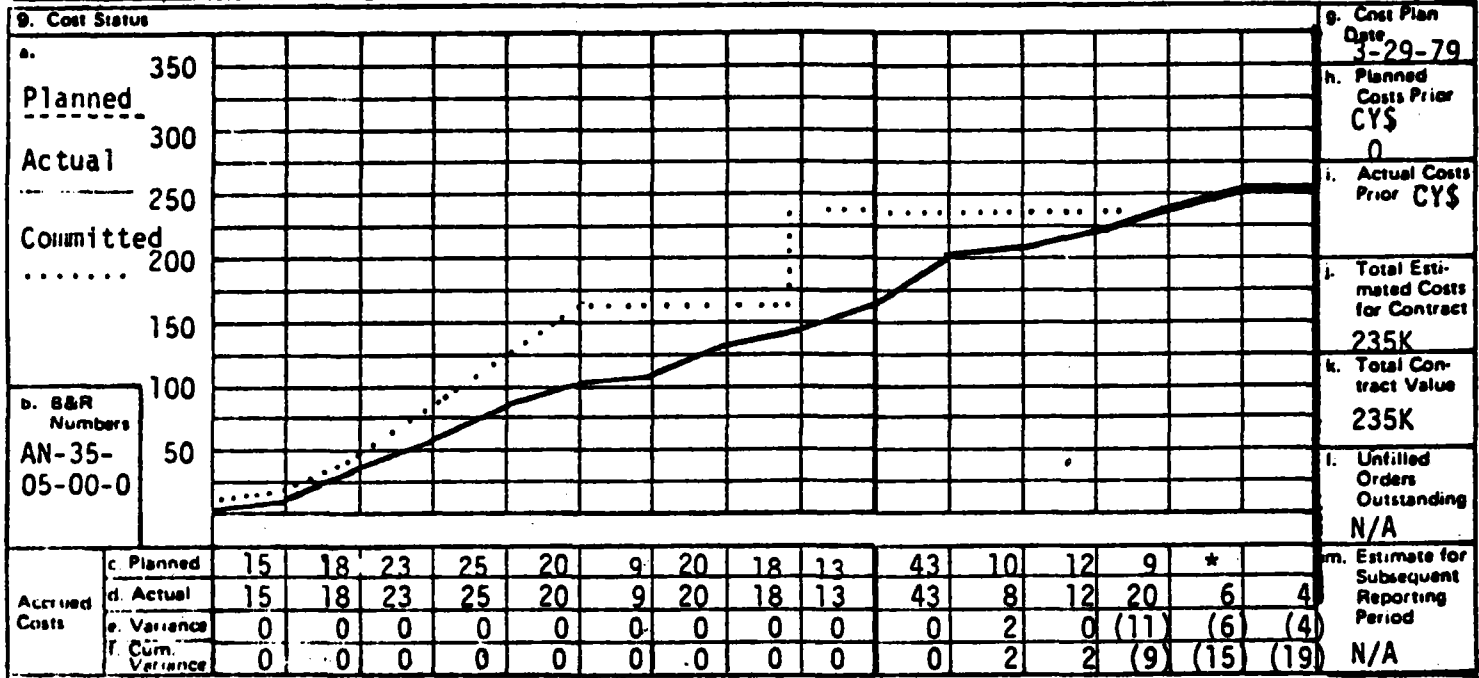
CONTRACT MANAGEMENT SUMMARY REPORT

FORM DOE 536
(1/78)

FORM APPROVED
OMB NO. 38R-0190

1. Contract Identification CENTRAL ENERGIA SOLAR ALMERICA-1 (CESA-1)		2. Reporting Period 1 Jun 79 through 29 Aug 80		3. Contract Number AN35-05-00-0	
4. Contractor (Name and Address) SANDIA LABORATORIES, LIVERMORE				5. Contract Start Date 1 June 1979	
				6. Contract Completion Date N/A	

7. Months 1979	J	J	A	S	O	N	D	J	F	M	A	M	J	J	A	8. CY-79
----------------	---	---	---	---	---	---	---	---	---	---	---	---	---	---	---	----------



11. Major Milestone Status

a. Salaries	Anticipated average total monthly salaries \$12K
b. P.O. 83-8963	Foster-Wheeler \$50K Period of Performance 18 Sep 79 to 29 Feb 80
c. P.O. 83-9673	Foster-Wheeler \$ 8K Period of Performance 9 Jul 79 to 30 Sep 79
d. N.T.I.S.	Deposit for reports requested \$10K 5 Sep 79 to Indefinite
e. P.O. 20-1142	Language Services \$10K 31 Dec 79 to 31 Dec 80

P.O. 20-8146 Badger Energy, Inc. \$10K Energy Storage Medium Consultation

- NOTE:
1. Previous reports stated total costs for the month of May 1980 as \$64K. Upon rechecking the computer reports, it was found that \$21K had been erroneously charged to the CESA-1 Project. A correction has been made.
 2. The Badger Energy, Inc. contract has not been placed as yet, and will not be placed until funding is received.
 3. Costs in August 1980 were a carry over of July 1980 activities.

Figure 1. June 1979 - July 1980 Financial Summary

Distribution:

G. W. Braun, DOE/HQ
S. Griffith, DOE/SAN (2)
L. Herwig, DOE/SAN (3)
R. W. Hughey, DOE/SAN
M. Goldberg, SERI
A. C. Skinrood, 8452
File 32.3
A. F. Baker, 8452

APPENDIX I

Bi-Monthly Status Letters

for the

June 1979 - July 1980

Budget Year

June - October 1979
Technical Assistance Status

Sandia's CESA-1 effort, which was scoped at the Reston, Virginia meeting on March 23-24, 1979 received funding in late June 1979. During the week of June 3rd Sandia hosted a series of joint US/Spanish working group sessions both in Livermore, California and Albuquerque, New Mexico. At these sessions Sandia reviewed technical information from the US program which would be applicable to CESA-1. Included was a visit to Central Receiver Test Facility in Albuquerque and a review of facility operational procedures. Many technical reports and papers were provided to the Spanish during this visit including lists of applicable test equipment and procedures. During this same period Sandia continued to aid the Spanish in the use of the HELIOS computer code. A number of shadowing and blocking calculations were made and both the HELIOS and MIRVAL computer codes were modified to provide thermal flux maps. The first preliminary flux calculations were reviewed with CEE during a visit to Madrid and Almeria by J. C. Gibson and T. D. Brumleve, Sandia's solar programs department, the week of July 16. Sandia awarded a contract to Foster Wheeler Development Company in the US to provide specific review and consulting on the Spanish receiver development contract. During the visit in July, the Spanish requested that the review effort by Foster Wheeler be increased. Also during this visit discussions concerning heliostat design, testing and evaluation continued.

Since this visit, Sandia has provided a specific list of test equipment based on a list of capabilities requested by the Spanish. Also two other visits have been planned with one completed.

Charlie Vittitoe visited Spain in September 1979 to continue his consultation on the use of the HELIOS computer code. During this trip, several areas were identified where additional documentation or explanation is needed and where clarifying comments in the HELIOS computer code output would be helpful to users. A new version of HELIOS was transferred to the Spanish.

Recently Sandia received mirror samples from CEE and both reflectivity and absorption measurements are being made. Weatherability tests will also be done. Sandia has begun to provide an indepth thermal analysis of the Spanish cavity receiver. Analysis so far is based on abbreviated and frequently revised design definition from CESA-1. It is hoped when these results are presented in Spain that the most recent receiver design information will be obtained.

Sandia's efforts on this project have been slowed by the fact that English translations of CESA-1 technical documentation are not available from the CESA-1 project office. Arrangements are being made by Sandia to award a contract for translation service for CESA-1 documents. It is hoped that this will make it possible for Sandia to provide information and guidance more quickly.

November - December 1979
Technical Assistance Status

An Abbreviated Technical Assessment of the CESA-I Project (November 15, 1979) was completed at Sandia Livermore and provided to the CESA-I Project Office. This assessment is abbreviated since all the information necessary for a more complete assessment is not yet available at Sandia Livermore. As a part of this, a list was prepared of all documents which have been received by Sandia Laboratories. A contract for \$10,000 has been awarded to Language Services, Knoxville, Tennessee for translation of documents from Spanish to English. Several of the documents received by Sandia written in Spanish have recently been sent to this service. In the future any documents Sandia receives written in Spanish will be sent for translation. It takes about six weeks for a document to be translated and returned to Sandia.

Carlos Fernandez visited Sandia Livermore (December 11-12, 1979) and participated in detailed discussion on the instrumentation used for heliostat performance evaluations. Both the backward gazing system (BGS) and beam characterization system (BCS) were reviewed and Carlos was provided basic component ordering information. Juan Diez from Technicas Reunidas visited Sandia Livermore (November 26 - December 3, 1979) and worked with Sandia personnel to perform a cavity thermal analyses of the CESA-I receiver. Copies of the computer results from MIRVAL and RADSOLVER for the receiver were given to Juan on an "information only" basis for him to take back to Spain.

On December 21, 1979 a Sandia internal meeting was held to review the status of Sandia support activities for CESA-I. Near term activities were defined. This meeting was held in preparation for the Sandia/CESA-I meeting in Madrid in January 1980.

Heliostats

Additional HELIOS calculations (December 20, 1979) using a theoretical definition of the SENER heliostats were performed by Charlie Vittitoe, Sandia Albuquerque. The results of these calculations with 312 SENER heliostats with prealignment set for March 21 at noon and one-dimensional facet curvature for the six focal lengths were sent to the CESA-I Project Office. These HELIOS calculations were done to compare with earlier MIRVAL results (November 29, 1979) and were informative but like the MIRVAL results do not represent the actual configuration of a combined SENER and CASA heliostat field. When the measured performance of both heliostat types and quantity of each heliostat is determined, confirming MIRVAL and HELIOS calculations will be made, if necessary. With the several heliostat field definition options available, it is becoming more and more important that a single drawing set that is updated periodically by controlled revisions for all major components be implemented. This is especially true for the receiver and heliostat field since this interface is very complicated. Such a drawing control system may be the only way that one can determine what plant configuration is or has been analyzed.

A test plan for the CESA-I heliostats was received by Sandia (in English thanks to the efforts of Claudio Arano). Sandia is preparing comments and suggestions and will provide these in January 1980.

Receiver

Preliminary thermal analysis of the CESA-I superheater (October 22, 1979) based on data from previous MIRVAL calculations (August, September 1979) with 312 theoretically defined SENER heliostats was provided to the CESA-I Project Office. This thermal analysis and data from the Sandia stress analysis was presented to the CESA-I Project Office on October 31 - November 2, 1979. The results of these calculations show that at the design point (10 a.m. winter solstice) fatigue stress are not severe but at equinox noon the fatigue stress do become significant. Since these calculations were completed the receiver design has been changed and Sandia has reconfigured its receiver numerical model (December 17, 1979). The results of the thermal analysis using the new receiver (December 17, 1979) and MIRVAL (November 29, 1979) calculation including assumptions will be sent to the CESA-I Project Office (January 3, 1980). Previous comments concerning drawing control will not be repeated but its need is obvious.

As requested by the CESA-I Project Office, the contract with Foster Wheeler Development Corporation for support of the CESA-I project was revised. The original scope-of-work (July 1979) emphasized a critical review of the receiver design specifications and requirements. The new scope-of-work has the following major CESA-I support tasks:

- Task 1 - Design Review and Analysis - critically review the instrumentation/hydraulic and structural and materials aspects of the design.
- Task 2 - Operational Considerations - critically review the receiver instrumentation, controls, and operational and safety aspects of the receiver.
- Task 3 - Progress Reviews and Coordination - attended project review meetings and report on the progress and results of the design reviews.

Based on the original scope-of-work Foster Wheeler provided Sandia and the CESA-I Project Office (August 1979) a review of the receiver specifications and requirements.

Storage

Only a general definition of the storage system has been provided to Sandia. As soon as the detail storage definition is received at Sandia, an assessment will be made if necessary.

Plant Control and Interface Definition

No definition concerning plant control, interface definitions, and instrumentation has been provided to Sandia.

January-February 1980

Technical Assistance Status

A CESA-I project design review was held in Madrid, Spain on the 14, 15, 16 and 17 January 1980. Those attending the design review from Sandia Livermore were M. Abrams, E. T. Cull, J. F. Jones, C. L. Mavis, and C. S. Selvage. B. Zoschak from Foster Wheeler Development Corporation, New Jersey, who is under contract to Sandia for technical support was also at the Madrid review. The primary subsystems covered during this design review were the receiver and heliostats. Both CEE and Sandia issued meeting summaries including action items and understandings shortly after the Madrid meeting. A combined list of those action items and understandings can be found in Appendix 1. During the course of the meetings CEE and Tecnicas Reunidas (T.R.) provided Sandia drawings and documents pertinent to the CESA-I project. A list of the information provided to Sandia can be found in Appendix 2. Appendix 3 contains a list of reports and papers which have been translated from Spanish to English and provided to the technical staff at Sandia.

On 28 February 1980 a letter was sent to Claudio Arano concerning the exchange of proprietary information. The letter identified what was required for Sandia to receive proprietary information if it was absolutely necessary for the success of the project. Two Spanish documents which were understood to contain proprietary information were returned to CEE without reviewing their contents.

Heliostats

Based on verbal information presented during the January Madrid review, discussions were held with the Sandia materials group about the foam cores used in the CESA-I mirror modules. The materials people felt the foam types (PVC and polyurethane) should be good in a mirror module application. However, without more information on foam density, blowing agent, and chemistry a more definite statement could not be made. This information was provided to the CESA-I project on 4 February 1980 by telex along with existing concerns about water permeability, dimensional stability and long term creep as they relate to the mirror module design. This telex contained a request for a set of heliostat drawings so that a more meaningful review can be provided. The current status of the Sandia heliostat assessment is that:

1. The heliostat structures seem sufficiently rigid and are probably adequate. Test data should demonstrate their preference.
2. The drive mechanics for the SENER and CASA heliostats are similar to those which Sandia has design experience and test data should show they function similarly.

3. The heliostat field control and heliostat control systems are understood to be preliminary. Details are needed defining the requirements, interfaces, modes of operation, and software. These will be discussed at a CESA-I and Sandia meeting in March.
4. A recommendation has been made to the CESA-I project concerning heliostat alignment and canting system.
5. Meetings have been set for March to discuss the necessary outstanding detailed information concerning the heliostat system.

Receiver

The January Madrid review covered in detail the current T.R. receiver design. Drawings defining the receiver with controlled revisions were supplied to Sandia and Foster Wheeler. As a consequence of the T.R. delays in the receiver design and new work to be done, CEE authorized Sandia to increase the Foster Wheeler contract. Since the review, Foster Wheeler provided the CESA-I project results of their calculations of the T.R. receiver superheater power. Foster Wheeler indicated that based on conventional boiler experience they recommend that the superheater be sized so that the attemperator water flow is not less than two percent of the total feedwater flow at any time during normal operation. This subject will be further discussed in March when the CESA-I project meets at Sandia with Foster Wheeler.

The current status of the Sandia receiver assessment is that:

1. Both T.R. and Sandia are in agreement on the basis and results of stress analysis for the receiver. Four materials are still being evaluated for possible superheater applications.
2. The radiant flux incident on the receiver are still based on 312 theoretically defined SENER heliostats. Flux spillage on the edge of the receiver aperture has not been studied.
3. Instrumentation and piping details provided to Sandia are being evaluated. This evaluation includes the applicability of the instrumentation for receiver control as defined in the "Conditions and Operation Procedure for the CESA-I Solar Receiver".
4. A receiver review will be held in mid-March with T.R., Foster Wheeler, and Sandia.

Storage

Only a general definition of the storage system has been provided as part of the CESA-I plant definition received at the January Madrid meeting. As soon as the detailed storage definition is received at Sandia, an assessment will be made if necessary.

Plant Control and Interface Definition

Definition concerning plant control, interfaces, and operation has not been supplied in sufficient detail for a worthwhile assessment.

Appendix 1

Summary of Action Items and Understandings
from Madrid, Spain Meeting, January 14-17, 1980

<u>Action CEE/SLL</u>	<u>Item</u>	<u>Responsible for Action</u>	<u>Requested Date</u>	<u>Completed Date</u>
1/-	Budget for project Spain-USA	CEE	17 Jan 80	23 Jan 80
2/2	Final results of tests performed on the SENER heliostat prototype	CEE	29 Feb 80	11 Mar 80
3/2	Final results of tests performed on the CASA-2 heliostat prototype	CEE	30 April 80	
4/2	Final results of tests performed on the new SENER mirror modules	CEE	15 June 80	
5/1	Provide recommendation on BCS/BGS and focus and alignment system	SLL	25 Jan 80	31 Jan 80
6/4	Information on CASA-2 heliostat prototype and control (English description)	CEE	15 Feb 80	
7/5	Recommendation on heliostat washing system equipment and water requirements	SLL	1 Feb 80	1 Feb 80
8/8	Information including handouts and an audio tape of pilot plant heliostat testing and analysis	SLL	1 Feb 80	28 Jan 80
9/6	Information on Heliostat Glass Survey and Specifications for second surface silvered mirrors	SLL	31 Jan 80	28 Jan 80
10/-	Final reports of the pilot plant tests results of MMC and MDAC heliostats	SLL	30 March 80	

Summary of Action Items and Understandings
from Madrid, Spain Meeting, January 14-17, 1980

(continued)

<u>Action CEE/SLL</u>	<u>Item</u>	<u>Responsible for Action</u>	<u>Requested Date</u>	<u>Completed Date</u>
11/-	Planning Program Cooperation	CEE	22 Jan 80	23 Jan 80
-/7	Information on how to modify a Cary 17I Spectrophotometer	SLL	25 Jan 80	4 Feb 80
-/-	Recommendation on need for more receiver superheater surface area	FWDC	25 Jan 80	29 Jan 80
-/-	Receiver convective loss prediction	SLL	June 80	
-/-	FWDC complete their task 2 and 3	FWDC	29 Feb 80	11 March 80
-/-	Periodic Receiver Review and Assessment	SLL	1 March 80	12 March 80
-/-	Information on mechanical alignment instrument explained by Mr. Mavis	SLL	No date	
-/-	CEE will provide the following	CEE		
	(1) One line electric diagram		31 Jan 80	
	(2) P&I Diagram, Rev. 1 (exclude receiver)		31 Jan 80	25 April 80
	(3) Spec. on tanks, drum, heat exchangers, & pumps		No date	11 March 80
	(4) Plant flow diagram		No date	
	(5) Siemens/Bazan turbine steam balance		No date	
	(6) Plant thermal balance		No date	
	(7) EISA bid for the Field Control System		No date	11 March 80
	(8) Overall CESA-I Project Planning Schedule		No date	
-/-	Heliostat field control system functional specification	CEE	15 April 80	11 March 80



Appendix 2

Centro de Estudios de la Energía
Ministerio de Industria y Energía

SANDIA LABORATORIES
LIVERMORE, Ca. 94550
U.S.A.

Att. Mr. Skinrood / Mr. Cull

10th January 1980

SUBJECT: CESA-1 Project - Almeria (Spain) = Receiver Subsystem.
Forwarding of new TR drawings and documents.

Gentlemen,

Please find herewith enclosed two copies of each one of the following documents just issued by Técnicas Reunidas:

<u>Drawing No.</u>	<u>Rev.</u>	<u>Title</u>
^A SD-8230-300	0	-Planta de Tuberías (Pipe Layout).
SD-8230-115-B	0	-Estructura de Receptor - Vigas (Planta superior), (Receiver structure - Upper Beams)
SD-8230-162	2	-Serpentin del sobrecalentador -- Alzado y detalles, (Reheater coil - Elevation and details).
^S SD-8230-112C	0	-Estructura del Receptor - Vigas (Planta superior), (Receiver structure - Upper Beams).
^E SD-8230-190A	0	-Estructura del Receptor - Marquesina y aletas laterales (alzado), (Receiver Structure - Outside and side protection wings).
^{AO} SD-8230-010A	2	-Diagrama de tuberías e instrumentación - Subsistema Receptor, (P & I Diagram - Receiver subsystem).
^{AO} SD-8230-010B	2	-Diagrama de tuberías e instrumentación - Subsistema Receptor, (P & I Diagram - Receiver Subsystem).
SE-8230-110	0	-Estructura del Receptor - Esquema estructural, (Receiver Structure - Structural Sketch).
SD-8230-164	0	Soportes del Sob



Centro de Estudios de la Energía

Ministerio de Industria y Energía

SANDIA LABORATORIES
LIVERMORE, Ca. 94550
USApage 2ATT. Mr. Skinrood / Mr. Cull

10th January 1980

.../...

SE-8230-113A	1	-Estructura del Receptor - Sección longitudinal, (Receiver Structure - Longitudinal section).
SE-8230-113 ^B 8	0	-Estructura del Receptor - Sección Longitudinal, (Receiver Structure - Longitudinal Section - Extended view).
SE-8230-190B	0	-Estructura del Receptor - Marquesina y aletas laterales - Puerta exterior de cierre rápido, (Receiver structure - Outside roof and side protection wings-Quick closure security doors).
SE-8230-163	0	-Colectores - Secciones y detalles (Manifolds - Sections & details).
A4-8230-487	1	-Hoja 1 de 7, Diagramas de lazos Electrónicos, (Sheet 1 of 7 - Diagram of - Electronic Loops).
A4-8230-487	1	-Hoja 3 de 7 - Diagrama de lazos electrónicos, (Sheet 3 of 7 - Diagram of - Electronic Loops).
A4-8230-487	1	-Hoja 4 de 7 - Diagramas de lazos electrónicos, (Sheet 4 of 7 - Diagram of - electronic loops).
A4-8230-487	1	-Hoja 6 de 7 - Diagramas de lazos electrónicos - (Sheet 6 of 7 - Diagram of electronic loops).
A4-8230-487	1	-Hoja 7 de 7 - Diagramas de lazos electrónicos, (Sheet 7 of 7 - Diagram of - electronic loops).
A4-8230-482	1	-Esquemas lógicos (hoja 1 de 1), (Logical sketch (sheet 1 of 1)).
Without number	1	-Descripción de los lazos de instrumentos y control, (Description of instrument and control loops, 10 pages).
Without number	0	-Condiciones y procedimientos de operación del receptor solar CESA-1, (CESA-1 Solar Receiver Operation Conditions and Procedures).

Appendix 2 (continued)



Centro de Estudios de la Energía
Ministerio de Industria y Energía

SANDIA LABORATORIES
LIVERMORE, Ca. 94550
USA

Page 3

Att. Mr. Skinrood / Mr. Cull

10th January 1980

.../...

180-8230-2020	0	Isométrica - (Isometric)	- Sheet 1 of 1
180-8230-2025	0	" "	- Sheet 1 of 1
180-8230-2026	0	" "	- Sheet 1 of 1
180-8230-2022	0	" "	- Sheet 1 of 1
180-8230-2023	0	" "	- Sheet 1 of 1
180-8230-2024	0	" "	- Sheet 1 of 1
180-8230FA-101	0	" "	- Sheet 1 of 1
180-8230-1021	0	" "	- Sheet 1 of 1
180-8230-2042	0	" "	- Sheet 1 of 1
180-8230-2041	0	" "	- Sheet 1 of 1
180-8230-2040	0	" "	- Sheet 1 of 1
180-8230-2010	0	" "	- Sheet 1 of 1
180 Without numb.	0	" "	- Sheet 1 of 1
180-8230-2050	0	" "	- Sheet 1 of 1
180-8230-2001	0	" "	- Sheet 1 of 1
180-8230-2030	0	" "	- Sheet 1 of 1
180-8230-2070	0	" "	- Sheet 1 of 1

Without number Anexo 5 (Annex Five - Strain at Tube Crown)

The above documentation will be hand delivered in Madrid to your Mr. Cull so that may be discussed in the course of the meetings to be held at T.R. Offices.

Best regards


G. Arano
Project Manager

Appendix 2 (continued)

In addition to the documents listed in your letter of January 10, 1980; subject: CESA-1 Project-Almerica (Spain) = Receiver Subsystem. Forwarding of New TR Drawings and Documents.

Ed Cull made available to me the following drawings and documents.

<u>Drawing No.</u>	<u>Rev.</u>	<u>Title</u>
SD-8230-111	--	Estructura Del Receptor Planta Inferior
SD-8230-112	--	Estructura Del Receptor Planta Superior
SD-8230-114A	--	Estructura Del Receptor Vigas (Planta Inferior)
SD-8230-114B	--	Estructura Del Receptor Vigas (Planta Inferior)
SD-8230-115A	--	Estructura Del Receptor Vigas (Planta Superior)
SD-8230-116A	0	Estructura Del Receptor Soportes Entre Plantas - Panel No. 1
SD-8230-116B	--	Estructura Del Receptor Soportes Entre Plantas - Panel No. 2
SD-8230-116C	--	Estructura Del Receptor Soportes Entre Plantas - Panel No. 3
SD-8230-116D	0	Estructura Del Receptor Soportes Entre Plantas - Paneles Nos. 4 & 5
SD-8230-116E	0	Estructura Del Receptor Soportes Entre Plantas Panel Central de Puerta
SD-8230-160	2	Serpentin Del Evaporador Panel Central
SD-8230-161	2	Serpentin Del Evaporador Paneles Laterales
SA-8230-185	2	Esquema Del Receptor CESA-1
SKC-700-0	--	Esquema De Placas De Anclaje Para Estructura Del Receptor
CESA-OM-G-01-1	0	Emplazamiento CESA-1

Appendix 2 (continued)

<u>Drawing No.</u>	<u>Rev.</u>	<u>Title</u>
CESA-OM-G-02-0	0	Disposicion General Zuna De Edificios
CESA-OM-G-02-0	0	Disposicion General Campo De Heliostatos.
CESA-OM-A-01-0	0	Disposicion General Sistema De Almacenamiento Planta ALA COTA - 1, 20
CESA-OM-A-02-0	0	Disposicion General Sistema De Almacenamiento Plantas A Las Cotas + 5'30, + 8'30y + 9'80
CESA-OM-A-03-0	0	Disposicion General Sistema De Almacenamiento Secciones
CESA-OM-A-01-2	--	Diagrama T. e I. Almacenamiento Termico M-200
CESA-OM-P-01-0	0	Disposicion General Edificio De Turbina Planta A La Cota \pm 0, 00
CESA-OM-P-02-0	0	Disposicion General Edificio Turbina Planta A La Cota + 4, 50
CESA-OM-P-03-0	0	Disposicion General Edificio De Turbina Plantas A Los Cotas - 3, 50 + 7, 50y + 10, 00
CESA-OM-P-04-0	0	Disposicion General Edificio De Turbina Seccion "A"
CESA-OM-P-05-0	0	Disposicion General Edificio De Turbina Seccion "B"
CESA-OM-P-01-2	--	Diagrama T. e I. Vapor-Condensado Y Aqua De Alimintacion M-100
(Spanish) July 1, 1979	0	Estudio De Los Modos De Operacion De La Central
(English) December 27, 1979	0	Conditions and Operation Procedures for the CESA-1 Solar Receiver
(Spanish) January 14, 1980	--	Analisis De Flujo Y AP

Appendix 2 (continued)

<u>Drawing No.</u>	<u>Rev.</u>	<u>Title</u>
(English) January 13, 1980	--	Evaporator Flux Analysis
K-Number (Spanish)	NA	Information concerning instrumentation (multiple pages)
512-8230-16Y	0	Soportes del Sobrecalentador En Interior de cabina

Appendix 3

Reports and Papers Which Have Been Translated to English

1. Report on Heliostat Prototype Tests.
2. Data on the Site - Revision 3.
3. Study of Diffuse and Specular Reflectance of Mirrors Used in the Design of Heliostat Prototypes Based on Information Furnished by the "Daza De Valdes" Institute.
4. General Plant Specifications - Revision 0.
5. Specifications for Solar Receiver Order.
6. "Selected" Instrumentation "K" Drawings.
7. Diagram of General Scheduling - Revision 3.

The following reports have not yet been received from the translating service.

8. Descripcion De Los Lazos De Instrumentos Y Control - Receptor Solar - CESA-I.
9. Estudio De Los Modos De Operacion De La Central - Rev 0.
10. Pruetas De Calificacion De Los Prototipos De Heliostats.

March - April 1980

Technical Assistance Status

Members of the CESA-1 project visited the U.S. during March to attend a CESA-1 project review, the CRTF Workshop, and the DOE Solar Central Receiver Semi-Annual Meeting. Those attending these meetings from Spain included, Carlos Ortiz and Fernando Sanchez (CEE), Loek De Gruijter and Jesus Cruz (TR), Jose Ramirez (EISA), and Carlos Garriga (SENER). The CESA-1 project review was held at Sandia Livermore on March 11-14, 1980 while the CRTF Workshop and semi-annual meetings were at Albuquerque, New Mexico on March 17-18, 1980 and March 19-20, 1980, respectively. The primary subsystems covered during the project review were the heliostat field control and heliostat control, receiver, and heliostats.

On April 24-25, 1980 Al Baker (SNLL) visited the CESA-1 project office at CEE and the CESA-1 heliostat test facility at I.N.T.A. in Madrid, Spain. The main purpose of this meeting was to establish with CEE a joint CEE/Sandia budget and work tasks for the time period between 1 May 1980 to 30 April 1981. The work for the next year is similar to last year but with less emphasis on the receiver design and more on the heliostat and storage subsystem design.

Sandia has recently completed a "Technical Assessment of the CESA-1 Project - 15 April 1980" which is now being typed. This assessment covers the information supplied to us thru 15 April 1980. The results of the reviews mentioned in this status letter are included in that Technical Assessment and have not been duplicated in this report.

Heliostats

During the March review meeting CEE provided a verbal description of their Group 1 - Optical, Group 2 - Mechanical, Group 3 - Ambiental, and Group 4 - Controls tests from the CESA-1 heliostat test plan. CEE delivered to Sandia several reports on their test results for the SENER heliostat from Groups 1 and 3. They also orally presented a description of both the SENER and CASA heliostats including the mirror modules, structure, and drive mechanism. When Al Baker was at CEE in April, he was given a complete set of SENER structure and gear box detailed drawings for Sandia to review and comment, however, mirror module drawings were not included in the drawing set. The results of Sandia's review of these SENER drawings will be included in the next status letter. The current status of the Sandia CESA-1 heliostat assessment is that:

1. All of the heliostat related reports CEE supplied at the March 11-14, 1980 meeting have been reviewed.
2. Sandia is in the process of reviewing the detailed design drawings of the SENER structure and gear box supplied in April 1980.

3. Sandia will review and provide comments to CEE on the revised heliostat test plan which is currently being prepared by CEE.

Receiver

The Sandia assessment of the CESA-1 water/steam receiver is based on a complete detailed drawing set and documentation of controls and instrumentation provided by CEE. Sandia has had a contract with Foster Wheeler Development Corporation (FW) to provide a detailed review and comments on the CESA-1 receiver. The Sandia and FW receiver evaluations have been based on solar heat flux distributions calculated by Sandia using an artificial 312 SENER heliostat field. The heat flux distribution is therefore the greatest uncertainty in the receiver assessment. The current status of the Sandia receiver assessment is that:

1. The contract Sandia has had with Foster Wheeler was completed and a draft of their final report was supplied to Sandia and CEE.
2. Sandia and FW will visit CEE in Madrid, Spain on May 21, 1980 for an oral presentation of the FW final report results.

Heliostat Field Control and Heliostat Control

Specifications for the heliostat field controller and heliostat controllers and the EISA bid for the heliostat field control system have been provided to Sandia. During the March review meeting Jose Ramirez, EISA, and Duncan Tanner, SNLL, had very detailed discussions on EISA's approach to meeting the heliostat field control requirements. The current status of the Sandia heliostat field and heliostat control assessment is that:

1. All of the reports on the heliostat field and heliostat controls have been reviewed by Sandia.
2. Sandia will review and provide comments to CEE on the response of their proposal for the supply of the heliostat controller when it is available.

Storage

CEE has provided Sandia with reports covering the storage system equipment sizing, data sheets on pumps, and a storage subsystem heat exchanger study. The current status of the Sandia storage subsystem assessment is that:

1. All of the reports on the storage subsystem have been reviewed.

May-June, 1980

TECHNICAL ASSISTANCE STATUS

Representatives for Sandia and Foster Wheeler visited the CESA-1 Project Office in Madrid during May, 1980. Those attending from Sandia included Al Skinrood, Ed Cull, and Bob Carling. Bob Zoschak attended from Foster Wheeler. The primary topics discussed at the meeting were final results of the receiver design review, status of heliostats and the storage subsystem.

The recently completed Sandia "Technical Assessment of the CESA-1 Project" was given to CEE and major points were discussed. CEE is satisfied with Sandia's overall project support and expressed their appreciation. Since Sandia's current funding for CESA-1 support was spent during May, Al Skinrood discussed with CEE interim funding needs until the May 80-April 81 budget is approved by the U.S./Spanish joint committee. Bob Goeckerman, Scientific Attache at the U.S. Embassy, informed Sandia that \$50K interim funding has been approved and a telegram was sent to the U.S. Department of State requesting them to provide the funds. Sandia will continue to support the project but will make no outside commitments until we receive written confirmation of the funding approval.

Heliostats

On April 25, 1980, CEE provided Sandia with a set of SENER heliostat drawings, except the mirror module and mirror module support structure were not included. SENER is in the process of redesigning their mirror module since CEE test results of its optical performance showed it did not meet the CESA-1 specifications. Sandia has completed its review of the SENER structure and drive mechanism. SENER's heliostat is very similar to the McDonnell Douglas (MDAC) Barstow prototype heliostat which has been extensively tested by Sandia. The Sandia review of the SENER heliostat included comparing like design features with the MDAC prototype and commenting on areas of concern. During the May meeting in Madrid, CEE provided Sandia with the CASA heliostat drawings including mirror modules. This drawing set did not include all piece part drawings; thus, only the major assembly drawings are being reviewed. CASA's heliostat is similar to the Martin Marietta (MMC) Barstow prototype, so the same type of review, by comparing the CASA heliostat design to the MMC heliostat (where Sandia again has test experience), is being done. The CASA review is almost complete. Results of these reviews will be sent to CEE in several days.

Using the CASA-II heliostat design definition, C. N. Vittitoe, SNLA, has begun some HELIOS calculations to determine the acceptable beam quality errors which are necessary to meet the CESA-1 heliostat specification. Heliostats with the shortest and longest slant ranges are being considered. Also, three focal lengths for a given slant range are being evaluated to determine how beam quality errors change. Preliminary results show that heliostats with the shortest slant range cannot meet the CESA-1 specification, even with very small beam quality errors. Since for the short slant range heliostats all of their energy does enter the cavity aperture, the impact of them not meeting the specification may not be that important on receiver performance.

Mr. Vittitoe plans to use the acceptable beam quality error he determines from his analysis, and predict the beam target image that CEE would measure at their INTA heliostat test facility for the CASA-II heliostat if it was tested at equinox noon. Beam pointing errors have not been considered at this time. Once beam pointing and beam quality errors are measured, they will be included in the field performance calculations. CEE will be making the HELIOS field performance calculations which will be compared to selected HELIOS and MIRVAL Sandia calculations. The current status of the Sandia CESA-1 heliostat assessment is that:

- 1) SENER and CASA-II heliostat structure and drive mechanism drawing have been reviewed.
- 2) CASA-II mirror module drawing review is in progress and results will be included with structure and drive mechanism review.
- 3) Sandia has not received test results from the Group I-Optional, Group 2-Mechanical, or Group 3-Environmental test from CEE for either CASA-II or SENER. Reports of the SENER tests with the mirror module that was not accepted by CEE were provided to Sandia earlier.
- 4) Single heliostat HELIOS calculations, using the current CASA-II heliostat definition, have been started. The calculation will be finalized after Sandia receives test data.

Receiver

The May meeting in Madrid was the final design review meeting prior to CEE placing the contracts for receiver fabrication and instrumentation. This meeting concluded Sandia's contract with Foster Wheeler (FW) for the CESA-1 receiver design review and included a presentation of the results in their final report. Recommendations by Sandia and FW were discussed with CEE and Technicas Reunidas (TR), the receiver designer. Since the biggest uncertainty in the receiver assessment is the heat flux distribution, based on an artificial 312 SENER heliostat field, TR has added provisions so that additional

superheater tubes can be added if necessary. TR has modified their design of the central panel inlet manifold to provide for common orificing for groups of five tubes. Sandia and FW had recommended the possible need for tube orificing to improve the tube-to-tube flow distribution, and this TR change is an improvement over the original design. The CEE project manager, supported by TR, decided not to follow the Sandia and FW recommendation to use Type 316 stainless steel for the last three passes of the superheater; TR will use X20CRMOV12. The recommendation to use 316 stainless steel was based on the United States experience with fossil and solar "fired" boilers. The current status of the Sandia CESA-1 receiver assessment is that:

- 1) Sandia will provide an introduction for the FW final report and FW will combine their reports on Tasks 1, 2 and 3 into one overall report.
- 2) Sandia will provide CEE with the results of our limited fatigue testing at 600°F on a sample of X20CRMOV12 material, supplied by TR, when the testing is completed.
- 3) Sandia will perform receiver heat flux calculations using the heliostat field layout and measured heliostat performance data when it is provided by CEE.

Storage

The two tank HITEC storage subsystem uses three U-tube heat exchangers for charging and three U-tube heat exchangers for discharging. There are two hot HITEC pumps and one cold HITEC pump. The storage subsystem uses an inert nitrogen atmosphere to keep the HITEC stable at temperature. During the May design review meeting, CEE provided Sandia with a list of questions concerning salt handling, hardware, and heat exchangers. Discussion on the storage subsystem included operation methods, selection and suppliers of equipment, and requirements for trace heating or draining of the storage components. CEE requested that Sandia subcontract Badger Energy Inc., similar to what was done on the receiver with FW, to provide support on answering these engineering type of questions. This idea of having Sandia subcontracting an engineering firm experienced in salt equipment was also discussed in April when we were establishing the May 80-April 81 budget, so funds were included in the budget for this activity. The current status of the Sandia CESA-1 storage assessment is that:

- 1) A scope of work has been drafted and sent to Badger Energy for them to quote on costs. No contract will be awarded until written assurance of funding authorization is received.
- 2) Reports on HITEC properties, compatibility with metals, and safety were provided to CEE.

July - August, 1980

TECHNICAL ASSISTANCE STATUS

Sandia National Laboratories has still not received official authorization from DOE that either the \$50K interim funding or the \$185K May 80 - April 81 budget funding is available to support the CESA-1 project. Both the interim and May 80 - April 81 funding have been approved by the United States/Spanish Joint Committee. Sandia reluctantly temporarily stopped its support of the CESA-1 project at the end of July, 1980 until additional funds are available. Attempts to expedite the process within DOE have been made but Sandia has no commitment for when the procedure will be completed.

Heliostats

The preliminary assessments of both the SENER and CASA-II heliostats were completed and sent to CEE during July, 1980. These assessments are considered preliminary since Sandia has not yet received any of the current SENER or CASA-II heliostat test data from CEE. General observation reported in the assessment covering the SENER and CASA-II heliostat designs are as follows:

SENER

The use of a harmonic drive system for azimuth rotation and a linear screw-jack to drive the elevation mechanism are design features which indicate similarity of the SENER design to McDonnell Douglas's (MDAC) prototype design. A particularly unique feature of the SENER design is the employment of a four-linkage system to accomplish a full 180° elevation travel (face-up to face-down stowage) with only a single linear actuator.

The SENER general arrangement drawings define a sophisticated and complex design. The SENER design has already been built and tested, and verbal reports from CEE indicate satisfactory operation. However, the complexity of the design is of concern because of the possible reduction in reliability.

CASA II

The general concept of the CASA-II design is much like the Martin Marietta Corporation (MMC) Barstow design, but specific features are significantly different. A split torque-tube flange is mounted to each side of the AZ-EL drive mechanism, in contrast to MMC's through torque-tube with its offset connecting arms. The CASA

concept has considerable merit in that mass/CG offset of the mirror assembly can be kept to a minimum, thus reducing the torsional load requirements on the gear drive mechanism. Additional benefits can also be realized in the logistics of assembling and installing the complete heliostat in the field, since the split torque-tube would permit preassembly of smaller, easier-to-handle reflector assemblies for each half of the heliostat.

Another area of notable difference between the CASA-II and MMC designs is the applied operational and survival specifications. Although the reasons for these differences are not fully understood at this time, it was deemed necessary to point them out as they affect the comparative capability of the two designs.

The HELIOS calculations by C. N. Vittitoe, SNLA, which were begun in the last reporting period were completed in July, 1980. Results from these calculations were sent to CEE.

A single CASA-II heliostat was analyzed to determine an acceptable beam quality error which would meet the CESA-I heliostat specification. The heliostat was located at four different positions within an early version of the CESA-I heliostat field layout. Based on the results of that study, predictions were made to obtain beam target images that CEE might measure at their I.N.T.A. heliostat test facility. The beam quality error for the CASA-II heliostat to meet the CESA-I requirement for all but the close-in heliostats location was predicted to be .9 MRAD. This value is slightly less than that which has been measured for the MMC #1 Barstow prototype at CRTF which was .98 MRAD. CESA-I close-in heliostats, even with small beam quality errors, cannot meet the heliostat specification.

The predictions of the target images for I.N.T.A. were very sensitive to heliostat canting time. To be able to determine the beam quality error from the I.N.T.A. test results, the exact cant time will have to be known. Also, the time it takes to cant the heliostat must be as short as possible.

Sandia is waiting to receive from CEE test results for the SENER and CASA-II heliostats from the Group I - Optical, Group II - Mechanical, and Group III - Environmental tests, so that the heliostat assessment can be continued.

Receiver

The only activity on receivers during this reporting period was the completion of our limited fatigue testing on a sample of X20CrMoV12 material supplied by Technicas Reunidas (TR). This material is used in the superheater of the CESA-1 received. The

results of our test were sent to CEE. The important feature of this test was that, after the initial test cycle, the relaxation of X20CrMoV12 appeared to be complete within several minutes. This behavior is similar to 316 stainless steel in which the relaxations have been complete within an hour of the start of the hold period and significantly different from relaxations on Alloy 800 which are not complete after 5.9 hours.

Storage

At the May, 1980 design review meeting in Madrid, Spain CEE requested that Sandia subcontract Badger Energy Inc. to provide support by answering engineering types of questions on the salt storage system. A scope of work was drafted and sent to Badger Energy for them to quote on the cost of this support. Based on Badger's quote a revised scope of work was written so that the cost would be within the desired value of \$10 K. This revised scope of work was sent to CEE for their concurrence. No contract to Badger has been awarded since funding for further CESA-1 project support has not been authorized by DOE.

TECHNICAL STATUS REPORT
Project IIIP - 3020
Franklin Research Center
September 1980

TASK 1, ENERGY AND ECONOMIC DATA

We obtained Spanish energy and economic data from AUXINI. We reviewed them and made suggestions which were transmitted to AUXINI in June, 1980 while their personnel visited here. This task was subcontracted by the Franklin Research Center (FRC) to General Electric Co. (GE).

TASK 2, METEOROLOGICAL DATA

We obtained meteorological data for Spain from AUXINI. We reviewed the proposed solar radiation model, noted certain deficiencies in it, and developed a revised model that is to be used. Comparisons with measured data verified the validity of this radiation model which permits an approximate determination of solar radiation from other meteorological data at locations where no measured solar radiation exist.

TASK 3, DEMOGRAPHIC DATA

We obtained Spanish demographic data from AUXINI, reviewed them, and made suggestions pertaining to the presentation of data and to voids in the data which should be filled. This task was subcontracted by FRC to GE.

TASK 4, COST/PERFORMANCE EVALUATION

Computer simulation programs available in the United States were reviewed as to their applicability for Spanish conditions and as to the practicality of their use by the equipment available to AUXINI. The programs initially selected were TRNSYS and f-Chart, both developed under U.S. Department of Energy sponsorship at the University of Wisconsin. Spanish meteorological data for five locations and Spanish physical and monetary units were entered into the f-Chart program. Tax credit routines applicable to the U.S. were eliminated. This modified f-Chart program readily usable for Spanish conditions was then transmitted to AUXINI.

TASK 6, BARRIER ANALYSIS

Real and potential barriers to the utilization of solar energy were identified. Possible actions to overcome these barriers were investigated, and pertinent recommendations were made. This task was sub-contracted by FRC to GE.

TASK 7, TRAINING PLAN

A training program was conducted for two groups of Spanish engineers in the United States. One group was familiarized with analytical methods used in economic and technical analysis. This included data preparation, data verification, and data use. The second group contained training in solar design, both passive and active, energy storage, and the use of the TRNSYS and f-Chart computer programs which were delivered to AUXINI. This group was also taken on an extended tour of U.S. solar research and test installations. During that tour, this group also saw a considerable number of solar passive residential installations.

TASK 8, HEAT PUMP APPLICATIONS

The applicability of heat pumps to Spanish conditions was investigated. Data on the cost of installed conventional heating and heat pump equipment and on different fuel costs were obtained from AUXINI for both present conditions and escalations through the year 2000. AUXINI also furnished heat loss data for typical multi-family residential units.

FRC then determined operational performance of the heat pump and the conventional systems in five geographical locations in Spain. Based on these, payback periods and return on investment were determined for the period from the present through the year 2000.

A complete set of TRNSYS tape, User's Manual, and printout was delivered to AUXINI in June, 1980 when their personnel visited FRC.

The OPSIS program developed by AUXINI was reviewed. Computer simulations for buildings at five locations corresponding to five Spanish climate regions were performed. The data obtained by AUXINI using OPSIS and the data obtained by FRC using TRNSYS were compared. It was found that the OPSIS simulation of solar radiation on an inclined surface produced results which were significantly different from those produced by TRNSYS. Apart from this shortcoming, the results obtained by OPSIS agree reasonably well with TRNSYS results. Recommendations for modifying OPSIS to overcome these shortcomings were made.

Computer simulations for different buildings and for the utilization of solar energy for industrial process heating were performed. These data were transmitted to AUXINI for use in Task 5, Market Potential.

Performance and cost analyses were performed for different solar systems for different applications and at different locations in Spain.

Copies of all the work performed by AUXINI on this task were sent to FRC by AUXINI, and the report covering this entire task was produced in Philadelphia and was mailed to AUXINI for inclusion in their report to the Joint Committee.

TASK 5, MARKET POTENTIAL

The market potential of solar energy for both residential and commercial and industrial applications was evaluated. It was found that most of it is in the residential sector concentrated in the Madrid and Barcelona regions of the country. A preliminary demonstration plan to accelerate the commercial development of solar energy utilization in Spain was prepared.

This task was subcontracted by FRC to GE.

PROPOSAL FOR ASSISTANCE FOR COOPERATIVE
RESEARCH PRESENTED TO THE ADVISORY
COMMISSION FOR SCIENTIFIC AND
TECHNICAL RESEARCH CHARGED TO THE
THIRD COMPLEMENTARY AGREEMENT
OF THE TREATY OF FRIENDSHIP AND
COOPERATION BETWEEN SPAIN AND
THE UNITED STATES OF AMERICA
COOPERATIVE SOLAR ENERGY PROGRAM
III - P - 3020, 2nd PHASE

1. Background:

In 1978 a proposal of assistance of cooperative Research for the development of a solar energy project to which was given the name and legal reference cited in the title of this document was present to the Advisory Commission for Scientific and Technical Research charged to the Program of the 3rd Complementary Agreement of the Treaty of Friendship and Cooperation between Spain and the United States of America.

Said project to be done in collaboration with the FRANKLIN RESEARCH INSTITUTE LABORATORIES of Philadelphia had an anticipated duration of 3 years and basically concentrated on the following activities.

1. Study of the possibility of introducing solar energy in thermal process of up to 100° C in our country.
2. Study of the developments of solar system components, based on fixed non-concentrating solar collectors, and the implementation of demonstration installations.
3. Participation in research programs on heat pumps and an energy and economic analysis of the heat pump in comparison with other heat producing systems, including solar energy.

This project was approved by the Advisory Commission for Scientific and Technical Research and in July, 1979 began its first year of activity.

The evolution of said project has been, in general terms, as it was expected as can be seen in the Reports presented up to now to the joint

Spanish-North American Committee for Scientific and Technological Cooperation, despite the late incorporation of the U.S. part to the Project due to the delay of the corresponding contract signature between Franklin Institute Research Laboratories and the Solar Energy Research Institute of the United States.

Currently two months from completing the first cycle we present a proposal, the purpose of the document, for the materialization (realization, implementation) of the 2nd phase of activity to begin starting August, 1980 maintaining the general terms of the original proposal but introducing certain changes recommended by the experience acquired in the period which we are now completing.

2. Proposal for Phase II of the Project

2.1.1. Updating of energy and economic data

The constant evolution of economic factors, price of combustibles, etc., and the appearance of energy data corresponding to the most recent years make it necessary to update the work package developed in the 1st phase of this project.

2.1.2. Finalization of the cost efficiency evaluation of the systems

This task contemplates the development and/or acquisition of computer programs for the simulation of the functioning of solar energy systems and the materialization of the past computer simulations necessary for assuring the knowledge of the efficiency relationship - cost, or in other words, the cost of energy produced by solar energy, in different applications and in different regions of our country.

This task was developed almost totally in the 1st phase, nevertheless the changes that may be introduced on the conditions of departure (energy and economic data, improvements of solar systems and their components, etc.) can compel and updating of the conclusions of said study.

2.1.3. Updating of the market studies

Just as the previous one, this task which contemplates the analysis of the possibilities of introducing solar energy in the market, will be practically finalized in the 1st phase of the project. Nevertheless, it will be right to proceed with the updating in view of variations in costs of components and performance of solar systems.

2.1.4 Finalization of the heat pump analysis of applicability

For the reasons cited previously it is suitable to do an up-date of the study done during the previous year. Besides, given the evaluation that this equipment are currently undergoing, the permanent contact with the American side is completely justified for the analysis of new types and concepts that may continue appearing on this theme, whether they be already in the American market or at the prototype stage.

2.1.5 Demonstration plan for solar heating and air conditioning for the residential sector, steam production and industrial and commercial thermal processes and the implementation of the heat pump.

The realization of a plan for demonstrations that may serve to test the technical and economic viability of the solar systems in the specific areas disclosed is a fundamental task for this second year of the project.

This task includes the following sections:

a) Plan for heating and air conditioning demonstrations

Once the technical and economic viability of solar energy is demonstrated for the purposed, the most adequate number of demonstrations will be determined in terms of the division of the country in climatic zones and in terms of the influence that said number of demonstrations can have over the results. The characteristics should join each one of the demonstrations planned ought to be prepared, a function of the different possibilities of the advisable solar systems; an evaluation criterion of the conditions of the demonstration candidates out to be done in order to select those most adequate ones; the types of buildings in which the demonstrations will be implemented ought to be selected and lastly a definite demonstration plan ought to be prepared.

b) Plan for demonstrations of industrial and commercial thermal processes.

In this case, the first task consists in identifying the industrial and commercial users who may utilize low temperature hot water or steam. Later the solar systems adequate to the necessities cited for analysing the influence over the market potential of the number of demonstrations ought to be defined and then a process similar to that described for the previous case ought to be repeated; that is: to determine the number of demonstrations, to analyze characteristics of the demonstrations to be done, and evaluation criteria for selecting candidates and an implementation plan.

c) Plan for heat pump demonstrations

As with the previously mentioned ones, this plan for demonstrations requires a selection for cities in which to install the demonstrations, a selection of types of heat pumps to use, an analysis of the influence of the number of demonstrations to be made selection criteria for candidates, technical and economic analysis of the installations to be done, and the preparation of a plan for demonstrations.

2.1.6 Implementation of two demonstration installations

With the objective of beginning the implementation phase of the demonstration installations as soon as possible, allowing at the same time the acquiring of necessary experience for the implementation of large-scale installations, the materialization of two installations, one in the residential sector and the other in the commercial or industrial sector is proposed during the next phase. These will form part of the plan for demonstrations to

to prepare during the same period of time.

In the beginning these demonstration installations will be considered pilot installations for the seasons explained and therefore ought to be small size.

2.1.7. Study of manufacture of vacuum collectors

The objective of this study is to determine the possibilities for the manufacturing of vacuum flat-plate collectors in our country and includes, therefore, an analysis of materials fabrication processes, identification of suppliers, determination of the size of collector series to be manufactured, the participation of U.S. technology in the process and an analysis of cost and technical and economic viability of the layout.

This study will be conditional, as far as size of the series and its evolution in time, on the study and updating of the market analysis, cited as a task in this same description of activities.

2.1.8. Training plan

Just as was done in the first phase of this project, the development of the activity ought to be accompanied by a training plan for Spanish people in the specific tasks to be developed.

During the first year of activity the training plan was of a general type and related mainly to software (studies of computer programs, methodology of market studies, etc.) while in this second year it ought to be more specific for design and implementation of solar installations and heat pumps as well as fabrication analysis.

2.2 Plan for Activity corresponding to the Second Phase of the Project.

The following diagram summarizes the tasks and subtasks cited in the activity description and places the materialization during the proposed 2nd phase proposed.

2.3 Distribution of Costs

The following table shows the cost distribution by task and by participants, that is the National Industrial Institute and the Franklin Research Center (new name for the old Franklin Institute Research Laboratories).

Translated from the Spanish. Solar Energy Research
Institute (December 1, 1980)

Plan for Second Phase
 PLANIFICACION DEL SEGUNDO CICLO

1.980

1.981

Nº	T A R E A	AGO	SEP.	OCT	NOV.	DIC.	ENE.	FEB.	MAR	ABR.	MAY	JUN	JUL	AGO	SEP	OC
0	<i>Detailed plan for the 2nd phase</i> PLANIFICACION DE DETALLE DEL 2º CICLO	▲	▼													
1	<i>Energy & Economic Information Update</i> ACTUALIZACION DATOS ENERGETICOS Y ECONOMICOS	▲				▼						▲		▼		
2	<i>Efficiency & System Cost Evaluation</i> EVALUACION EFICIENCIA-COSTE DE SISTEMAS	▲				▼						▲		▼		
3	<i>Update of Market Studies</i> ACTUALIZACION DE LOS ESTUDIOS DE MERCADO			▲				▼					▲	▼		
4	<i>applicability Analysis of Heat Pumps</i> ANALISIS APLICABILIDAD DE LA BOMBA DE CALOR	▲						▼					▲	▼		
5	<i>Demonstration Plan</i> PLAN DE DEMOSTRACIONES			▲						▼						
5.1	<i>Heating & Air Conditioning</i> CALEFACCION Y AIRE ACONDICIONADO			▲				▼								
5.2	<i>Thermal Processes in Industries & Businesses</i> PROCESOS TERMICOS EN INDUSTRIAS Y COMERCIOS					▲			▼							
5.3	<i>Heat Pump</i> BOMBA DE CALOR							▲				▼				
6	<i>Implementation of Two demonstration installations</i> IMPLEMENTACION DE DOS INSTALACIONES DE DEMOSTRACION					▲								▼		
6.1	<i>Installation Project</i> PROYECTO DE INSTALACION					▲		▼								
6.2	<i>Installation and final touches</i> INSTALACION Y PUESTA A PUNTO							▲						▼		
7	<i>Manufacturing of Vacuum Collector Study</i> ESTUDIO DE FABRICACION DE COLECTORES DE VACIO							▲				▼				
8	<i>Trainer Plan</i> PLAN DE FORMACION (DISEÑO, INSTALACION Y FABRICACION)	▲							▼							
9	<i>Final Report of 2nd phase</i> REPORT FINAL DEL 2º CICLO													▲	▼	
10	<i>Continuance of the demonstration</i> SEGUIMIENTO DE LAS DEMOSTRACIONES													▲	---	---

DISTRIBUCION DE COSTES POR INSTITUCION (\$)

Nº	TAREA	INI	FRC	TOTAL
1	<i>Energy & Economic Information Update</i> ACTUALIZACION DATOS ENER- GETICOS Y ECONOMICOS.	1.000	-	1.000
2	<i>Efficiency & System Cost Evaluation</i> EVALUACION EFICIENCIA- COSTE DE SISTEMAS	8.000	6.000	14.000
3	<i>Market Studies Update</i> ACTUALIZACION ESTUDIOS DE MERCADO.	5.000	3.000	8.000
4	<i>applicability analysis of</i> ANALISIS APLICABILIDAD BOMBA DE CALOR <i>Heat Pump</i>	15.000	15.000	30.000
5	<i>Demonstration Plan</i> PLAN DE DEMOSTRACIONES	20.000	20.000	40.000
6	<i>Two Demonstration Installation</i> IMPLEMENTACION DOS INS- TALACIONES DEMOSTRACION(*) <i>Implementation</i>	117.000	67.000	184.000
7	ESTUDIO FABRICON COLEC- TORES. <i>Collector Manufacture</i>	25.000	25.000	50.000
8	<i>Study</i> PLAN DE FORMACION	25.000	45.000	70.000
T O T A L E S		216.000	181.000	397.000

(*) *This part corresponds to the hardware of the demonstration*
Esta partida corresponde al hardware de las instalaciones
de demostración. *installations*

Cooperative Research Grant
(Spain and the United States of America)
Annual Progress Report

"FURTHER DEVELOPMENT OF TWO-SIDED SOLAR CELLS"

U. S. State Department Designation: III-P-3008

U. S. Principal Investigators: J. G. Fossum
F. A. Lindholm
A. Neugroschel

Department of Electrical Engineering

University of Florida

Gainesville, FL 32611

U. S. A.

April 1980

A. INTRODUCTION

This cooperative program of scientific research involving the United States and Spain was initiated to advance the development of double-sided illuminated (DSI) solar-photovoltaic cells. These cells differ from conventional ones in that they are designed to be used in solar concentrators that illuminate both the front and back surfaces of the solar cell. The primary goal of this program is to extend the theory and the technology for DSI cells to the point where high efficiencies ($>11\%$ at AM1 on both sides) can be achieved.

The United States (University of Florida) involvement in the program is to provide technical assistance to the Spanish investigators who will do the actual fabrication of the high-efficiency DSI cells. Three U. S. tasks were accordingly defined:

- (1) Develop experimental techniques to measure carrier lifetimes and diffusion lengths in the quasi-neutral base regions, and effective surface recombination velocities at the p-n and low-high (L-H) junctions of the basic DSI solar-cell structures, i.e., n^+pp^+ , p^+nn^+ , n^+pn^+ , and p^+np^+ .
- (2) Identify and characterize the physical mechanisms occurring in DSI solar cells that limit their conversion efficiencies.
- (3) Based on the results of Tasks (1) and (2), propose and evaluate cell design modifications for improving the DSI cell efficiency.

Section B of this report describes the essential completion of Task (1). New experimental-theoretical methods are presented and illustrated that enable accurate determinations of the minority-carrier diffusion length in the narrow base region of basic DSI solar-cell structures. These methods are unlike more conventional diffusion-length measurements in that they enable the evaluation of diffusion lengths longer than the base width. For back-surface-field (BSF) cells, i.e., n^+pp^+ or p^+nn^+ structures, these methods enable also the determination of the effective surface recombination velocity at the L-H junction.

Using the methods described in Section B, and relying on a recently developed description of the physics underlying the performance of BSF solar cells [reported in our semiannual report], we present in Section C results of our work under Task (2). The work is concerned primarily with tandem-junction, front-surface-field, and interdigitated-back-contact cells, all of which are basic DSI cell structures. A unifying view of the physics underlying the performance of these cells is presented. Special emphasis is given to qualitative treatments of the important multi-dimensional transport problems introduced by these cells, treatments which can be applied directly to the study of solar cells being illuminated on both sides.

Task (3), and related, necessary work described in our request for renewal, will be undertaken during the second year of our involvement in this program.

In Section D, we describe briefly the U. S.-Spain technical interaction supported by this program. Exchanges of technical information during the first year and plans for additional exchanges during the second year are described.

The current financial report is given in Section E. Because the Annual Progress Report has been requested early, the financial report does not account for the total annual budget, which will not be completely spent until July 1980.

SECTION B

DETERMINATION OF LIFETIMES AND RECOMBINATION CURRENTS IN p-n JUNCTION SOLAR CELLS AND DIODES *

(Arnost Neugroschel)

Abstract

New methods are presented and illustrated that enable the accurate determination of the diffusion length of minority carriers in the narrow regions of a solar cell. Other methods now available are inaccurate for the desired case in which the width of the region is less than the diffusion length. Once the diffusion length is determined by the new methods, this result can be combined with measured dark I-V characteristics and with small-signal admittance characteristics to enable determination of the recombination currents in each quasi-neutral region of the cell--for example, in the emitter, low-doped base, and high-doped base regions of the BSF cell. For BSF cells, this leads to a value for the effective surface recombination velocity of the high-low junction forming the back-surface field.

I. INTRODUCTION

The minority carrier base diffusion length is an important material parameter determining the performance of solar cells. Very long diffusion lengths, longer than the base width, are desirable for the successful operation of BSF, IBC, FSF, and TJ cells [1] - [4]. Such long diffusion lengths are necessary to achieve large values of the short circuit current J_{SC} , to minimize the base dark current, and thus lead to large cell efficiency η . A long diffusion length is also necessary in the emitter of the HLE cell [5] for similar reasons.

Numerous methods exist to measure the base diffusion length L_B [6,7]. These methods are based on the measurement of some device parameter, such as current, capacitance, etc., which is dependent on L_B . To measure L_B accurately, L_B has to be smaller than the base width W_B , i.e., $L_B < W_B$. In this case, the minority carriers recombine within the base without interacting with a back contact. If, however, $L_B \sim W_B$ the minority carriers interact with the back contact and the measured parameter is dependent on a slowly varying (hyperbolic) function of W_B/L_B [7]. If $L_B > W_B$, the measured parameters depends on W_B only, and is independent of L_B . Thus, existing methods of measurement do not work well for cells with $L_B > W_B$.

An accurate knowledge of L_B is still very important even if $L_B > W_B$, since the dark base recombination current Q_B/τ_B can still significantly contribute to the total dark current of the device.

In this paper, methods for the accurate measurement of L in a narrow region W in cells for which $L > W$ are described. The methods are applicable to essentially all cells and diodes with a narrow region either in the base or in the emitter.

The first method, described in Section II, is based on basewidth-modulation of n-p-n or p-n-p transistor-like structures. The method involves measurement of the low-frequency small signal conductances which arise from the basewidth-

modulation by a small ac signal. TJ cells are directly applicable for the method, since they are, in essence, transistor structures. For other cells, transistor-like structures can be obtained by modification of the cell structures done at low temperature. The method requires only a knowledge of the base width W_B and the base doping, and the accuracy is better than about $\pm 10\%$. The method applies for both high and low levels of carrier injection.

Section III discusses the small-signal admittance method. This method can be applied to practically any cell with a narrow region either in the base, or in the emitter which is the case for the HLE cell [5]. It also leads to determination of the recombination velocity at the back of the narrow region. Section IV describes a simple method to determine the diffusion length, which is based on measurements of dc currents on two related structures.

Based on an accurate knowledge of L , a simple analysis of the cells can be made. This analysis, described in Section V, uses measurement of dark currents and small-signal admittance, and leads to determination of the recombination currents in each region of the cell. Section VI shows illustrative examples of the analysis of three cells: $n^+ - p - n^+$ TJ cell, $n^+ - p - p^+$ BSF cell, and $p^+ - n - n^+$ BSF cell. Section VII discusses the accuracy of the measurements.

II. BASEWIDTH-MODULATION METHOD

A. Minority carrier lifetime

The basewidth-modulation (BWM) method for determination of the minority carrier base lifetime of junction transistors was recently published (8). This method is applied here for the case of very wide base regions in solar cells. The method is also extended to determine the recombination currents in the quasi-neutral emitter and collector regions of the cells.

The basewidth-modulation effects arise from voltages appearing across the base-collector junction of the transistor. Any change in the base-collector voltage will produce a change in the width of the junction space-

charge-region (SCR) which, in turn, produces a change in the width, W_B , of the quasi-neutral base (QNB) region, as illustrated in Fig.1 for an $n^+ - p - n^+$ transistor. The change in the base width, ΔW_B , produces three effects: a) the amount of excess minority carrier (electron) charge Q_B stored in the QNB changes by ΔQ_B ; b) the component of the base current due to recombination within the QNB changes by $\Delta Q_B / \tau_B$; and c) the collector current changes because of the change in the slope of the excess minority electron distribution $N(x)$ in the base.

The BWM effects can be detected by measuring a low-frequency small-signal output conductance G_o and a reverse transconductance G_r [2] of the device:

$$G_o = \left. \frac{i_c}{v_{ce}} \right|_{v_{be}=0} = \frac{\partial I_c}{\partial W_B} \cdot \frac{W_B}{V_{CB}} \bigg|_{V_{BE}} \quad (1)$$

$$G_r = \left. \frac{i_b}{v_{ce}} \right|_{v_{be}=0} = \frac{\partial I_B}{\partial W_B} \cdot \frac{\partial W_B}{\partial V_{CB}} \bigg|_{V_{BE}} \quad (2)$$

G_o and G_r result from modulation of the base width by a small ac signal applied between the collector and emitter terminals with base-emitter voltage V_{BE} kept constant. For an n-p-n transistor (for example) with a uniform base doping N_{AA} , under condition of low-injection and negligible recombination in the QNB ($L_n \gg W_B$), the charge-control minority carrier (electron) lifetime τ_n is [8]

$$\tau_n = -\tau_F \frac{G_o}{G_r} \quad (3)$$

where

$$\tau_F = \frac{W_B^2}{2D_n} \quad (4)$$

is the minority-carrier transit time across the QNB and D_n is the electron diffusion coefficient. The minus sign in (3) results from the fact that G_r is negative. G_o and G_r are both proportional to $\exp(qV_{BE}/kT)$ [8]. The minority carrier lifetime in the base can thus be determined by measuring G_o and G_r and calculating τ_F from the base width and base doping.

This method can be extended for use under the condition of high-injection occurring in the p-type base. In high injection [9]

$$N(0) \approx n_i \exp \frac{qV_{BE}}{2kT} \quad (5)$$

Using (5), we obtain for the collector and base currents:

$$I_C \approx \frac{A_{BE} 2qD_n n_i}{W_B} \exp \frac{qV_{BE}}{2kT} \quad (6)$$

$$I_B \approx \frac{A_{BE} qn_i W_B}{2\tau_H} \exp \frac{qV_{BE}}{2kT} \quad (7)$$

where $\tau_H = \tau_n + \tau_p$ is the high-injection lifetime [9].

Using (1) and (2) we obtain:

$$\tau_H = -\frac{1}{2} F \frac{G_o}{G_r} \quad (8)$$

This expression is similar to (3) for the low-injection case except for a factor of 1/2. Note also that G_o and G_r are both proportional to $\exp(qV_{BE}/2kT)$ in high-injection [9]. Equation (6) is valid if $W < L$ and if the recombination current in the emitter is negligible [9]. This will apply to many devices with a wide low-doped base region. If the above conditions do not apply, then a more general solution is required to obtain τ_H [9].

Our treatment was restricted so far to the case for which $L_n > W_B$, resulting in a linear dependence of $N(x)$ on distance within the base. The method, however, is applicable also for $L \sim W_B$. It can be easily shown that for this general case:

$$\frac{G_o}{G_r} = -\frac{\cosh \frac{W_B}{L_n}}{\sinh \frac{W_B}{2L_n}} \quad (9)$$

This expression converges to (3) for $W_B/L_n < 1$. For $W_B/L_n = 1$, the difference between L_n determined from (3) and (9) is only about 8%, i.e., for $W_B \approx L_n$, (3) can be used with only a small error.

Conductances G_o and G_r are due only to changes in the QNB region provided V_{CB} is low enough to make the generation currents in the collector depletion layer negligible. They are independent of the recombination currents in the emitter and in the base-emitter space-charge region, since V_{BE} is held constant. Therefore, G_o and G_r will follow the ideal $\exp(qV_{BE}/kT)$ dependence in low-injection and $\exp(qV_{BE}/2kT)$ dependence in high-injection. This ideal exponential dependence of both G_o and G_r on voltage serves as a very convenient self-consistency measurement check of the method. This check also assures us that series resistance is low enough, mainly in high-injection, to validate the assumptions underlying the method.

B. Determination of the emitter current

Once the base lifetime, τ_n , is measured using the BWM technique, the emitter contribution to the base current can be easily found. The total measured base current I_{BT} for forward-active operation in low-injection is [10,11]

$$I_{BT} = \frac{Q_B}{\tau_n} + \frac{Q_E}{\tau_E} + \frac{Q_{SCR}}{\tau_{SCR}} \quad (10)$$

where Q_B , Q_E and Q_{SCR} are the excess minority carrier charges in the base, emitter, and SCR, respectively; and τ_n , τ_E and τ_{SCR} are the respective charge-control time constants. The SCR recombination current Q_{SCR}/τ_{SCR} can be removed from the measured $I_B - V_{BE}$ characteristic by an appropriate subtraction [10,11]. The remaining base saturation current, I_{B0} is then

$$I_{B0} = \frac{Q_{B0}}{\tau_n} + \frac{Q_{E0}}{\tau_E} \quad (11)$$

where Q_{B0} and Q_{E0} are the minority charges at equilibrium: $Q_B \approx Q_{B0} \exp(qV_{BE}/kT)$, $Q_E \approx Q_{E0} \exp(qV_{BE}/kT)$.

The ideal common emitter current gain is given by [11]

$$h_{FE}(\text{ideal}) = \frac{I_{C0}}{I_{B0}} = \frac{Q_{B0}/\tau_F}{Q_{B0}/\tau_n + Q_{E0}/\tau_E} \quad (12)$$

Solving for Q_{E0}/τ_E and combining with (3), the recombination current occurring within the quasi-neutral emitter is

$$\frac{Q_{E0}}{\tau_E} = \frac{Q_{B0}}{\tau_n} \left(\frac{G_o/G_r}{h_{FE}(\text{ideal})} - 1 \right) \quad (13)$$

Q_{E0}/τ_E is thus found by combining the small-signal ac measurements (G_o/G_r) with dc characteristics of the transistor (h_{FE}).

For a transistor with negligible recombination losses in the emitter, $Q_{E0}/\tau_E \ll Q_{B0}/\tau_B$, note that

$$h_{FE}(\text{ideal}) = \frac{Q_{B0}/\tau_F}{Q_{B0}/\tau_n} = \frac{\tau_n}{\tau_F} \quad (14)$$

in accord with conventional transistor theory. The minority carrier base lifetime is then simply $\tau_n = \tau_F h_{FE}(\text{ideal})$. This provides a method for finding τ_n that is an alternative to that based on (3). But finding $h_{FE}(\text{ideal})$ requires subtraction of the SCR current component from I_{BT} . This subtraction is subject to errors depending on magnitude and voltage dependence of components in (10). Thus, the method based on (3) is the more accurate method.

The current due to recombination in the n^+ -collector quasi-neutral region can be measured by reversing the roles of collector and emitter and using (13) again.

III. SMALL-SIGNAL ADMITTANCE METHOD

A. Minority carrier lifetime

The BWM technique described in the previous section is directly applicable for TJ cells, since the TJ cell is actually a transistor-like structure. It cannot, however, be applied directly to some other cells with a narrow base or emitter region which are diode structures only, without a collector. In these cases, a different measurement method has to be used. In this section we present a method applicable to all cells with a narrow base or emitter region.

Fig. 2 shows two different cells with either narrow base, BSF cell--Fig. 2(a), or narrow emitter, HLE cell--Fig. 2(b). In both cases a high-low junction exists in the narrow region of the cell, and is characterized by an effective surface recombination velocity S_{eff} for the minority carriers. Fig. 2(c) shows the basic structure of the IBC, FSF, and TJ cells [2,3,4]. In this structure both the n^+ -region and the p^+ contacts to the base are on the bottom nonilluminated surface. The p^+ regions cover only a small portion ($\sim 10\%$) of the total area. The top illuminated surface is left floating and is characterized by the surface recombination velocity S for the IBC cell. If a p^+ - p junction (FSF cell) or a n^+ - p junction (TJ cell) is used on the top surface, then the surface region can be characterized by an effective surface recombination velocity S_{eff} . Due to structural similarities which are evident in Fig. 2, the cells shown in Fig. 2 will all have a similar treatment for the narrow region small-signal admittance. The treatment shown below is done for a n^+ - p - p^+ BSF cell as an illustration.

Consider, for example, a n^+ - p - p^+ BSF cell, Fig. 3, with a base width W_p and minority carrier base lifetime τ_n corresponding to the diffusion length $L_n = \sqrt{D_n \tau_n}$. The electron current at the high-low junction ($x = W_p$) is [12]

$$J_n(W_p) = qS_{\text{eff}}N(W_p) \quad (15)$$

where S_{eff} is the effective surface recombination velocity for electrons at $x = W_p$. By solving a continuity equation [13] in low-injection for an ac signal superimposed on a steady forward bias, and using boundary condition (15), we can derive the expressions for the small-signal quasi-neutral base capacitance C_{QNB} and conductance G_{QNB} valid for a low frequency signal with $\omega\tau_n \ll 1$:

$$C_{\text{QNB}} = \frac{q}{kT} \frac{AqD_n n_i^2}{2N_{AA}L_n} \left[\frac{\frac{W_p D_n}{L_n} - \frac{L_n W_p S_{\text{eff}}^2}{D_n} - S_{\text{eff}}L_n}{2 \sinh^2 \left(\frac{W_p}{L_n} \left(\frac{D_n}{L_n} \coth \frac{W_p}{L_n} + S_{\text{eff}} \right) \right)^2} + \tau_n \frac{\frac{D_n}{L_n} + S_{\text{eff}} \coth \frac{W_p}{L_n}}{\frac{D_n}{L_n} \coth \frac{W_p}{L_n} + S_{\text{eff}}} \right] \left[\exp\left(\frac{qV}{kT}\right) - 1 \right] \quad (16)$$

$$G_{QNB} = \frac{q}{kT} \frac{AqD_n n_i^2}{L_n N_{AA}} \left[\frac{\frac{D_n}{L_n} + S_{eff} \coth \frac{W_p}{L_n}}{\frac{D_n}{L_n} \coth \frac{W_p}{L_n} + S_{eff}} \right] \left[\exp\left(\frac{qV}{kT}\right) - 1 \right] \quad (17)$$

The expression for C_{QNB} can be simplified for the following conditions:

$$W_p/L_n \approx 1 \quad (18)$$

$$S_{eff} \sim 100 \text{ cm/sec} \quad (19)$$

These conditions are not restrictive for an actual device, with good performance and a narrow base. Under these conditions the first term inside of the parentheses in (16) can be neglected and combining (16) and (17) yields

$$\tau_n \approx 2 \frac{C_{QNB}}{G_{QNB}} \quad (20)$$

This expression for τ_n is similar to that valid for $W_p \gg L_n$ [14].

To determine C_{QNB} , we measure the capacitance at two frequencies: C_{LF} at $\omega\tau_n \ll 1$ and C_{HF} at $\omega\tau_n \gg 1$ to obtain [14]:

$$C_{QN} \approx C_{QNB} = C_{LF} - C_{HF} \quad (21)$$

This results because the n^+ base and p^+ emitter regions are much narrower than W_p and the amount of minority-carrier charge in these regions will be negligible compared to that in the wide base, giving $C_{QN} \approx C_{QNB}$.

To determine G_{QNB} , we measure a total conductance G at the terminals which consists of a few components [10]:

$$G = G_{QNE} + G_{QNB} + G_{SCR} \quad (22)$$

where G_{SCR} is the conductance from the bulk and surface base-emitter space-

charge region, and G_{QNE} designates the contribution of the emitter quasi-neutral region. G_{SCR} can be eliminated from the data by a subtraction technique to give

$$G_{QN} = G_{QNE} + G_{QNB} \quad (23)$$

If $G_{QNE} < G_{QNB}$, then $G_{QN} \approx G_{QNB}$ and τ_n can be then determined from (20). This condition will apply for many devices made on high resistivity substrates ($\sim 1-10 \Omega\text{cm}$) with wide base. If G_{QNE} is not negligible, an independent method is required to determine it before we can calculate τ_n from (20).

One simple method involves thinning the base region to assure $W_p < L_n$ and providing an ohmic contact to the base instead of a high-low junction.

The narrow-base current can then be calculated using a conventional formula and subtracted from the total measured diode current to give the emitter current or G_{QNE} .

For the case of the HLE cell of Fig. 4, we note that the n-type emitter is the narrow region of interest, with a minority carrier (hole) lifetime τ_p . To determine τ_p , we proceed as follows: we measure the electron diffusion length in a wide base by an X-ray technique, [15] or some other suitable method, and calculate C_{QNB} and G_{QNB} . These two values are then subtracted from measured C_{QN} , G_{QN} to give C_{QNE} , G_{QNE} , and

$$\tau_p = 2 \frac{C_{QNE}}{G_{QNE}} \quad (24)$$

The small-signal admittance method can be also applied for conditions of high-injection in the narrow region. Following the derivation of (16) and (17) for $P \approx N$ we obtain for high-injection lifetime:

$$\tau_H \approx 4 \frac{C_{QNB}}{G_{QNB}} \quad (25)$$

Equation (25) is similar to (20) except for a factor of two which results because the electron diffusion constant D_n is doubled in high-injection [9]. This

equation is valid for the common case of a negligible emitter current and $W_p/L_n < 1$ [9].

A more complicated, but accurate way to determine both G_{QNE} and τ_n in the BSF cell and other structures of Fig. 2 is to use the BWM technique described in the previous section. In order to do that, we have to first create a modified transistor-like structure from the actual cells. This can be done quite easily as shown in Fig. 5. For the case of p^+-n-n^+ BSF cell, the n^+ region on the back can be etched-off from about 90% of the area and Al can be evaporated on n-type base to create a Schottky barrier collector; the remains of n^+ BSF region serve as a contact to the base, see Fig. 5(a). This procedure can be also used for n^+-n-p HLE cell from Fig. 2(b). In the case of a n^+-p-p^+ BSF cell, Fig. 5(b), an n^+ -diffusion is performed simultaneously from both sides of the p-type substrate. Emitter can then be a mesa-type and the p^+ region for the base contact over about 10% of the area can be done by a standard method used to create a BSF region. Schottky barrier collector using Al cannot be used on p-type substrates because a metal-semiconductor junction on p-type substrates is usually very poor. Similar transistor-like structures can be made also from the FSF and IBC cells.

B. Determination of S (S_{eff})

Once the minority carrier lifetime in the narrow region is found, then $S(S_{eff})$ can be determined either from small-signal quasi-neutral conductance or capacitance of this region. The capacitance is, however, a much better choice because of reasons discussed earlier (see also Section VI C). This procedure is strictly valid only if $S(S_{eff})$ is constant, independent of applied voltage. This condition will be satisfied at low-injection for BSF, FSF, and HLE cells [12], but may not be satisfied for TJ and IBC cells. If $S(S_{eff})$ is not constant, then using (16) or (17) will result in an average value.

BSF and for n^+-n-p HLE cell shown in Figs. 3 and 4, which also show distribution of minority carriers in these cells. The analysis is based on independent measurement of τ_n by one of the three methods described before. The effective surface recombination velocity is determined from a small-signal capacitance using (16). This allows us to calculate $N(x)$ [9] and the recombination currents in the p and p^+ portions of the base. The SCR current, I_{SCR} is determined graphically [10], the recombination current in the emitter region can be obtained by the BWM technique or using the dc method. The sum of all currents recombining within the cell has to be equal to the total measured dark current I . This serves as a self-consistency check of the analysis. Another check for dark current I results from measurement of the short circuit current I_{SC} and open-circuit voltage

$$V_{OC} \text{ through } V_{OC} = \frac{kT}{q} \ln \frac{I_{SC}}{I_0} \quad (29)$$

where I_0 is the dark saturation current corresponding to I .

The analysis of the n^+-n-p HLE solar cell, Fig. 4, starts with the wide p -type base. The electron diffusion length is measured by the X-ray method [15], and the base dark current and small-signal quasi neutral capacitance [14] are calculated. The hole lifetime τ_p and S_{eff} at the n^+-n junction are then evaluated as was described in Section 3A, 3B. The rest of the analysis follows the BSF case above.

For high-injection conditions in the low-doped part of the base in the BSF cell or low-doped part of the emitter in the HLE cell, we again measure τ_H in these regions as described in Sections IIA, IIIA, and IV. The value of S_{eff} increases with applied voltage in high-injection [12]. The analysis has to be then made for a certain voltage, for example $V = V_{OC}$ corresponding to a certain illumination level; S_{eff} can then be calculated based on its low-injection value provided that the voltage drop in the quasi neutral low-doped portion of the base is negligible [12]. The high-doped regions of the cell will remain in low-injection. The analysis then follows the low-injection case.

IV. MINORITY CARRIER BASE LIFETIME FROM DC CURRENT MEASUREMENTS

An alternative method, suitable for TJ cells or the transistor-like structures, Fig. 5, is proposed. This method requires only dc current measurements on two related structures. The first structure is the actual TJ cell (for example), Fig. 6(a). The other structure, Fig. 6(b), is created by removing the n^+ layer on one side of the cell and replacing it by an ohmic contact.

We will neglect the contribution of the SCR, which can be removed by an experimental procedure [10]. The base saturation current of the transistor-like structure is given by (11), the collector saturation current is $I_{CO} = Q_{BO}/\tau_F$. The saturation current I_0 of the narrow-base diode from Fig. 6(b) is

$$I_0 = \frac{Q_{BO}}{\tau_F} + \frac{Q_{EO}}{\tau_E} \quad (26)$$

Combining (11) and (26), we obtain for τ_n :

$$\tau_n = \frac{I_{CO}}{I_{BO} + I_{CO} - I_0} \tau_F \quad (27)$$

In (27) all currents are measured and $\tau_F = W_B^2/2D_n$ is calculated.

The disadvantage of this procedure is that the separation of SCR current components [10] is subject to errors. This will limit the applicability of this method, mainly if $I_{BO} + I_{CO} \sim I_0$, which is the case when the emitter dominates the current. The recombination current in the emitter is simply found from (26)

$$\frac{Q_{EO}}{\tau_E} = I_0 - I_{CO} \quad (28)$$

An expression similar to (28) can be derived for τ_H , differing only by a factor of 1/2 on the right side of (28). Note that in this case the currents in (27) are proportional to $\exp(qV/2kT)$. Also note that a highly-doped emitter will remain in low-injection.

V. ANALYSIS OF DARK CURRENTS IN THE CELL

The analysis of dark currents in the cell is demonstrated for a $n^+ - p - p^+$

BSF and for $n^+ - n - p$ HLE cell shown in Figs. 3 and 4, which also show distribution of minority carriers in these cells. The analysis is based on independent measurement of τ_n by one of the three methods described before. The effective surface recombination velocity is determined from a small-signal capacitance using (16). This allows us to calculate $N(x)$ [9] and the recombination currents in the p and p^+ portions of the base. The SCR current, I_{SCR} is determined graphically [10], the recombination current in the emitter region can be obtained by the BWM technique or using the dc method. The sum of all currents recombining within the cell has to be equal to the total measured dark current I . This serves as a self-consistency check of the analysis. Another check for dark current I results from measurement of the short circuit current I_{SC} and open-circuit voltage

$$V_{OC} \text{ through } V_{OC} = \frac{kT}{q} \ln \frac{I_{SC}}{I_0} \quad (29)$$

where I_0 is the dark saturation current corresponding to I .

The analysis of the $n^+ - n - p$ HLE solar cell, Fig. 4, starts with the wide p -type base. The electron diffusion length is measured by the X-ray method [15], and the base dark current and small-signal quasi neutral capacitance [14] are calculated. The hole lifetime τ_p and S_{eff} at the $n^+ - n$ junction are then evaluated as was described in Section 3A, 3B. The rest of the analysis follows the BSF case above.

For high-injection conditions in the low-doped part of the base in the BSF cell or low-doped part of the emitter in the HLE cell, we again measure τ_H in these regions as described in Sections IIA, IIIA, and IV. The value of S_{eff} increases with applied voltage in high-injection [12]. The analysis has to be then made for a certain voltage, for example $V = V_{OC}$ corresponding to a certain illumination level; S_{eff} can then be calculated based on its low-injection value provided that the voltage drop in the quasi neutral low-doped portion of the base is negligible [12]. The high-doped regions of the cell will remain in low-injection. The analysis then follows the low-injection case.

VI. ILLUSTRATIVE EXAMPLES

To demonstrate the various methods for analysis of the cells, we have done measurements on three different types of cells. The complete analysis for these devices is summarized in this section.

A. $n^+ - p - n^+$ TJ cell

This cell is fabricated on $6 \Omega\text{cm}(N_{AA} \approx 2 \times 10^{15} \text{ cm}^{-3})$ p-type substrate. The top illuminated n^+ -layer is about $0.3 \mu\text{m}$ deep, the surface is texturized and covered by an AR coating. The bottom n^+ -layer is about $0.7 \mu\text{m}$ deep. The base width is $160 \mu\text{m}$. Measured performance at one-sun AMO illumination at 25°C with top junction floating was: $V_{OC} = 577 \text{ mV}$, $J_{SC} = 30.5 \text{ mA/cm}^2$.

An ohmic contact to the top junction was provided after removing the AR coating. The measured dc and ac characteristics for this transistor-like structure are shown in Fig. 7. The data were taken with the bottom n^+ -region serving as an emitter. The BWM conductances were measured at 2kHz using a Wayne-Kerr B224 admittance bridge. The dependencies of I_c , G_o and G_r are proportional to $\exp(q(V_{BE}/kT))$, which confirms that the BWM effects alone are responsible for G_o and G_r . For $V_{BE} < 0.4 \text{ V}$ the leakage of the base-collector junction may dominate G_o and G_r , in some devices, giving almost constant values independent on V_{BE} . These values can be then subtracted from the measured G_o and G_r to extend the range of the exponential dependence on V_{BE} .

From Fig. 7 we have for the low-injection case: $G_o/G_r \approx \tau_n/\tau_F \approx 13$; $h_{FE}(\text{ideal}) \approx 13$. Using (4) and (13) we then obtain: $\tau_n \approx 50 \mu\text{sec}$ ($L_n \approx 410 \mu\text{m}$) and $Q_{EO}/\tau_E \approx 0$, i.e. $Q_{EO}/\tau_E \ll Q_{BO}/\tau_n$. Examination of the $I_B - V_{BE}$ dependence in Fig. 7 shows that the base will be in high-injection for $V_{BE} > 0.6 \text{ V}$. The base current follows an $\exp(q(V_{BE}/2kT))$ dependence in accord with (7), provided that the effects of series resistance R_s are negligible. Because $Q_E/\tau_E \ll Q_B/\tau_B$, τ_H can be found from (7): $\tau_H \approx 200 \mu\text{sec}$. Further analysis of the cell, described in Section V, with the top junction left floating leads to determination

of recombination losses in the top n^+ -layer and in the p-base region. A summary of all results obtained for this cell are shown below. The dark currents are given as a fraction of the total dark current density $J = 3 \times 10^{12}$ A/cm² measured at $V = V_{OC} = 577$ mV. The results are:

$$\begin{aligned}\tau_n &\approx 50 \text{ } \mu\text{sec} \\ L_n &\approx 410 \text{ } \mu\text{m} \\ \tau_H &\approx 200 \text{ } \mu\text{sec} \\ S_{\text{eff}} &\approx 350 \text{ cm/sec} \\ J_E &\approx 0.52 \text{ J} \\ J_B &\approx 0.42 \text{ J} \\ J_{\text{SCR}} &\approx 0.06 \text{ J} \\ J_C &\ll J_B\end{aligned}$$

The measurements of G_o and G_r in high-injection were not possible, because the collector current in this region exceeded the maximum allowable current of the bridge for the large area (4 cm²) device used.

B. n^+ -p- p^+ BSF cell

This cell was fabricated on $1.5 \text{ } \Omega\text{cm}(N_{AA} = 1 \times 10^{16} \text{ cm}^{-3})$ substrate. The n^+ -region is about 0.3 μm deep, sheet resistance is about 55 Ω/square . The BSF high-low junction was created by an Al-paste alloying [16]. The cell was 220 μm thick and has a Ta_2O_5 AR coating on the top. The parameters measured at one-sun (AM0, 25°C) illumination are: $V_{OC} = 617$ mV, $J_{SC} = 38 \text{ mA/cm}^2$.

The values for τ_n and Q_E/τ_E were measured by the BWM method on a modified structure shown in Fig. 5(b). The recombination currents in the p and p^+ -region were then measured on the actual BSF cell, S_{eff} was determined from the dark base current using (17). The inspection of the dark I-V characteristic showed that this cell is in low-injection at one-sun illumination level.

The results are:

$$\begin{aligned}\tau_n &\approx 120 \text{ } \mu\text{sec} \\ L_n &\approx 600 \text{ } \mu\text{m}\end{aligned}$$

$$S_{\text{eff}} \approx 380 \text{ cm/sec}$$

$$J_E \approx 0.4 \text{ J}$$

$$J_B \approx 0.15 \text{ J}$$

$$J_{B^+} \approx 0.4 \text{ J}$$

$$J_{\text{SCR}} \approx 0.05 \text{ J}$$

where $J \approx 3.8 \times 10^{-2} \text{ A/cm}^2$ is the measured total dark current density at $V = V_{\text{OC}} = 617 \text{ mV}$.

C. p^+-n-n^+ BSF cell

This cell was fabricated on about $7 \Omega\text{cm}$ ($N_{\text{DD}} \approx 6 \times 10^{14} \text{ cm}^{-3}$) float zone silicon wafer. The p^+ -emitter is about $0.25 \mu\text{m}$ deep. The n^+ -layer on the back is about $1 \mu\text{m}$ deep. Thickness of the cell was $320 \mu\text{m}$. The details of the fabrication process are in Ref. 17.

The one-sun (AM0, 25°C) data were: $V_{\text{OC}} = 605 \text{ mV}$, $J_{\text{SC}} = 39 \text{ mA/cm}^2$.

We will demonstrate here the use of the small-signal admittance method, described in Section III. Fig. 8 shows the measured dependencies of C and G on voltage V. The low frequency capacitance C_{LF} and conductance G_{LF} were measured at 500 Hz, C_{HF} was measured at 100 kHz using a Wayne-Kerr B224 bridge. Subtraction of these two dependencies yields $C_{\text{QN}} = C_{\text{LF}} - C_{\text{HF}}$ which follows the $\exp(qV/kT)$ dependence for about 2 decades. Similar procedure is used to extract G_{QN} [10].

Using a simple test described in Section IIIA we found that $G_{\text{QNE}} \ll G_{\text{QNB}}$.

The hole lifetime is then obtained from (20) and S_{eff} from (16):

$\tau_p \approx 200 \mu\text{sec}$, $S_{\text{eff}} \approx 80 \text{ cm/sec}$. Using these values for τ_p and S_{eff} , we find that the first term in the parentheses in (16) is indeed small compared to the second term, which then validates (20). These results are consistent with measurements on p^+-n-n^+ cells reported by others [17, 18].

The advantages of calculating S_{eff} from C_{QN} (instead of from) G_{QN} are clearly evident in Fig. 8. The measured C_{LF} characteristic is almost an ideal one; the correction by subtracting C_{HF} is very small. On the other hand, the correction due to G_{SCR} to obtain G_{QN} is very substantial.

For $V > 0.6$ Volts the n-region of the base is in high-injection as shown by $G_{QN} \propto \exp(qV/2kT)$ for $V > 0.6$ Volts, which was obtained by subtracting G_{SCR} from G . The C_{LF} dependence on voltage for $V > 0.6$ Volts is also expected to be proportional to $\exp(qV/2kT)$. The C_{LF} in Fig. 8 shows, however, an excessive bending due to the contact resistance between the cell and the measurement probes. The C_{LF} was measured using only 2 probes, however 4 probe measurements are necessary to eliminate the contact resistance. Such capacitance measurements are possible. The series resistance R_s will have a negligible effect on C_{LF} [19]. The $G-V$ curve was taken using 3 probe arrangement, effectively suppressing R_s for $V < 0.7$ Volts. Due to the difficulty with the high-injection value of C_{LF} , τ_H could not be found using the admittance method. The estimate of τ_H follows from recognizing that $G_{QNE} < G_{QNB}$ at $V \approx 600$ mV, $W_n < L_p$ and S_{eff} is small. This will result in a nearly flat profile of $P(x)$ in the n-base, and $I_B = Aq n_i W_n / \tau_H [\exp(qV/2kT)]$, which yields $\tau_H = 320$ μ sec. The fact that $G_{QN} \propto \exp(qV/2kT)$ indicates that the low-doped portion of the base dominates the dark current at $V = V_{OC} = 605$ mV.

The results for this cell are summarized below:

$$\tau_p \approx 200 \mu\text{sec};$$

$$L_p \approx 500 \mu\text{m}$$

$$\tau_H \approx 320 \mu\text{sec}$$

$$S_{eff} \approx 80 \text{ cm/sec (low injection)}$$

$$J_B \approx 0.8 \text{ J}$$

$$J_{SCR} \approx 0.2 \text{ J}$$

$$J_E \ll J_B$$

$$J_{B+} \ll J_B$$

where $J = 2.9 \times 10^{-2} \text{ A/cm}^2$ is the measured total dark current density at $V = V_{OC} = 605$ mV.

VII. SUMMARY

This work presented new methods for determining the minority-carrier lifetime in narrow regions of solar cells. This leads to a simple analysis which results in determination of recombination currents in each region of the cell. Such an analysis was demonstrated for three different types of cells. The basewidth-modulation (BWM) and the small-signal admittance method involve measurements using very accurate admittance bridges. The accuracy of the BWM method depends on the accuracy with which τ_F can be determined from (4). This can be done very accurately for wide regions with a uniform doping. No other material parameter is required to obtain the lifetime from (3) or (8). Additional reasons for the high accuracy of this method are that it is independent of the currents not associated with the region in which the lifetime is measured and that it has a self-consistency check. The accuracy of the BWM method is estimated to be about $\pm 5\%$.

The lifetime measured by the small-signal admittance method, as determined from (20) or (25), does not require knowledge of any material parameter of the cell. The high frequency capacitance C_{HF} can be measured at relatively small frequencies ($\sim 100\text{kHz}$) because of very long lifetimes in the measured cells. This allows measurements on large area devices ($\sim 1\text{cm}^2$) using commercially available bridges. This method also has a self-consistency check. The total accuracy of this method is estimated to be about $\pm 10\%$. The dc current method is less accurate than the previous two methods, mainly if the emitter current is dominant.

The determination of lifetimes and recombination currents in the cell allows identification of regions that limit cell efficiency. It will also allow monitoring of fabrication steps and material properties.

ACKNOWLEDGEMENT

The author thanks F. A. Lindholm for discussions concerning this work and J. A. Mazer for his comments. The author also thanks J. G. Fossum and J. Minahan for supplying some of the devices used for the measurements.

REFERENCES

1. J. Mandelkorn and J. H. Lamneck, Jr., "Simplified Fabrication of Back Surface Electric Field Silicon Cells and Novel Characteristics of Such Cells," in Record of 9th IEEE Photovoltaic Specialists Conf. pp. 66-72, 1972.
2. M. D. Lammert and R. J. Schwartz, "The Interdigitated Back Contact Solar Cell: A Silicon Solar Cell for Use in Concentrated Sunlight," IEEE Trans. Electron Devices, Vol. ED-24, pp. 337-342, April 1977.
3. O. von Roos and B. Anspaugh, "The front surface field solar cell, a new concept," Record of 13th IEEE Photovoltaic Specialists Conf., pp. 1119-1120, 1978.
4. S. Y. Chiang, B. G. Carbajal, and G. F. Wakefield, "Thin Tandem Junction Solar Cell," in Record of 13th IEEE Photovoltaic Specialists Conf. 78CH1319-3ED, 1978.
5. F. A. Lindholm, A. Neugroschel, S. C. Pao, J. G. Fossum, and C. T. Sah, "Design considerations for silicon HLE solar cells," in Record of 13th IEEE Photovoltaic Specialists Conf., pp. 1300-1305, 1978.
6. W. M. Bullis, NBS Technical Note 465, Nov. 1968.
7. J. H. Reynolds and A. Meulenber, Jr., "Measurement of diffusion length in solar cells", J. Appl. Phys., Vol. 45, pp. 2582-2592, June 1974.
8. M. S. Birrittella, A. Neugroschel, and F. A. Lindholm, "Determination of the Minority-Carrier Base Lifetime of Junction Transistors by Measurements of Basewidth-Modulation," IEEE Trans. Electron Devices, Vol. ED-26, pp. 1361-1363, Sept. 1979.
9. A. K. Jonscher, Principles of Semiconductor Device Operation, New York: Willey, 1960.
10. A. Neugroschel, F. A. Lindholm, C. T. Sah, "A method for determining the emitter and base lifetimes in p-n junction diodes," IEEE Trans. Electron Devices, Vol. ED-24, pp. 662-671, June 1977.
11. A. Neugroschel, F. A. Lindholm, C. T. Sah, "Experimental determination of the stored charge and effective lifetime in the emitter of junction transistors," IEEE Trans. Electron Devices, Vol. ED-24, pp. 1362-1365, Dec. 1977.
12. J. R. Hauser and P. M. Dunbar, "Minority carrier reflecting properties of semiconductor high-low junctions," Solid-State Electron., Vol. 18, pp. 715-716, July 1975.
13. W. Shockley, "The theory of p-n junctions in semiconductors and p-n junction transistors," Bell Syst. Tech. J., Vol. 28, pp. 435-489, July 1949.
14. A. Neugroschel, P. J. Chen, S. C. Pao, and F. A. Lindholm, "Diffusion length and lifetime determination in p-n junction solar cells and diodes by capacitance measurements," IEEE Trans. Electron Devices, Vol. ED-25, pp. 485-490, April 1978.
15. W. Rosenzweig, "Diffusion length measurement by means of ionizing radiation," Bell Syst. Tech. J., Vol. 41, pp. 1573-1588, Sept. 1962.

16. C. F. Gay, "Thin silicon solar cell performance characteristics", Record of 13th IEEE Photovoltaic Specialists Conf., pp. 444-449, 1978.
17. J. G. Fossum, R. D. Nasby, and E. L. Burgess, "Development of High-Efficiency p^+n-n^+ Back-Surface-Field Silicon Solar Cells", in Record of 13th IEEE Photovoltaic Specialists Conf., pp. 1294-1299, 1978.
18. J. G. Fossum, R. D. Nasby, and S. C. Pao, "Physics Underlying the Performance of Back-Surface-Field Solar Cells," to be published in IEEE Trans. Electron Devices, April 1980.
19. P. J. Chen, S. C. Pao, A. Neugroschel, F. A. Lindholm, "Experimental determination of series resistance of p-n junction diodes and solar cells," IEEE Trans. Electron Devices, Vol. ED-25, pp. 386-388, March 1978.

FIGURE CAPTIONS

- Fig. 1 Basewidth-modulation effects in n^+p-n^+ TJ cell.
- Fig. 2 Schematic illustration of (a) n^+p-p^+ BSF solar cell; (b) n^+-n-p HLE solar cell; and (c) the basic structure of the TJ (with floating front surface), FSF, and IBC cells.
- Fig. 3 (a) Schematic diagram of a n^+p-p^+ BSF cell; (b) Qualitative sketches of minority carrier distribution in dark.
- Fig. 4 (a) Schematic diagram of a n^+-n-p HLE cell; (b) Qualitative sketches of minority carrier distribution in dark.
- Fig. 5 (a) p^+-n-n^+ BSF cell and a modified transistor-like structure with a Schottky barrier collector, (b) n^+p-p^+ BSF cell and a modified n^+p-n^+ transistor-like structure.
- Fig. 6 (a) Schematic diagram of TJ cell; (b) Schematic diagram of a n^+-p diode structure obtained from the TJ cell.
- Fig. 7 Measured I_C , I_{BT} , G_0 , and G_r versus forward bias V_{BE} for n^+p-n^+ TJ cell. The base quasi-neutral current components are indicated by the dashed lines, I_{SCR} is the extrapolated SCR current component.
- Fig. 8 Measured capacitance and conductance versus forward bias V for p^+-n-n^+ BSF cell. The quasi-neutral components are shown by the dashed lines, G_{SCR} is the extrapolated SCR conductance component.

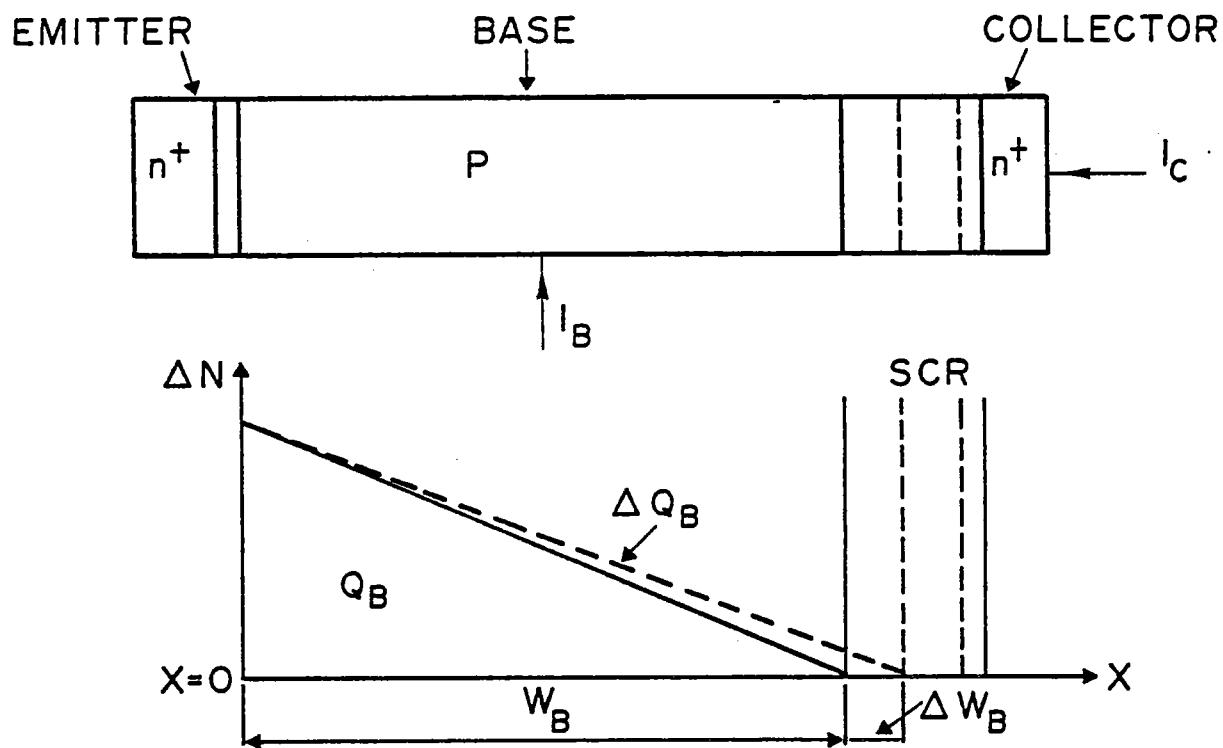
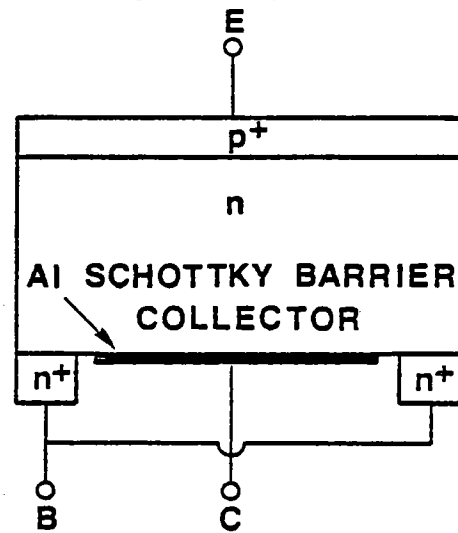
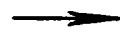
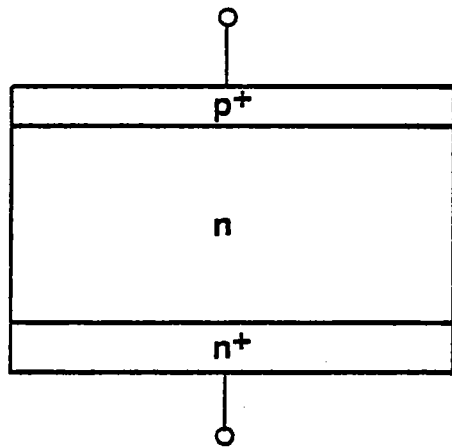
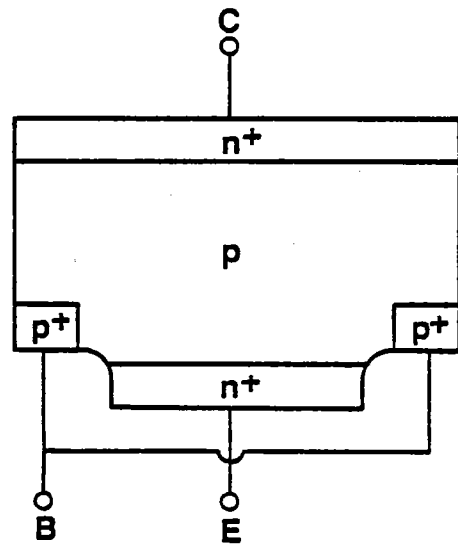
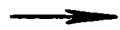
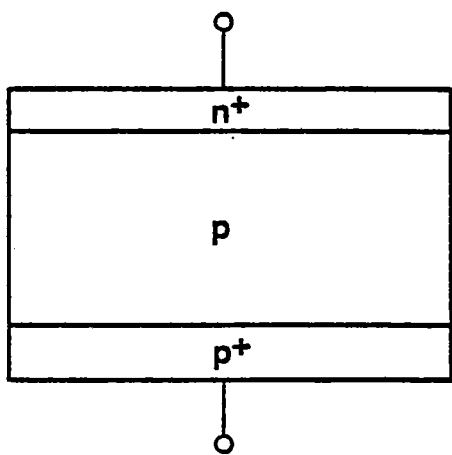


Figure 1

$p^+ - n - n^+$ BSF cell



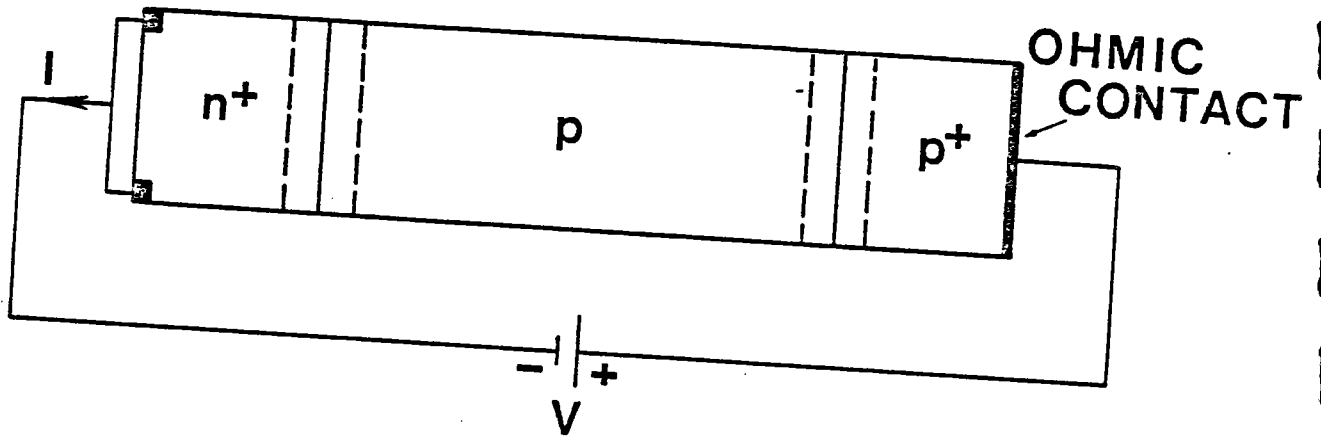
(a)



(b)

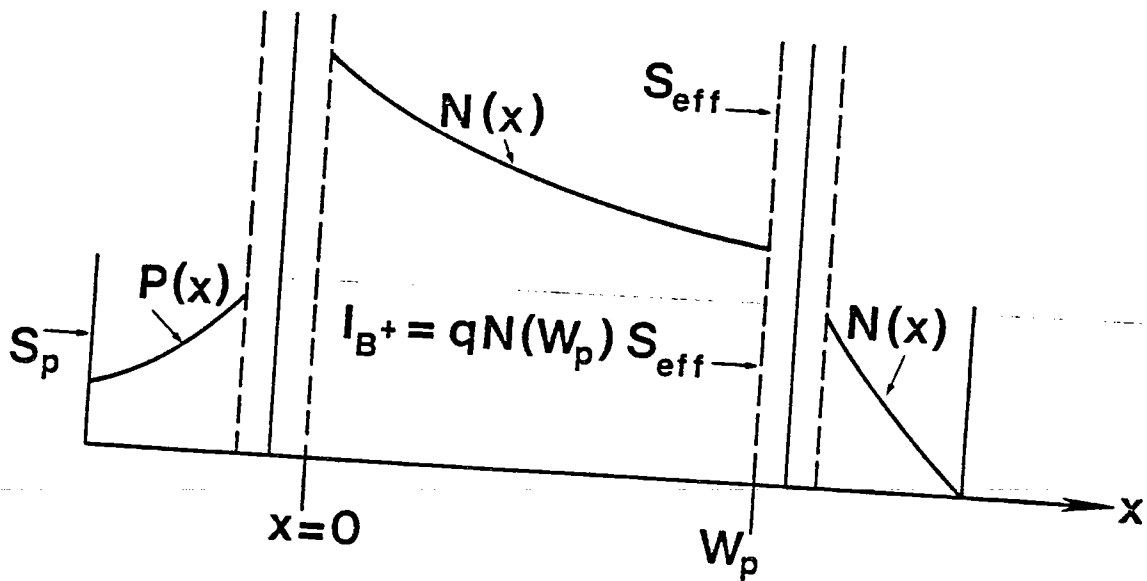
$n^+ - p - p^+$ BSF cell

Figure 2



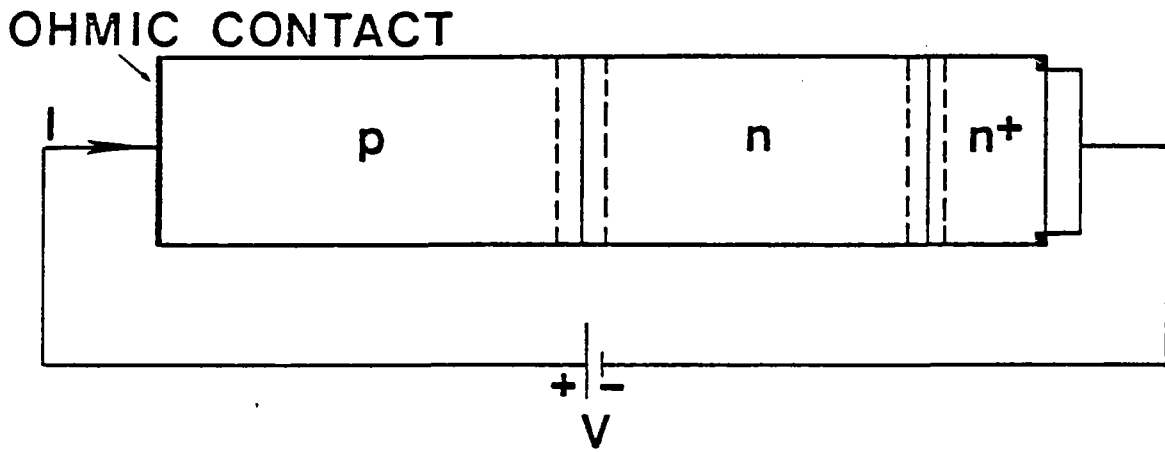
(a)

$$I = I_E + I_{SCR} + \frac{1}{\tau_n} \int_0^{W_p} N(x) dx + I_{B^+}$$



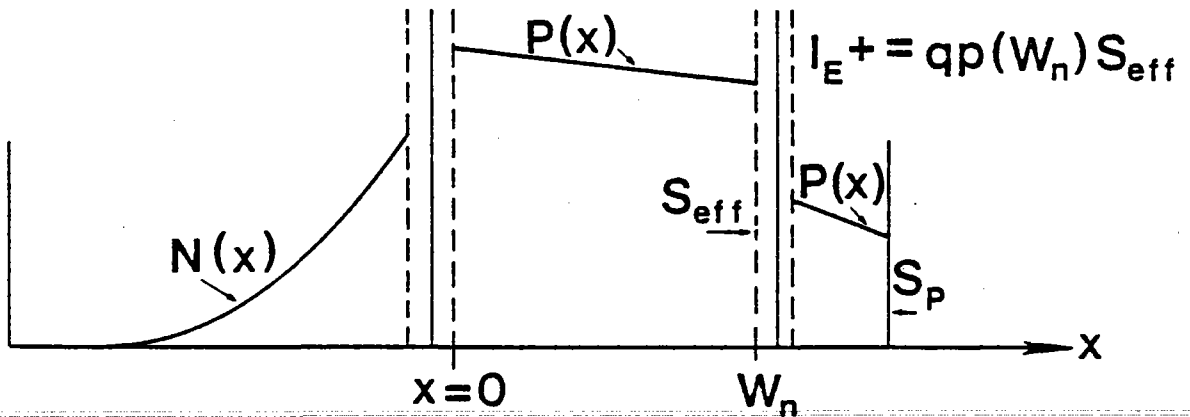
(b)

Figure 3



(a)

$$I = I_B + I_{SCR} + \frac{1}{\tau_p} \int_0^{W_n} P(x) dx + I_E$$



(b)

Figure 4

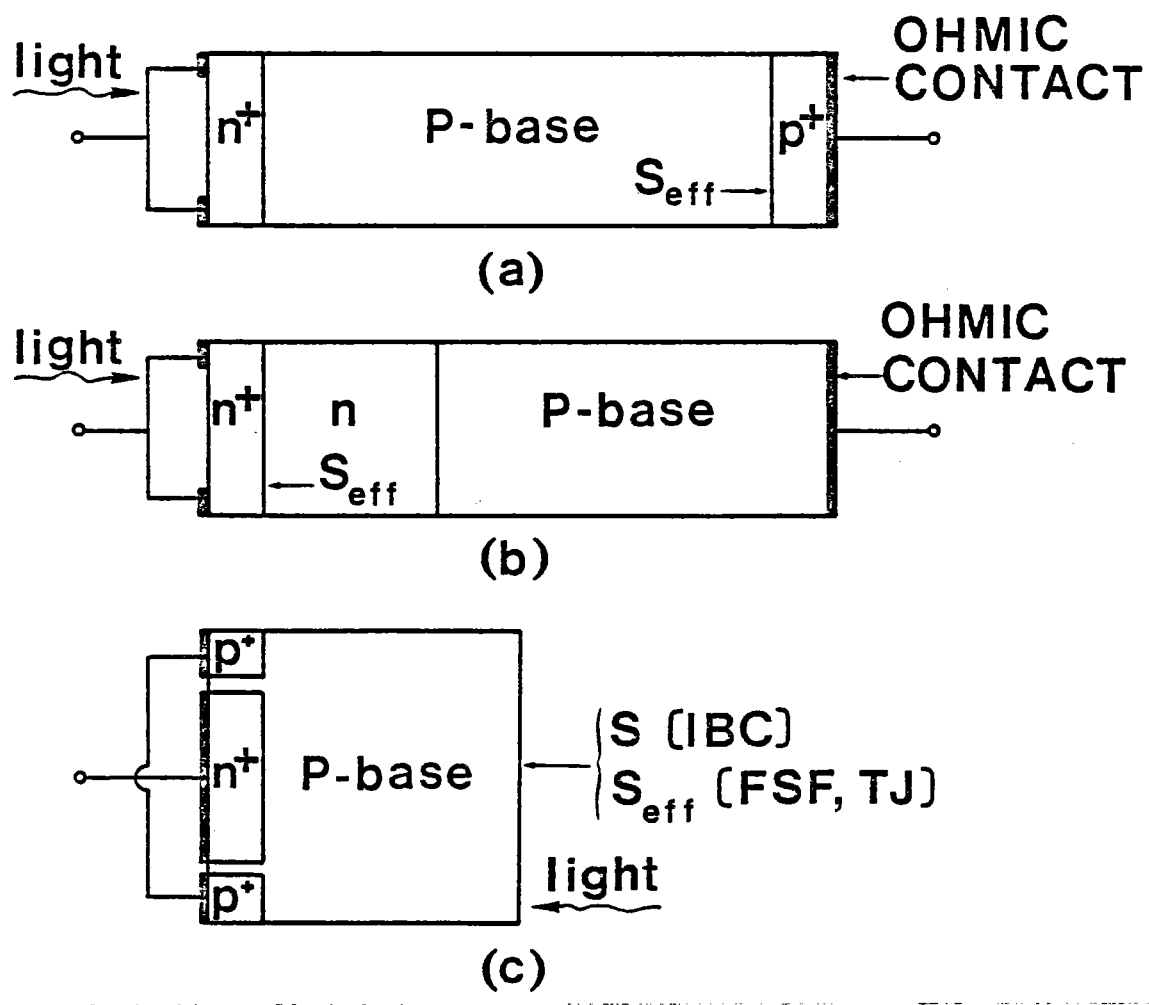
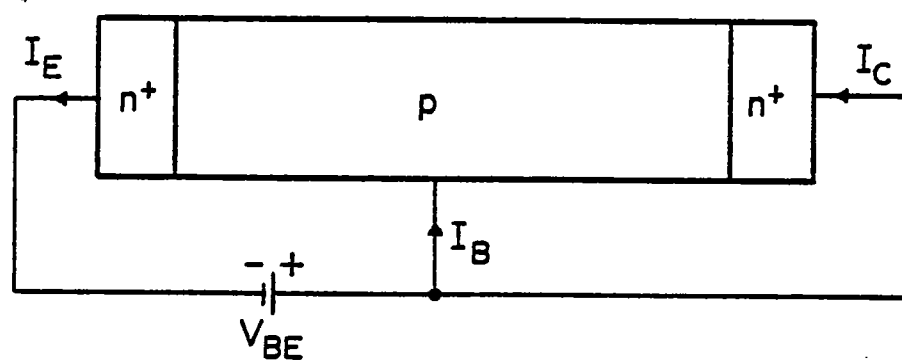
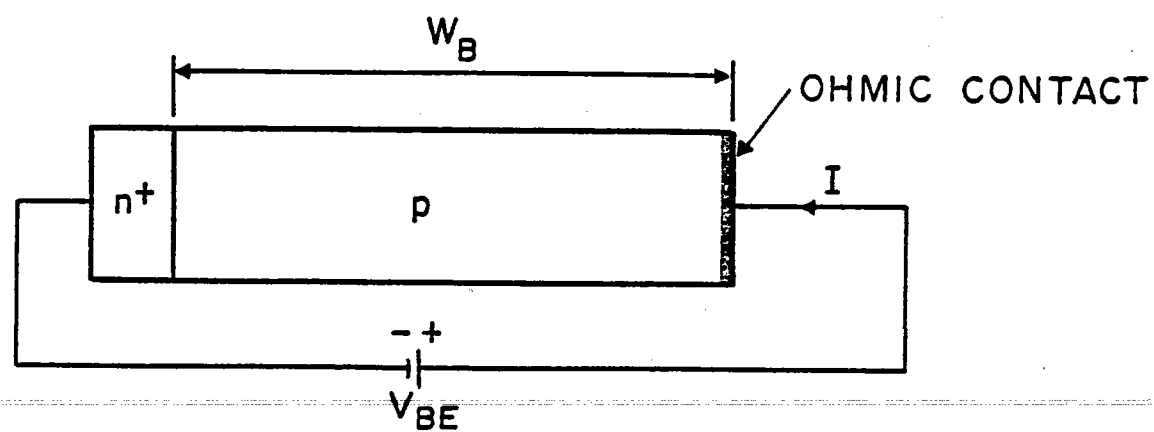


Figure 5



(a)



(b)

Figure 6

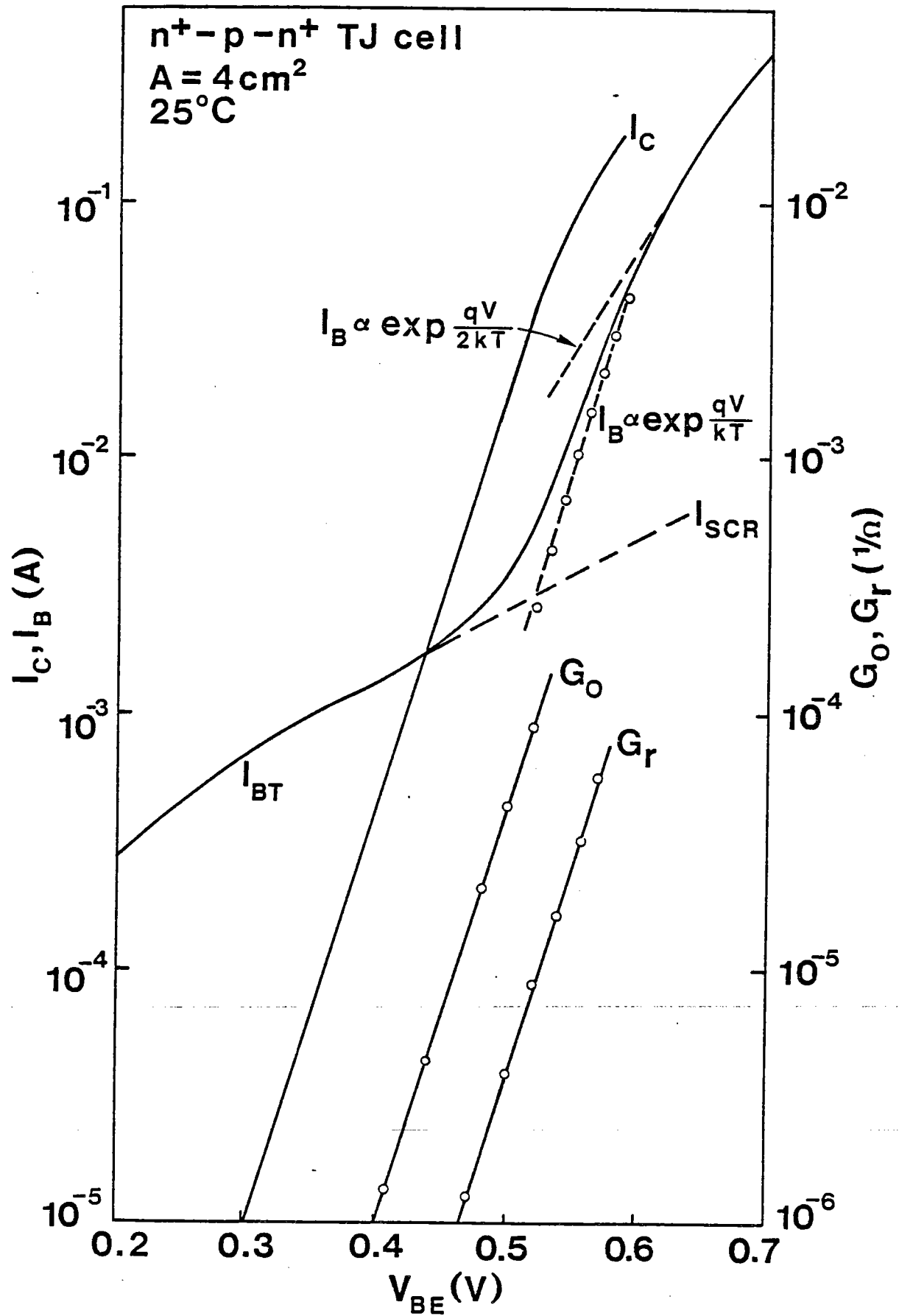


Figure 7

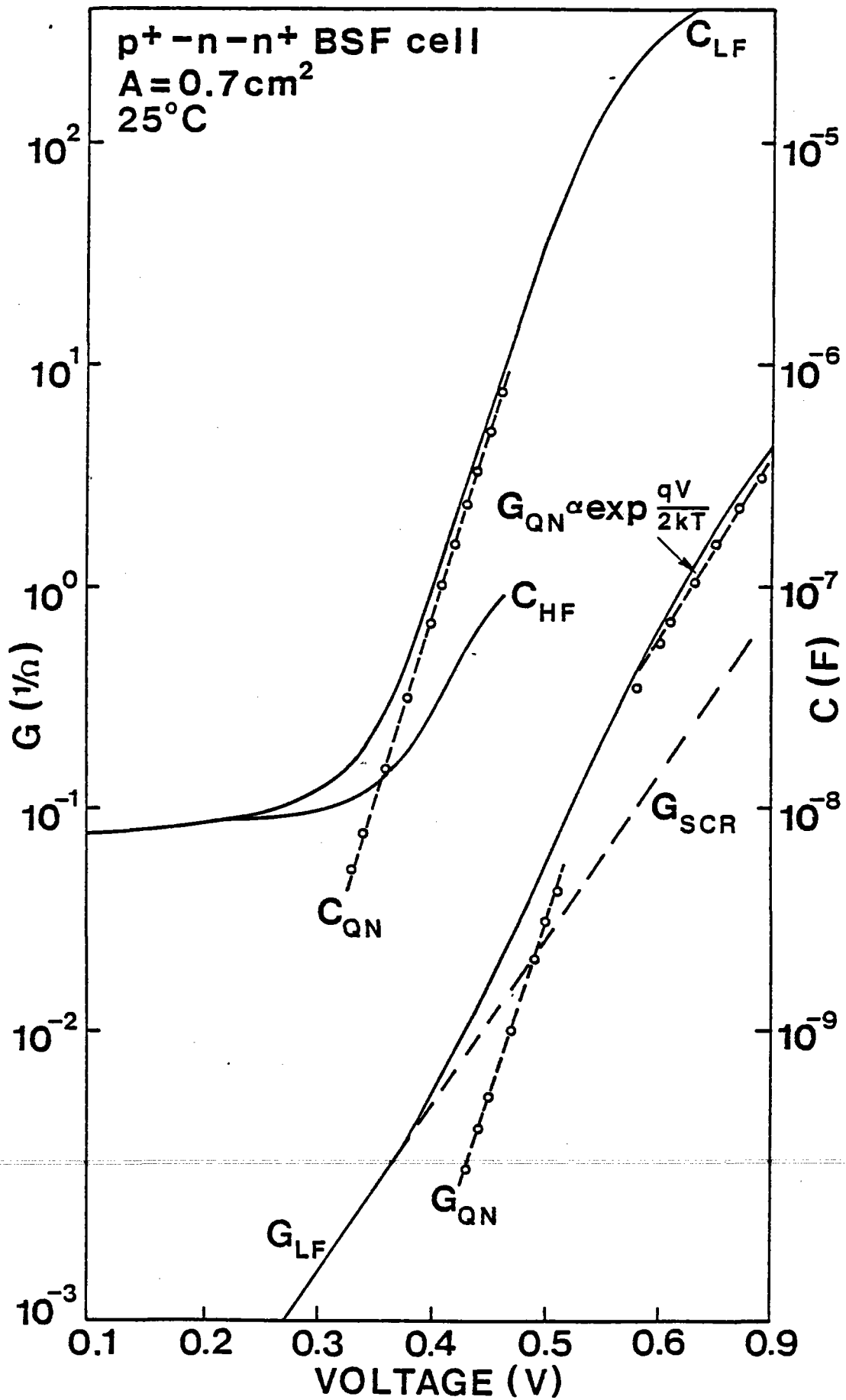


Figure 8

SECTION C

A UNIFYING STUDY OF TANDEM-JUNCTION, FRONT-SURFACE-FIELD, AND INTERDIGITATED-BACK-CONTACT SOLAR CELLS

(J. G. Fossum, A. Neugroschel, and F. A. Lindholm)

ABSTRACT

A theoretical-experimental study of tandem-junction, front-surface-field, and interdigitated-back-contact solar cells is presented. The study provides a unifying view of the physics underlying the performance of these cells. The important physical mechanisms that occur in these cells are described, and cell-design considerations are discussed.

I. Introduction

The purpose of this paper is to analyze the performance potential of the tandem-junction (TJ) solar cell [1], and to compare it with that of more conventional cells, for example, the back-surface-field (BSF) solar cell [2], [3]. Because the structure of the TJ cell has much in common with that of the front-surface-field (FSF) [4] and the interdigitated-back-contact (IBC) [5] solar cells, the development of an understanding of the TJ cell is helped by comparing it with the FSF and IBC cells. The paper will provide this comparison as well.

One of the major problems in dealing with the TJ, FSF, and IBC cells is that their structure emphasizes two- and three-dimensional current flow; boundary-value problems in more than one space dimension are difficult to treat rigorously. Throughout the paper, we focus on a simple analysis yielded by reducing the multi-dimensional boundary-value problem to a one-dimensional boundary-value problem or to coupled one-dimensional problems.

Section II of the paper considers the short-circuit current J_{SC} . Our treatment here reviews the work of others, but gives more complete attention than was given previously to the multidimensionality of the current flow. In the TJ cell, one has the option of using a second junction for collection. But, this advantage is compromised by the increased grid shadowing that results when the front surface is used as a collector. Thus a design trade-off exists, and this is discussed. The TJ, FSF, and IBC cells have a potential problem, not present in the BSF cell: the reduction of J_{SC} by edge-recombination effects. This problem is discussed in terms of experimental observations.

The physics governing the spectral response of the TJ cell is somewhat different from that underlying J_{SC} . In Appendix A we modify our treatment of J_{SC} described in Section II to provide a physical explanation for the spectral response and its observed dependence on light bias.

Section III contains a main new contribution to the theory of TJ cells: a sound description of the open-circuit voltage V_{OC} . Previous performance projections ignored the degrading effects of heavily doped regions. Being based on classical p-n junction theory, they projected maximum open-circuit voltages far in excess of that which we believe can be achieved. Our treatment takes the degrading effects of heavily doped regions into account. The treatment involves a reduction to a one-dimensional boundary value problem, but the neglect of the two-dimensionality of the current flow and of the excess carrier distribution receives careful attention. We base our modeling approach on charge control, which reveals the importance of the heavily doped n^+ and p^+ regions in terms of simple pictures. To make the analysis quantitative, we focus on the dark current-voltage characteristics, and use a first-order model for the heavily doped regions which assumes that the quasi-fields produced by a space variation in the effective intrinsic carrier density just balance the drift fields arising from the gradient in the net impurity concentration. This simple model has proved highly useful in our previous studies of the mechanisms underlying the observed values of V_{OC} , and we have considerable confidence that despite its simplicity, it is accurate enough for the purposes of engineering design. Both high-level and low-level injection conditions in the base region are considered. The main conclusion stemming from this work is that the performance projections previously given were far too optimistic; our analysis indicates that no particular advantage in V_{OC} results from the TJ structure, in the form it has been presented up to now.

Using our analysis of the dark current-voltage characteristic of the TJ cell developed in Section III, we discuss the physical mechanisms controlling the fill factor FF in Section IV. This discussion identifies possible benefits of high-level injection occurring in the base of the cell and of the associated base conductivity modulation.

A thorough understanding of a solar cell, sufficient to enable systematic

improvements in the design and performance, must contain methods for measuring the important material and structural parameters. In Section V, new experimental methods particularly suited to the TJ cell are presented and illustrated for determination of the low- and high-injection carrier lifetimes in the base region of the cell. We also present and illustrate methods for determining the various components of recombination current in the cell, and thus the degrading influence of the heavily doped regions. The experimental results also provide corroboration for our theoretical modeling of the TJ, FSF, and IBC cells.

The combination of the theory and experiment thus provided furnishes a framework for considering the relative performances of the TJ, FSF, IBC, and BSF solar cells. The work also suggests design trade-offs for these cells.

II. Short-Circuit Current

The basic structure of the TJ cell is illustrated in Figure 1. Generally, the front junction is left floating and hence serves only as a minority-carrier barrier to reduce the effective surface recombination velocity. In this configuration, the cell is not a tandem-junction cell in the strict sense of the term since no current is collected by the front junction.

The analytic description of the short-circuit current density J_{SC} of the TJ cell is complicated by the three-dimensional nature of the problem. The collecting n^+p junction on the back of the cell is interdigitated with the p^+ ohmic-contact diffusion to reduce lateral ohmic drops in the base region. Consequently the current flow and the carrier density gradients in the base are not one-dimensional.

A worst-case condition is illustrated in Figure 2. We have assumed that (a) the electron diffusion length L_n in the base is greater than both the p^+ -region width w_{p^+} and the spacing w_s between the n^+ and p^+ regions, and (b) the electron surface recombination velocity S_n is large in the spacing regions. Because the n^+p junction results in a low effective recombination velocity for electrons, all

of the electrons generated in the regions directly above the p^+ contacts, as well as those generated above the spacings, recombine predominantly at the spacing surfaces and do not contribute to J_{SC} . Only those electrons generated directly above the n^+ regions contribute to J_{SC} . Note that when the cell is delivering power, the n^+p junction is forward-biased ($V > 0$), and the electron-density gradient at the junction decreases. Thus, even more electrons are diverted toward the spacing surfaces where they recombine, as shown in Figure 2. This effect, if significant, invalidates the current-shifting approximation [6], and reduces FF and V_{OC} .

If S_n is sufficiently small, and w_{p+} and w_s are both much smaller than L_n , the electron flow is still two-dimensional as indicated in Figure 3. However, all electrons generated throughout the base can potentially be collected by the n^+ junction, and the problem can be solved approximately in one-dimension.

Rigorous one-dimensional solutions of the short-circuit carrier-transport problem in the base region have been published [7]-[9]. These treatments yield evaluations of J_{SC} and the cell spectral response in terms of the cell geometry and device parameters like carrier lifetime and effective surface recombination velocities at the front and back junctions. The studies are parametric and offer little physical insight, and no indication of how the effective recombination velocities are determined.

To provide a basis for estimating the effective front surface recombination velocity, we qualitatively discuss the behavior of the photo-generated electrons and holes in the short-circuited TJ cell. Consider the instant immediately following the application of the illumination. Photo-generated electrons near the front p-n junction space-charge region will diffuse to that space-charge region where the large electric field present there will force them toward the front n^+ quasi-neutral region. Because the front junction is open-circuited, the excess electrons thus directed toward the n^+ region cannot leave the region, and hence Coulomb forces restrain them to the space-charge-region edge. There they partially compensate the charge of the donor ions, thereby lowering the potential

barrier height. Thus the junction becomes forward-biased, resulting, in the steady state, in net equal fluxes of electrons and holes to the n^+ region where the carriers recombine.

A critical parameter in the determination of J_{SC} in the TJ cell, and in the FSF cell, is the effective surface recombination velocity at the front junction for minority carriers in the base region. Under conditions of low injection, this effective recombination velocity, S_E , is given by

$$qS_E N(W_B) = J_{EO} \exp\left(\frac{qV_{JE}}{kT}\right) \quad (1)$$

where $N(W_B)$ is the electron (minority-carrier) density at the edge of the front-junction space-charge region in the base, and V_{JE} is the forward bias developed across the junction. In writing (1), we have neglected the junction space-charge-region recombination current, which is a reasonable assumption for calculating J_{SC} . The justification of this assumption, and its necessary modification in the analysis of the cell spectral response, will be discussed in Appendix A. This assumption allows us to equate the electron current at W_B , which is equal in magnitude to the hole current at W_B , to the hole recombination current in the emitter J_E :

$$J_E = J_{EO} \exp\left(\frac{qV_{JE}}{kT}\right) \quad (2)$$

Implicit also in (1) and (2) is the assumption that J_E is not strongly influenced by the optical generation occurring in the emitter. Since the emitter junction depth is (should be) shallow, the generation current from the emitter is small ($\approx 1 \text{ mA/cm}^2$ at AM1), and this assumption is suitable for estimating S_E to an accuracy sufficient to avoid sizable errors in the calculation of J_{SC} . It follows from this assumption that J_{EO} is the emitter saturation current density in the non-illuminated cell whose evaluation is discussed in Section III.

In (1), if we assume quasi-equilibrium in the junction space-charge region,

$$N(W_B) = \frac{n_i^2}{N_{AA}} \exp\left(\frac{qV_{JE}}{kT}\right) \quad (3)$$

where N_{AA} is the dopant density in the base. Combining (1) and (3) yields

$$S_E = \frac{N_{AA} J_{E0}}{qn_i} \quad (4)$$

Note that S_E is proportional to N_{AA} for the assumed low-injection conditions. Knowledge of S_E for the TJ (and the FSF) cell enables direct comparison of the achievable value of J_{SC} with that of the IBC cell in which we focus attention on the actual front surface recombination velocity.

Regardless of the complexity of the general problem of characterizing J_{SC} , we can discuss the current collection of TJ and FSF cells by referring to previous theoretical and experimental work involving BSF and IBC cells. A p^+nn^+ BSF cell has been recently developed in which extremely long carrier diffusion lengths ($\sim 700 \mu\text{m}$) have been achieved, resulting in nearly 100% internal quantum efficiency [3]. These results have been ascertained by comparing experimental results with a charge-control analysis [10] of the BSF cell. Although the optical carrier generation in this cell occurs predominantly near the collecting (p^+n) junction, these results, supplemented by computer-aided numerical and experimental analysis of the current collection in an IBC cell [11], suggest that high values of quantum efficiency can be achieved with the TJ and FSF cells. This conclusion has been corroborated experimentally with an IBC cell whose fabrication evolved from the p^+nn^+ BSF cell process, and resulted in very long carrier diffusion lengths and small effective surface recombination velocities [11]. Neglecting losses due to recombination at the edges of this IBC cell, which we discuss later, the internal quantum efficiency of this cell, in which the carrier generation occurs nearly $300 \mu\text{m}$ away from the collecting junction, is about 93% [11]. Numerical solution of the basic differential equations describing J_{SC} in the IBC cell indicates that to attain quantum efficiencies this high, the front surface recombination velocity cannot be much greater than 10 cm/sec [11].

Based on these results, we conclude that if $L_n > 2W_B$, then the internal quantum efficiency of the TJ cell can approach 100%, at least in those regions directly above the back n^+ diffusion. If the p^+ contact stripes and the n^+-p^+ spacings are sufficiently narrow, and if the spacings are passivated to reduce the surface recombination velocity, then virtually all the carriers generated in the cell can be collected. In that case, if the front surface is texturized such that the reflection loss is negligible after the anti-reflection coating is deposited, then

$$J_{SC} = q \int_0^W G^o(x) dx \quad (5)$$

where G^o is the optical carrier generation rate, and W is the "optical thickness" of the cell which can exceed W_B because of the refraction of the light at the front surface and the reflection at the back surface. If W_B is increased to about 300 μm from its value in present cells [1] of about 100 μm , and if L_n is improved to values comparable to those achieved in the p^+nn^+ BSF cell, (5) implies

$$J_{SC} \rightarrow = 40 \text{ mA/cm}^2 \quad (6)$$

for the AM1 spectrum with an insolation of 100 mW/cm^2 . To indicate the feasibility of achieving this limit value of J_{SC} , we note that an IBC cell (without texturizing) has been fabricated that delivers 37 mA/cm^2 (corrected for reflection loss) [11]. This result suggests that the TJ and FSF cells cannot offer large advantages over the IBC cell with respect to J_{SC} .

In a TJ cell, the attainment of the limit value of J_{SC} given in (6) requires (a) sufficiently narrow p^+ contact strips and n^+-p^+ spacings, (b) sufficiently long carrier diffusion lengths in the base region, (c) sufficiently low surface recombination velocity in the spacings, and (d) sufficiently low effective surface recombination velocities at both the front n^+p and the back p^+p junctions. The latter requirement calls for proper design of the heavily doped n^+ and p^+ regions to suppress minority-carrier recombination. The designs of these regions, and the physics underlying the recombination in them and their effective surface recombination velocities, will be discussed in detail in Section III.

A possible technological problem that tends to limit J_{SC} to values less⁴¹ than the limit value stems from excessive recombination that can occur at the edges of TJ, FSF, and IBC cells [11]. In these cells, carriers are photo-generated near the front surface, away from the collecting junction. It is difficult to passivate the edge of a silicon chip, and consequently, if L_n is long, significant losses can result from generated carriers moving to the cell edge and recombination there. This limitation on J_{SC} has been observed in the IBC cells discussed earlier [11]. In a 1-cm² IBC cell, the recombination loss at the edge has been experimentally determined to be about 20% of the actual value of J_{SC} [11]. This loss obviously becomes less significant as the area-to-perimeter ratio of the cell increases. Hence, with proper geometrical design, the recombination loss at the cell edge might be made negligible.

Based on this discussion, and the likelihood of attaining the limit value of J_{SC} given in (6), we conclude that the use of the front n^+p junction as a second collecting junction is not advantageous in the TJ cell. If (5) and (6) are applicable to the cell when the front junction is floating, which permits no electrode shadowing, then a second current-collecting junction will provide no benefit. Even if (5) and (6) overestimate J_{SC} somewhat, the benefit of the second collecting junction is not obvious since it requires a front electrode that would shadow the cell and produce a direct reduction in J_{SC} . Our studies indicate that in good TJ cells, i.e., cells in which the carrier lifetimes in the base are sufficiently long to allow acceptable values of V_{OC} , any increase in J_{SC} provided by the second collecting junction is negated by the required front-electrode shadowing.

Without the necessity of the second current-collecting junction, new TJ cell design concepts, based on the underlying physics, can be considered. The sole purpose of the front n^+p junction is now only to provide a minority-carrier barrier to reduce the effective surface recombination velocity. This can be done alternatively with a p^+p high-low (H-L) junction (FSF cell structure [4]) or with direct surface passivation (IBC cell structure [5]).

III. Open-Circuit Voltage

The study of V_{OC} of the TJ cell is greatly facilitated by the current-shifting approximation,

$$I(V) = I_{SC} - I_D(V) \quad , \quad (7)$$

where $I(V)$ is the current-voltage characteristic of the illuminated cell, and $I_D(V)$ is the characteristic of the non-illuminated cell, neglecting nonlinear effects like ohmic drops [6]. The validity of (7) is based on the application of the superposition principle to the TJ cell, which requires linearity of the describing boundary-value problem [6]. As suggested by the discussion of Figure 2 in Section II, the bending of the carrier flow lines that occurs as V increases produces a nonlinear effect that may invalidate (7). This effect becomes stronger as the illumination level, or V , increases. Note therefore that the following analysis of V_{OC} , which is based on (7), may be inaccurate for high values of V_{OC} , for example, those resulting from high illumination levels.

From (7), V_{OC} is given implicitly by

$$I_{SC} - I_D(V_{OC}) = 0 \quad . \quad (8)$$

To identify and characterize the fundamental limitations of V_{OC} , we now analyze $I_D(V)$.

We base this analysis on the one-dimensional model of the TJ cell shown in Figure 4 for which the following are sufficient conditions for its adequacy:

- (a) The surface recombination velocity S_n at the spacings between the n^+ and p^+ diffused regions is no larger than the effective surface recombination velocity S_{pp} at the low-high junction between the p-type base and the p^+ diffused region.
- (b) The diffusion length L_n for minority electrons is large enough (i.e., $L_n \gg w_{p+} + 2w_s$) that the fringing of the electron flow lines at the edges of the back n^+ diffused regions overlap, and the flow lines are predominantly in the vertical (x) direction throughout the entire quasi-neutral base region.

- (c) The lateral communication between the n^+ and p^+ diffused regions is negligible because their junction depths are much less than W_n^+ and because S_{pp^+} is low.
- (d) Ohmic voltage drops that result from majority hole flow supporting recombination in the cell are negligible; these drops will be included later as a perturbation effect in the treatment of series resistance and fill factor.

For simplicity, we assume low-injection conditions, setting aside for now discussion of possible benefits that may result from designing a TJ cell for operation at high-level injection.

Because of these conditions, the recombining minority-carrier charge is located throughout the entire volume of the cell, and is not defined by the edges of the back n^+ diffused regions, as might be inferred from Figure 4. The following analysis, based on Figure 4, yields expressions for important components of current density, which can properly account for minority-carrier recombination through consideration of the cell geometry.

In Figure 4, we have included three terminals, labeled the emitter, the base, and the collector in accordance with the terminology of the bipolar transistor whose intrinsic structure is identical to that of the TJ cell. We will study $I_D(V)$ both for the common terminal configuration in which the emitter is left floating ($I_E = 0$) and for the tandem-junction configuration in which the emitter and the collector are tied together ($V_E = V_C$). We then will analyze the FSF structure in which the front n^+p junction has been replaced by a floating p^+p junction, and we will compare the results of this analysis to those of the TJ cell studies. Finally, we will discuss V_{OC} of the IBC cell.

Consider first the case in which the front n^+p junction is floating. This terminal configuration is shown in Figure 5 where we also illustrate the minority-

carrier storage in the three quasi-neutral regions of the cell. We neglect recombination in the junction space-charge regions. This does not limit the usefulness of our analysis since these components of current are rarely important at forward biases near V_{OC} in good silicon solar cells.

We assume low-level injection in the base. Using a charge-control representation for I_D [10], we write

$$I_D = \left(\frac{Q_N}{\tau_n} + \frac{Q_{PE}}{\tau_{pE}} \right) A + \left(\frac{Q_{PC}}{\tau_{pC}} \right) A_{n+} \quad (9)$$

where A is the total area of the cell and A_{n+} is the area of the collector; τ_{pC} and τ_{pE} are effective hole recombination times in the collector and emitter respectively. The physical interpretations of τ_{pC} and τ_{pE} will be discussed later.

To describe minority-carrier transport in the heavily doped regions, we use a first-order model based on the assumption that the quasi-field resulting from the gradient of the bandgap narrowing, influenced by Fermi-Dirac statistics, nearly offsets the built-in field resulting from the gradient of the actual doping density [12]. The application of this model to the collector region, in which the surface recombination velocity is very high because of the ohmic contact, yields

$$\frac{Q_{PC}}{\tau_{pC}} = \frac{qn_i^2}{N_{DC(eff)}} \left(\frac{\bar{D}_p}{W_C} \right) \exp \left(\frac{qV}{kT} \right) \quad (10)$$

where $N_{DC(eff)}$ is the effective doping density [12] in the collector.

Applying the model [12] to the emitter region, in which the surface recombination velocity S_{pE} can be made relatively small by properly passivating the surface, we obtain

$$\frac{Q_{PE}}{\tau_{pE}} = \frac{qn_i^2}{N_{DE(eff)}} \left(\frac{1}{S_{pE}} + \frac{1}{\bar{D}_p/W_E} \right)^{-1} \left(1 + \frac{\tau_{tp}}{\bar{\tau}_p} \right) \exp \left(\frac{qV_{BE}}{kT} \right) \quad (11)$$

where $N_{DE(eff)}$ is the effective doping density in the emitter, $\bar{\tau}_p$ is the average hole lifetime, and τ_{tp} is the hole transit time given by [12]

$$\tau_{tp} = \frac{W_E^2}{2\bar{D}_p} + \frac{W_E}{S_{pE}} \quad (12)$$

The voltage V_{BE} in (11) is the forward bias developed across the base-emitter junction to satisfy the $I_E = 0$ constraint. It can be evaluated by equating the hole recombination current Q_{pE}/τ_{pE} to the electron current from the emitter:

$$\frac{Q_{pE}}{\tau_{pE}} = -J_N(W_B) \quad (13)$$

To express $J_N(W_B)$ in terms of the junction voltages, we assume that, in the base,

$$L_n > W_B \quad (14)$$

As discussed in Section II, the inequality in (14) is a requirement of good TJ cells. With (14), we find that typically the hole and electron quasi-Fermi levels are nearly flat across the base region provided the effective recombination velocities at surfaces bounding the base region are sufficiently small [10]. Consequently, neglecting ohmic drops, we have

$$V_{BE} \approx V_{BC} \approx V \quad (15)$$

(11) and (15) now define Q_{pE}/τ_{pE} .

Since the quasi-Fermi levels are nearly flat across the base, $N(x)$ is nearly constant and is given by

$$N(x) \approx \frac{n_i^2}{N_{AA}} \exp\left(\frac{qV}{kT}\right) = \text{constant} \quad (16)$$

for low-injection conditions; N_{AA} is the doping density in the base. Consequently,

$$\frac{Q_N}{\tau_n} = \frac{qn_i^2 W_B}{N_{AA} \tau_n} \exp\left(\frac{qV}{kT}\right) \quad (17)$$

For a set of sufficient conditions analogous to (a) - (d) stated earlier, but appropriate for high injection, the preceding one-dimensional analysis can be regarded as general. For high injection levels in the base, i.e., $P \approx N$, the assumption

of nearly flat quasi-Fermi levels can remain valid for common operating conditions [10]. Therefore, the base recombination current becomes [10]

$$\frac{Q_N}{\tau_n} \rightarrow \frac{Q_N}{\tau_H} = \frac{q n_i W_B}{\tau_p + \tau_n} \exp\left(\frac{qV}{2kT}\right) \quad (18)$$

if we neglect ohmic drops.

The open-circuit voltage of the TJ cell with the front n^+p junction floating is then given implicitly by the combination of (8), (9), (10), (11), (17), and (18) for low- and high-injection conditions in the base. To maximize V_{OC} , the three components of I_D must all be minimized. Depending on the cell design, any of the three components can be significant. Note that under conditions of high injection, the relative significance of the base recombination current (18) diminishes because of its slower increase with increasing V . This means that at very high injection levels, V_{OC} is limited primarily by recombination in the heavily doped surface regions.

Consider next the case in which the emitter is shorted to the collector producing two current-collecting (tandem) junctions. We thus force the condition (15), and the results of the preceding analysis of $I_D(V)$ are directly applicable to this case. Fundamentally then, to first-order accuracy, the open-circuit voltage of the TJ cell is the same whether the emitter is floating or is shorted to the collector!

Let us now consider the FSF cell configuration pictured in Figure 6, which also indicates the minority-carrier charges stored in the quasi-neutral regions. The p^+p junction floats, constraining the front-terminal current to zero.

For this case, we write, analogously to (9),

$$I_D = \left(\frac{Q_N}{\tau_n} + \frac{Q_{NE}}{\tau_{nE}}\right)_A + \left(\frac{Q_{PC}}{\tau_{pC}}\right)_{A_{n^+}} \quad (19)$$

for low-injection conditions. Referring back to our analysis of the TJ cell, we see that Q_{PC}/τ_{pC} is identical to the collector recombination current given by (10).

We once again use our argument that the quasi-Fermi levels are nearly flat across the base region [10], and thereby obtain (17) for the base recombination current. When the injection level becomes high, this current component is described by (18). Finally, applying our first-order model for minority-carrier transport in heavily doped regions [12] to the front p^+ layer ("emitter"), we get

$$\frac{Q_{NE}}{\tau_{nE}} = \frac{qn_i^2}{N_{AE(eff)}} \left(\frac{1}{S_{nE}} + \frac{1}{\bar{D}_n/W_E} \right)^{-1} \left(1 + \frac{\tau_{tn}}{\tau_n} \right) \exp\left(\frac{qV}{kT}\right) \quad (20)$$

in which the parameters are defined analogously to those in (11).

The open-circuit voltage of the FSF cell is given implicitly by (8), (10), (17), (18), (19), and (20). Comparison of this result with those for the TJ cell indicates that there is no obvious advantage, with respect to V_{OC} , of the FSF structure over the TJ structure, or vice versa. The only significant difference between the analytic characterizations of V_{OC} for the FSF and the TJ cells is due to the different descriptions of minority-carrier recombination in the front surface layer: (11) describes the hole recombination in the n^+ emitter of the TJ cell, and (20) describes the electron recombination in the p^+ "emitter" of the FSF cell.

There are fundamental reasons why it may be technologically easier to suppress electron recombination in p^+ regions than hole recombination in n^+ regions [13]. These reasons involve the difference between the effective density of states in the conduction and valence bands in silicon, or, equivalently, the difference between the electron and hole effective masses, as well as the difference between the Auger recombination coefficients for electrons and holes. We have experimental evidence that, for similar p^+ and n^+ doping profiles, the electron current described by (20) can be less than the hole current described by (11) by a factor as high as ten [14]. This fundamental advantage favors the p^+pn^+ FSF structure over the n^+pn^+ TJ structure. It furthermore suggests that a p^+np^+ TJ cell could yield a higher V_{OC} than either of these structures.

The analysis of V_{OC} for an IBC cell is similar to the preceding charge-control analysis for the TJ and FSF cells. The only difference is that the front-surface recombination current is given by the product of the surface recombination velocity and the excess carrier charge-density at the surface. This product replaces Q_{PE}/τ_{pE} in (9) and Q_{NE}/τ_{nE} in (19). Using again the approximation of nearly flat quasi-Fermi levels across the base region, we find that this surface-recombination current is proportional to $\exp(qV/kT)$ for low injection and $\exp(qV/2kT)$ for high injection. This current, as well as the base recombination current, tend to become insignificant as V increases, and V_{OC} is limited primarily by recombination in the heavily doped regions at the back surface. This result, together with our earlier discussion, suggests that an np^+ IBC cell may yield the highest V_{OC} for this class of solar cells.

IV. Fill Factor

The fill factor of a solar cell, defined as

$$FF \equiv \frac{\max\{IV\}}{I_{SC}V_{OC}}, \quad (21)$$

depends on, in addition to I_{SC} and V_{OC} , parameters that describe the $I(V)$ characteristic of the cell, i.e., series resistance, shunt resistance, and reciprocal slope factor of the $I_D(V)$ characteristic, excluding ohmic drops. Generally, in silicon cells, the shunt resistance is so high that it can be neglected.

From our descriptions of $I_D(V)$ for the TJ, FSF, and IBC cells developed in Section III, we see that, because of the possible occurrence of high-level injection in the base and the consequent variation of the functional dependence of the base recombination current on V , $I_D(V)$ can appear to vary with V in the following manner:

$$I_D(V) = I_{D0}(V) \exp \left[\frac{qV}{n(V)kT} \right] \quad (22)$$

where $1 < n(V) < 2$ [10]. The reciprocal slope factor n is largest when the base recombination current, under high-injection conditions, dominates the $I_D(V)$ characteristic. Since the cell fill factor FF decreases as n increases [16], this dominance results in low values of FF .

This physical mechanism that decreases FF is less significant in cells operating at high values of V , for example, cells with high V_{OC} or concentrator cells. The base recombination current, increasing as $\exp(qV/2kT)$, becomes a less significant component of $I_D(V)$ since the collector and emitter components are increasing faster with V as $\exp(qV/kT)$. At sufficiently high values of V , $n \approx 1$, and FF attains its ultimate value, limited only by series resistance [16]. At one-sun illumination, this degradation of FF can be eliminated by suppressing the base recombination current. This demands increases in carrier lifetimes and/or a reduction in the base width (and, in the IBC cell, a reduction in the front surface recombination velocity). This effect can also be eliminated by increasing the base doping level, thereby decreasing the excess carrier charge stored in

the base, as well as extending the onset of high-level injection to higher values of V . The benefits of higher base doping levels, however, are compensated by the associated lower carrier lifetimes [15] and, in the TJ and FSF cells, by the higher effective surface recombination velocities indicated in (4).

Ohmic drops in the solar cell also degrade FF. It is therefore necessary to minimize the series resistance R_S of the cell. One distinct advantage that TJ and FSF cells have over conventional cells is the apparent relative ease of doing this. With the electrodes on the non-illuminated side of the cell, shadowing is not a concern, and large areas of metal can be used, thereby reducing the contributions to R_S from the metal and the back n^+ and p^+ layers. This leaves only the base to contribute significantly to R_S .

The design of the cell then must focus on the back contact geometry and the sheet resistivity R_{BS} of the base. Simple quasi-two-dimensional ohmic-drop calculations will imply satisfactory geometries yielding sufficiently small R_S for given values of R_{BS} , provided R_{BS} is sufficiently small.

Under low-injection conditions, R_{BS} of the n^+pn^+ TJ cell is determined by the base doping level and the base thickness:

$$R_{BS} = \frac{1}{q\mu_p N_{AA} W_B}, \quad (23)$$

where μ_p is the hole mobility. A possible advantage of the FSF structure over the TJ structure now becomes obvious. With a p^+p junction at the front surface, lateral conductivity in the p-type base is supplemented by the conductivity of the p^+ "emitter". The effective sheet resistivity of the base in the FSF cell is given by the parallel combination of R_{BS} in (23) and the sheet resistivity of the front p^+ layer, R_{ES} :

$$R_{BS(\text{eff})} = \frac{R_{BS}R_{ES}}{R_{BS} + R_{ES}} \quad (24)$$

The reduction in R_{BS} implied by (24) can be quite significant. For example, in a 100- μm -thick TJ cell with a 10- $\Omega\text{-cm}$ base, (23) yields $R_{BS} = 1000\Omega/\square$. In the FSF

counterpart, with a typical $R_{ES} = 100\Omega/\square$, (24) implies $R_{BS(eff)} = 90\Omega/\square$!

For conditions of high injection in the base, the ambipolar conductivity results in lower values of R_{BS} ; both holes and electrons contribute to the conductivity. With $P = N = n_i \exp(qV/2kT)$, as discussed in Section III,

$$R_{BS} = \frac{1}{q(\mu_p + \mu_n)n_i W_B \exp(qV/2kT)} \quad (25)$$

For the cell described above then, at $V = 700$ mV, which may correspond to an intermediate concentration ratio, (25) yields $R_{BS} = 40\Omega/\square$ at 25°C . The conductivity modulation due to high injection in the base can reduce the series resistance of the cell substantially, and thereby significantly enhance the fill factor, provided the base recombination can be suppressed ($n = 1$). This result, together with the benefits of nearly complete metal coverage on the back of the TJ, FSF, and IBC cells, make them candidates for high-efficiency concentrator solar cells.

The accuracy of (25) and the benefits of high injection to FF are threatened by the possibility of current-crowding effects in the base region. The study of current crowding involves the solution of the three-dimensional carrier transport problem in the base, as do rigorous treatments of the overall performance of TJ, FSF, and IBC solar cells.

V. Experimental Characterization of a TJ and an FSF Solar Cell

The experimental characterization described in this section has the following purposes:

- (a) to determine material and structural parameters basic to the theoretical models described in the previous sections;
- (b) to determine the relative importance of the various recombination currents modeled; and
- (c) to assess the validity of the assumptions used in the modeling.

The geometry of the TJ cell used in this study is shown in Figure 7. After an ohmic contact to the top n^+ layer (emitter) was made, as indicated in Figure 7, the dc current-voltage characteristics of the cell were measured in the transistor configuration of Figure 8. The measured dependencies of I_E and I_B on V_{BC} (inverse-active region of operation) are shown in Figure 9. The data were taken at 24°C with the base-emitter junction shorted. As expected, I_E follows an $\exp(qV_{BC}/kT)$ dependence. The total measured base current, $(I_B)_{total}$, exhibits a large leakage current that probably originates at the edges of the cell. This large leakage current can possibly decrease the accuracy with which the quasi-neutral base current I_B can be separated from $(I_B)_{total}$ [17]. This separation, illustrated in Figure 9, estimates the base saturation current density to be

$$J_{B0} \approx 1.0 \times 10^{-12} \text{ A/cm}^2 \quad (26)$$

The emitter saturation current density is found from Figure 9 to be

$$J_{E0} \approx 1.7 \times 10^{-11} \text{ A/cm}^2 \quad (27)$$

and

$$\beta(\text{ideal}) \triangleq \frac{J_{E0}}{J_{B0}} \approx 17 \quad (28)$$

The base doping density can be determined from J_{E0} :

$$N_{AA} = \frac{qn_i^2 D_n}{J_{E0} W_B} = 2.1 \times 10^{15} \text{ cm}^{-3} \quad (29)$$

which corresponds to a base resistivity of 6 Ω -cm. (The base width W_B was measured with a dial-gauge indicator and was found to be about 160 μm .)

To determine the minority-carrier (electron) lifetime in the base region, we use a method involving the measurement of base-width-modulation conductances [18]. The small-signal output conductance G_o and the reverse transconductance G_r were measured using a Wayne-Kerr B224 admittance bridge at a frequency of 2 KHz. The base-emitter junction was reverse-biased (1-2 V) during this measurement. Since $W_B \approx 160 \mu\text{m}$, which is large compared with the modulation of the base width, the ac measurements done with $-V_{BE} = 1-2 \text{ V}$ will be consistent with the previously described dc measurements done with $V_{BE} = 0$. The dependencies of G_o and G_r on V_{BC} are shown in Figure 10. Both G_o and G_r are proportional to $\exp(qV_{BC}/kT)$. These ideal dependencies of G_o and G_r on V_{BC} confirm that they are due predominantly to base-width modulation [18]. For $V_{BC} < 0.4 \text{ V}$, the leakage of the base-emitter junction dominates in determining G_o and G_r , resulting in almost constant values of the conductances. For $V_{BC} > 0.4 \text{ V}$, however, the intrinsic parts of G_o and G_r due to the base-width modulation prevail, and the ideal exponential dependencies extend for about two orders-of-magnitude variation in the measured conductances.

From Figure 10, we obtain [18]

$$\frac{G_o}{G_r} = \frac{\tau_n}{\tau_F} \approx 13 \quad , \quad (30)$$

where τ_F is the minority-carrier base transit time ($\tau_F = W_B^2/2D_n$). From (30), the electron diffusion length in the base is

$$L_n = \left(\frac{\tau_n W_B^2}{2\tau_F} \right)^{1/2} \approx 410 \mu\text{m} \quad . \quad (31)$$

The experimental determination of L_n involving base-width modulation requires $L_n > W_B$; the result (31) is self-consistent with this requirement, and also validates assumption (14) of our theoretical modeling. From (31), the electron lifetime is

$$\tau_n = \frac{L_n^2}{D_n} \approx 50 \text{ } \mu\text{sec} \quad , \quad (32)$$

and

$$\tau_F \approx 3.9 \text{ } \mu\text{sec} \quad . \quad (33)$$

The base saturation current density J_{B0} , whose value is given in (26), consists of components due to recombination in the quasi-neutral base region, Q_B/τ_n , and in the quasi-neutral (n^+) collector region, Q_{PC}/τ_{pC} . To relate these recombination currents to our previously described modeling, we note that Q_B/τ_n is approximately one-half of Q_N/τ_n given in (17), and Q_{PC}/τ_{pC} is the current described in (10). From charge-control transistor theory, we know that

$$\beta(\text{ideal}) = \frac{Q_B/\tau_F}{Q_B/\tau_n + Q_{PC}/\tau_{pC}} \quad (34)$$

Using the measured values of $\beta(\text{ideal})$, τ_F , and τ_n in (34), we determine that

$$\frac{Q_B}{\tau_n} > \frac{Q_{PC}}{\tau_{pC}} \quad (35)$$

Thus, the dark $I_D(V)$ characteristic of the TJ cell in this configuration (Figure 8) is determined primarily by base recombination.

Examination of the $I_B(V_{BC})$ characteristic of Figure 9 for $V_{BC} > 600$ mV reveals a portion varying as $\exp(qV_{BC}/2kT)$. This variation yields an estimate of the high-injection lifetime τ_H appearing in (18). We find $\tau_H \approx 200$ μsec .

Consider now the TJ cell in the floating-emitter mode illustrated in Figure 11. As discussed in Section III, when the base-collector junction is forward-biased, the base-emitter junction becomes forward-biased to constrain the emitter current to zero. As concluded previously on theoretical grounds, the front and back junction voltages are nearly equal [see (15)]. By direct measurement of these voltages, we find, for example, with V_{BC} set at 578 mV, $V_{BE} = 573$ mV.

We show in Figure 12 the measured $(I_B)_{\text{total}}(V_{BC})$ characteristic with the emitter floating, and we compare it with the $(I_B)_{\text{total}}(V_{BC})$ characteristic for the transistor configuration with the base-emitter junction shorted. Subtracting the space-charge-region current components from the measured currents (as illustrated in Figure 9), we find

$$(I_B)_{I_E=0} \approx 4(I_B)_{V_{BE}=0} \quad (36)$$

Since $V_{BE} = V_{BC}$ when $I_E = 0$, (36) implies

$$\frac{Q_{PE}}{\tau_{pE}} \approx 2 \frac{Q_B}{\tau_n} \quad (37)$$

Hence, although recombination in the heavily doped collector region is negligible in this TJ cell [see (35)], the recombination current in the emitter region is comparable to the base recombination current and therefore limits V_{OC} .

Consider now a companion FSF cell biased as shown in Figure 13. The fabrication processing of this cell is the same as that of the TJ cell except for the front-surface junction formation. In Section III, we concluded, from a theoretical standpoint, that the only possibly significant difference between the dark $I_D(V)$ characteristics of the FSF cell and the TJ cell would result from fundamental differences in the minority-carrier recombination currents from the heavily doped p^+ and n^+ emitters (provided τ_n , N_{AA} , and W_B are the same in both cells).

The measured dependence of $(I_B)_{total}$ on V_{BC} for the FSF cell is illustrated in Figure 14. Graphical removal of the space-charge-region recombination current components yields

$$J_{B0} \approx 2.3 \times 10^{-12} \text{ A/cm}^2 \quad (38)$$

This value is questionable because of the high leakage current in this cell, exhibited in Figure 14. Nonetheless, comparison of Figure 14 with Figure 12, and of (38) with (26), suggests that recombination in the p^+ emitter is insignificant. This is consistent with the theoretically implied advantage of p^+ over n^+ layers discussed in Section III.

VI. Summary

A theory describing the performance of TJ, FSF, and IBC solar cells has been presented. Careful attention has been given to the three-dimensionality of carrier flow in these devices. Qualitative discussions of possible degrading effects of the three-dimensional flow have been given. However, arguments supporting quasi-one-dimensional theoretical modeling were presented, and the quantitative analyses were based on one-dimensional models.

The study of J_{SC} in these cells indicates that, with proper design, values of J_{SC} approaching the theoretical limit are possible. In the TJ cell, this can be approached more readily without collection from the front pn junction. The analysis reveals that the physical mechanisms governing J_{SC} differ from those governing the spectral response. This difference is discussed in Appendix A.

The theoretical study of V_{OC} is based on a quasi-one-dimensional charge-control model of the dark current-voltage characteristic. It reveals the possible importance of recombination in the heavily doped surface regions and the possible benefit of high-level injection in the base region due to the effective suppression of the base recombination.

The treatment of FF is based in part on our analysis of the dark current-voltage characteristic, which reveals that high injection can also be beneficial to FF. This can occur because of higher values of V_{OC} and lower values of R_S due to base conductivity modulation. With regard to FF, a possible advantage of the FSF cell over the TJ and the IBC cells derives from the shunt lateral conductance provided by the high-doped side of the front H-L junction.

Experimental studies of an n^+pn^+ TJ and a companion p^+pn^+ FSF cell yielded results that are consistent with our theory and that provided evaluations of material and structural parameters. In particular, τ_n in the base was determined to be about 50 μsec , and $\tau_H (= \tau_p + \tau_n)$ was estimated to be 200 μsec . Although these lifetimes are respectable, the base recombination current nevertheless contributes to the

dark current-voltage characteristics, and limits V_{OC} to about 600 mV. If the cell designs are improved to yield values of V_{OC} comparable to those being achieved in more conventional cell structures (≈ 620 mV), then the recombination currents from the heavily doped surface regions will limit V_{OC} , consistent with our theoretically based anticipations.

Based on our theoretical and experimental studies of TJ, FSF, and IBC cells, we note the following observations concerning optimal cell designs:

- (a) The base recombination current can be decreased, and V_{OC} increased, by decreasing W_B (with possible sacrifice of J_{SC}), by increasing the minority-carrier lifetime (by impurity gettering for example), by increasing the base doping density (with possible decrease of carrier lifetime, and, in the TJ and FSF cells, increase of the effective front surface recombination velocity), and/or by designing the cell to operate at high-injection levels in the base.
- (b) The recombination currents in the heavily doped back surface regions can be minimized by maximizing the p^+ area and minimizing the n^+ area; these design criteria require an n-type base.
- (c) To minimize the recombination current in the front surface region, either a p^+ layer (forming a p^+np^+ TJ structure) or a surface-passivating film, e.g., a thermal SiO_2 layer (forming an IBC structure), should be used.
- (d) All non-metallized surfaces should be covered with a surface-passivating film, and the metallized areas should be minimized.
- (e) To reduce ohmic power loss, e.g., for concentrated-sunlight applications, several design options exist: increase W_B , increase the base doping density, rely on conductivity modulation due to high-level injection, use an H-L junction at the front surface (FSF structure), and of course properly define the back p^+ and n^+ geometries and diffusions.

Generally, device design involves trade-offs, and the design of TJ, FSF, and IBC cells is no exception. Thus, we note that the design considerations listed above are not necessarily all compatible.

Appendix A. Spectral Response

It has been experimentally observed that a white-light bias considerably improves the spectral response of the TJ cell [19]. In this Appendix, we modify our previous treatment of J_{SC} to provide a physical explanation for this observation.

Consider first the portion of the spectral response originating from hole-electron-pair generation in the p-type base region, i.e., the long-wavelength portion. As was discussed in Section II, the application of a white-light (solar-spectrum) bias to a TJ cell in which the top junction (emitter) floats leads to a forward bias V_{JE} across that junction. In contrast to the treatment in Section II, we now include the influence of the top junction space-charge-region recombination current J_{SCR} on the effective surface recombination velocity S_E seen by the minority electrons in the base:

$$S_E \triangleq \frac{J_N(W_B)}{qN(W_B)} = \frac{J_{SCR} + J_{PE}}{qN(W_B)} \quad (A-1)$$

in which J_{PE} , the hole recombination current in the quasi-neutral emitter, and $N(W_B)$ are both proportional to $\exp(qV_{JE}/kT)$, whereas J_{SCR} is proportional to $\exp(qV_{JE}/nkT)$ where $1 < n < 2$ according to the Sah-Noyce-Shockley theory [20]. Thus S_E is of the form

$$S_E = A \exp \left[\frac{qV_{JE}}{kT} \left(\frac{1}{n} - 1 \right) \right] + B \quad (A-2)$$

From (A-2), it follows that S_E decreases as V_{JE} (and the intensity of the light bias) increases. Thus, the spectral response is poor for zero or low light bias and increases when a sizable light bias is applied. This result is consistent with the experimental observations.

Consider now the portion of the spectral response due to carrier recombination in the front (floating) n^+ region (emitter) of the TJ cell, i.e., the short-wavelength portion. In the absence of white-light bias, V_{JE} is nearly zero since the monochromatic illumination level is small. Upon the generation of a hole-electron pair in the emitter, the hole will be forced into the base by the built-in electric

field of the junction, but the electron, which must be collected at the back n^+p junction to contribute to the photocurrent, is forced toward the front surface. Since there is no means by which the electron can easily enter the base (since V_{JE} is so small), it will probably recombine with an optically generated hole in the emitter.

If, however, the front emitter-base junction is forward-biased, for example by the white-light bias of a common solar-spectrum insolation, the optically generated electron can be injected into the base where it becomes a minority carrier and can possibly contribute to the photocurrent. Thus, the forward bias of the front junction is critical in determining the short-wavelength response of the TJ cell, and any effect by which V_{JE} is increased will enhance the TJ-cell spectral response.

Note that the effects discussed in this appendix do not occur in either the FSF or the IBC cell. With regard to the FSF cell, space-charge-region recombination is not significant in the high-low junction, and the minority carriers in the (p^+p) base are always repelled from the front surface by the built-in field of the high-low junction; the effective front surface recombination velocity is constant for low-injection conditions. In the IBC cell, there is no front junction (built-in field), and hence no separation of the optically generated holes and electrons occurs near the front surface; the front surface recombination velocity is constant for all injection levels.

The theoretical discussion in this appendix is consistent with an experimental study by Schwartz, et al. [21] of the influence of the front surface potential on the short-circuit current of an IBC cell.

Acknowledgements

This work was supported, in part, by the Jet Propulsion Laboratory. We thank L. J. Cheng for providing the TJ and FSF solar cells used in our experimental studies and for providing information about their structures. Partial support was also provided by the U. S. Foreign Assistance Act, administered by the U. S. Department of State and by the Solar Energy Research Institute, through Grant III-P-3008.

References

1. S. Y. Chiang, B. G. Carbajal, and G. F. Wakefield, "Improved Performance Thin Solar Cells," IEEE Trans. Electron Devices, Vol. ED-25, pp. 1405-1409, Dec. 1978.
2. J. Mandelkorn and J. H. Lamneck, Jr., "Simplified Fabrication of Back Surface Electric Field Silicon Cells and Novel Characteristics of Such Cells," in Record of 9th IEEE Photovoltaic Specialists Conference, 72CH0613-OED, 1972.
3. J. G. Fossum and E. L. Burgess, "High-Efficiency $p^+ - n - n^+$ Back-Surface-Field Silicon Solar Cells," Appl. Phys. Lett., Vol. 33, pp. 238-240, Aug. 1978; J. G. Fossum, R. D. Nasby, and E. L. Burgess, "Development of High-Efficiency $p^+ - n - n^+$ Back-Surface-Field Silicon Solar Cells", in Record of 13th IEEE Photovoltaic Specialists Conference, 78CH1319-3ED, 1978.
4. S. Y. Chiang, B. G. Carbajal, and G. F. Wakefield, "Thin Tandem Junction Solar Cell," in Record of 13th IEEE Photovoltaic Specialists Conf., 78CH1319-3ED, 1978.
5. M. D. Lammert and R. J. Schwartz, "The Interdigitated Back Contact Solar Cell: A Silicon Solar Cell for Use in Concentrated Sunlight," IEEE Trans. Electron Devices, Vol. ED-24, pp. 337-342, April 1977.
6. F. A. Lindholm, J. G. Fossum, and E. L. Burgess, "Application of the Superposition Principle to Solar-Cell Analysis," IEEE Trans. Electron Devices, Vol. ED-26, pp. 165-171, March 1979.
7. O. von Roos, "The Spectral Response of a Front Surface Field (FSF) Solar Cell," to be published in J. Appl. Phys. .
8. O. von Roos, "The Spectral Response of Tandem Junction Solar Cells," JPL Engineering Memo 341-78-4336, 1978.
9. C. Goradia, "Theory and Design of the Tandem Junction Solar Cell," IEEE Trans. Electron Devices, Vol. ED-27, April 1980.
10. J. G. Fossum, R. D. Nasby, and S. C. Pao, "Physics Underlying the Performance of Back-Surface-Field Solar Cells," IEEE Trans. Electron Devices, Vol. ED-27, April 1980.
11. H. T. Weaver and R. D. Nasby, private communications, 1979.
12. J. G. Fossum, F. A. Lindholm, and M. A. Shibib, "The Importance of Surface Recombination and Energy-Bandgap Narrowing in p-n-Junction Silicon Solar Cells," IEEE Trans. Electron Devices, Vol. ED-26, pp. 1294-1298, Sept. 1979.
13. M. A. Shibib, "Device Physics and Engineering Design of Heavily Doped Silicon PN-Junction Solar Cells, Diodes, and Transistors," Ph.D. dissertation, University of Florida, Gainesville, 1979.
14. J. G. Fossum, unpublished data, 1979.
15. J. G. Fossum, "Computer-Aided Numerical Analysis of Silicon Solar Cells," Solid-State Electron., Vol. 19, pp. 269-277, April 1976.
16. M. A. Green, "General Solar Cell Curve Factors Including the Effects of Ideality Factor, Temperature and Series Resistance," Solid-State Electron., Vol. 20, pp. 265-266, March 1977.

17. F. A. Lindholm, A. Neugroschel, C. T. Sah, M. P. Godlewski, and H. W. Brandhorst, Jr., "A Methodology for Experimentally Based Determination of Gap Shrinkage and Effective Lifetimes in the Emitter and Base of p-n Junction Solar Cells and Other p-n Junction Devices," IEEE Trans. Electron Devices, Vol. ED-24, pp. 402-410, April 1977.
18. M. S. Birrittella, A. Neugroschel, and F. A. Lindholm, "Determination of the Minority-Carrier Base Lifetime of Junction Transistors by Measurements of Basewidth-Modulation," IEEE Trans. Electron Devices, Vol. ED-26, pp. 1361-1363, Sept. 1979.
19. W. T. Matzen, S. Y. Chiang, and B. G. Carbajal, "A Device Model for the Tandem Junction Solar Cell," IEEE Trans. Electron Devices, Vol. ED-26, pp. 1365-1368, Sept. 1979.
20. C. T. Sah, R. N. Noyce, and W. Shockley, "Carrier Generation and Recombination in P-N Junctions and P-N Junction Characteristics," Proc. IRE, Vol. 45, pp. 1228-1243, Sept. 1957.
21. R. J. Schwartz, J. L. Bouknight, and M. S. Worley, "The Effects of Surface Potential on Surface Recombination and the Performance of Silicon Solar Cells," in Tech. Digest of 1978 International Electron Devices Meeting, 78CH1324-3ED, 1978.

Figure Captions

- Fig. 1 Basic structure of the TJ cell with the front junction floating.
- Fig. 2 Influence on electron flow of surface recombination between the p^+ and n^+ fingers. The solid flow lines are for $V = 0$; the dashed lines are for $V > 0$.
- Fig. 3 Electron flow when surface recombination is negligible.
- Fig. 4 One-dimensional model of the TJ cell.
- Fig. 5 One-dimensional model of the TJ cell, with the emitter floating, and the corresponding minority-carrier storage in the quasi-neutral regions.
- Fig. 6 One-dimensional model of the FSF cell and the corresponding minority-carrier storage in the quasi-neutral regions.
- Fig. 7 Cross-section and top view of the TJ cell used in the experiments.
- Fig. 8 Transistor configuration (inverse-active mode) used in the experiments.
- Fig. 9 Measured $(I_B)_{total}$ and I_E dependencies on V_{BC} . The graphical determination of I_B is indicated by the dashed lines.
- Fig. 10 Measured base-width-modulation conductances.
- Fig. 11 Bias configuration of the TJ cell in the floating-emitter mode.
- Fig. 12 Measured $(I_B)_{total}(V_{BC})$ characteristic with the emitter floating compared with the $(I_B)_{total}(V_{BC})$ characteristic with the base-emitter junction shorted.
- Fig. 13 Bias configuration of the FSF cell.
- Fig. 14 Measured $(I_B)_{total}(V_{BC})$ characteristic for the FSF cell. The graphical determination of I_B is indicated.

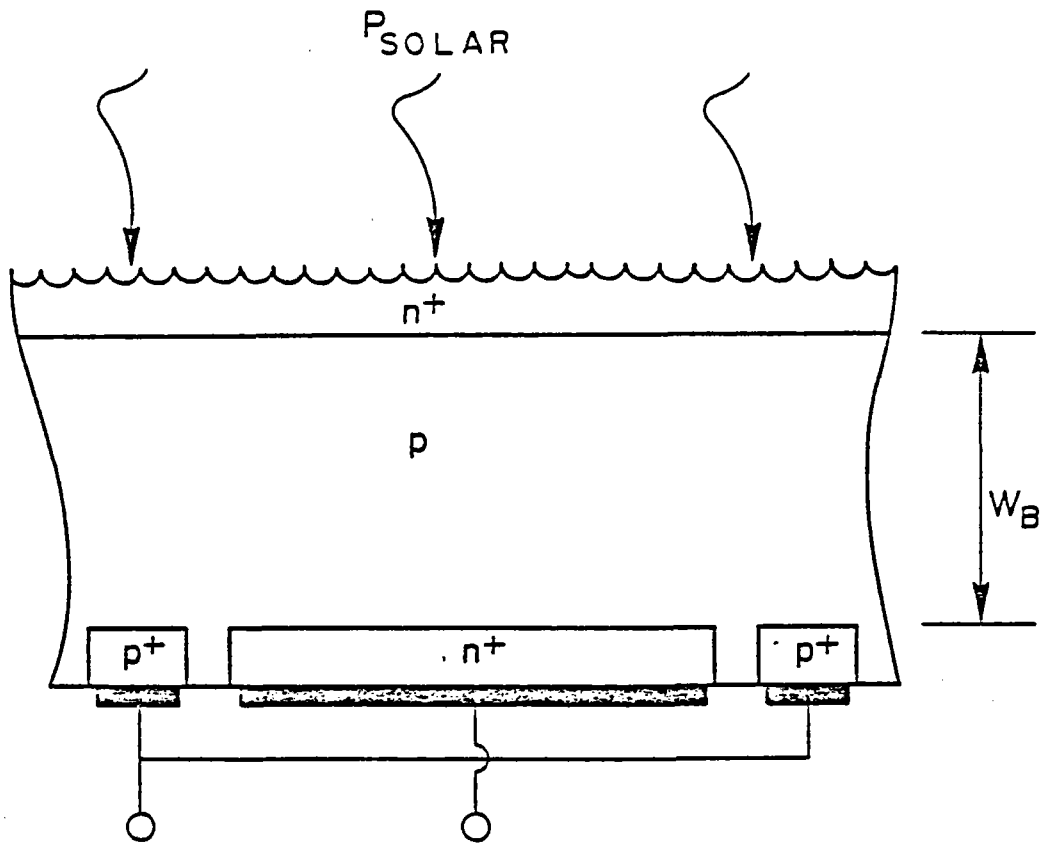


Figure 1

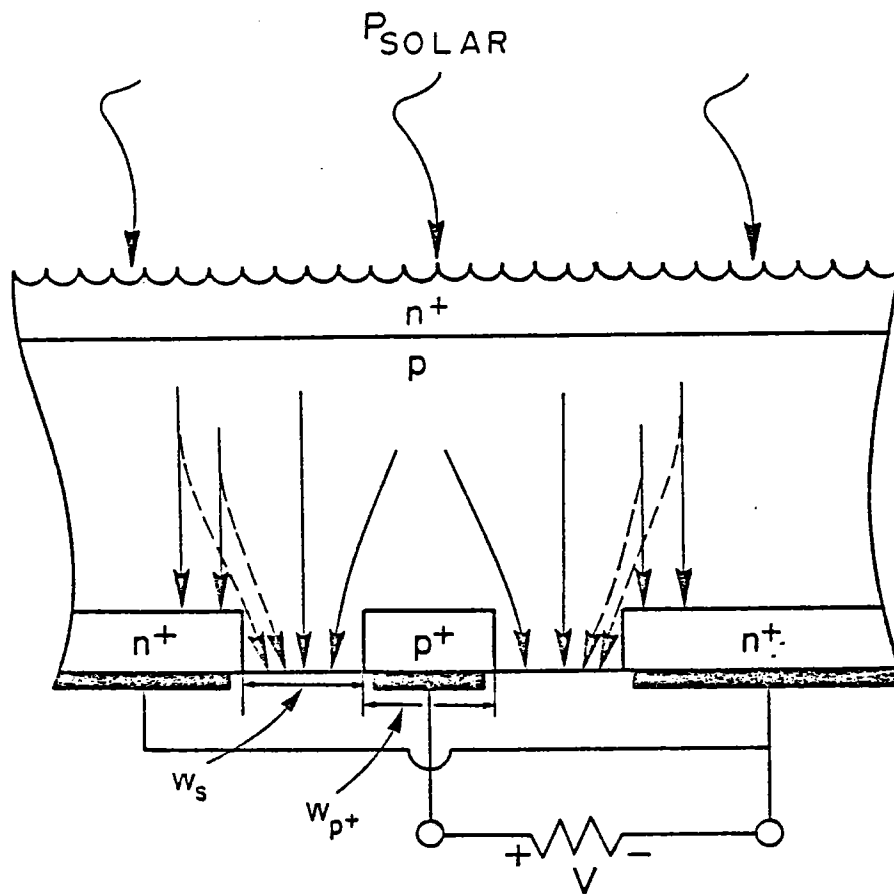


Figure 2

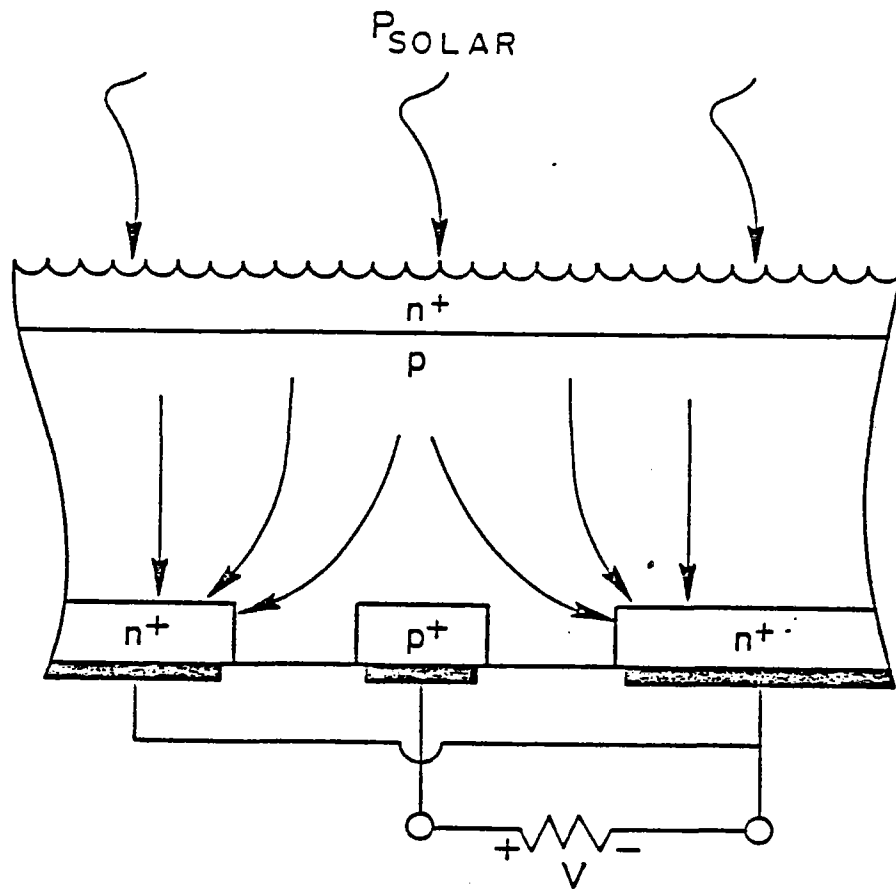


Figure 3

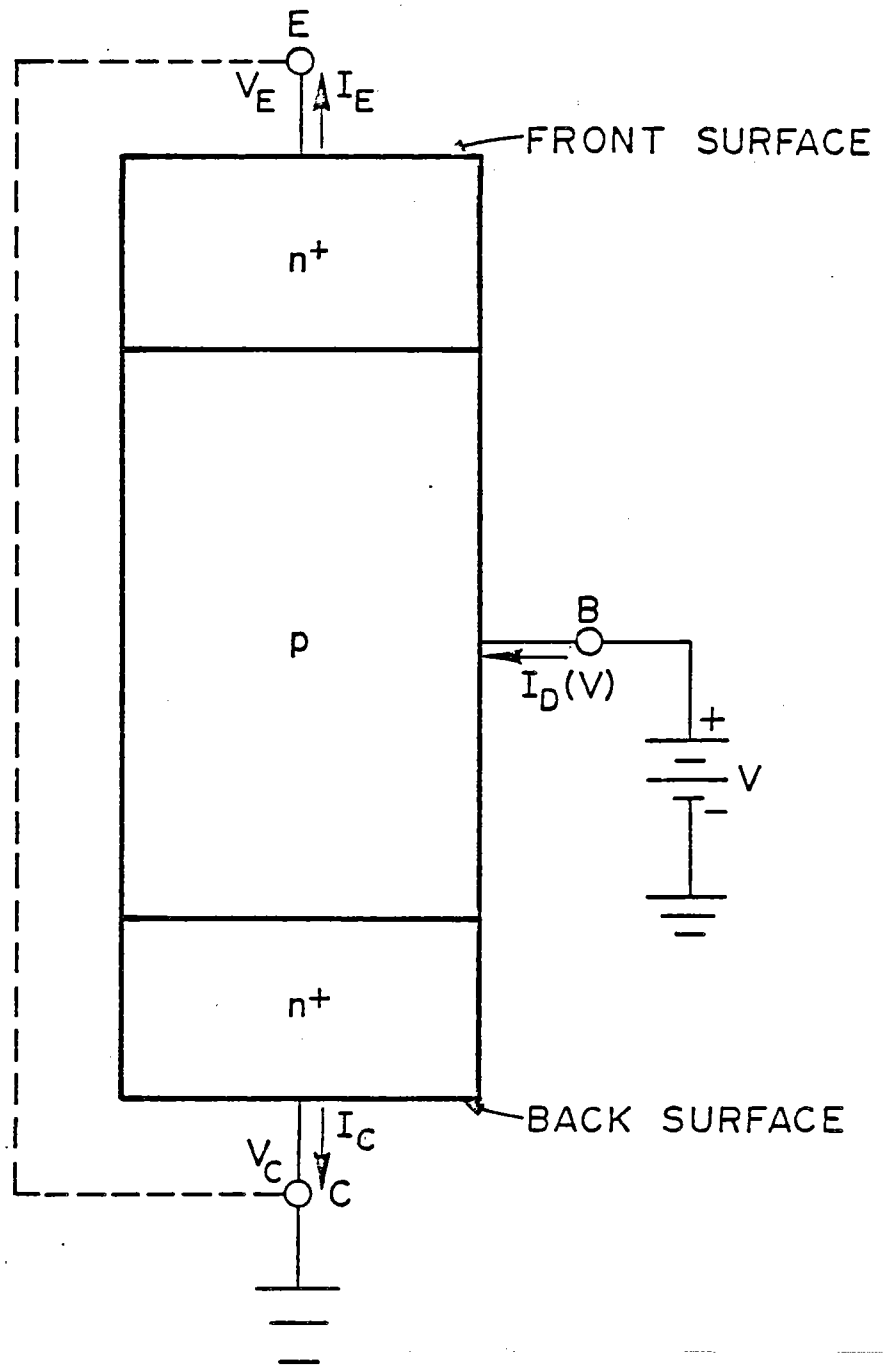


Figure 4

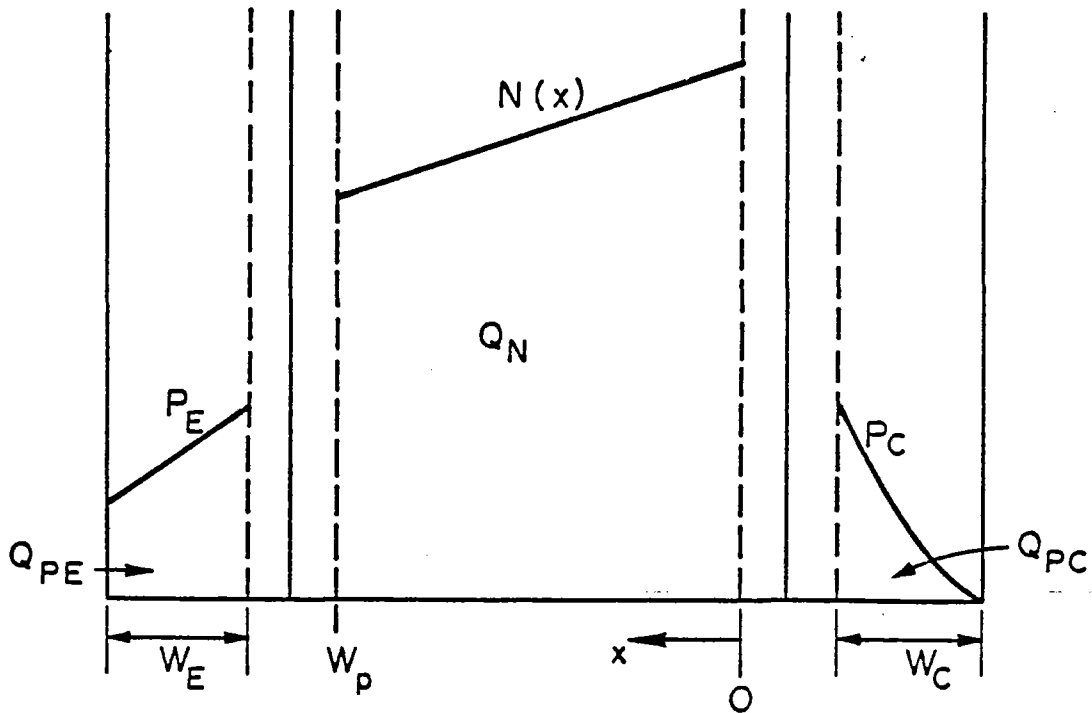
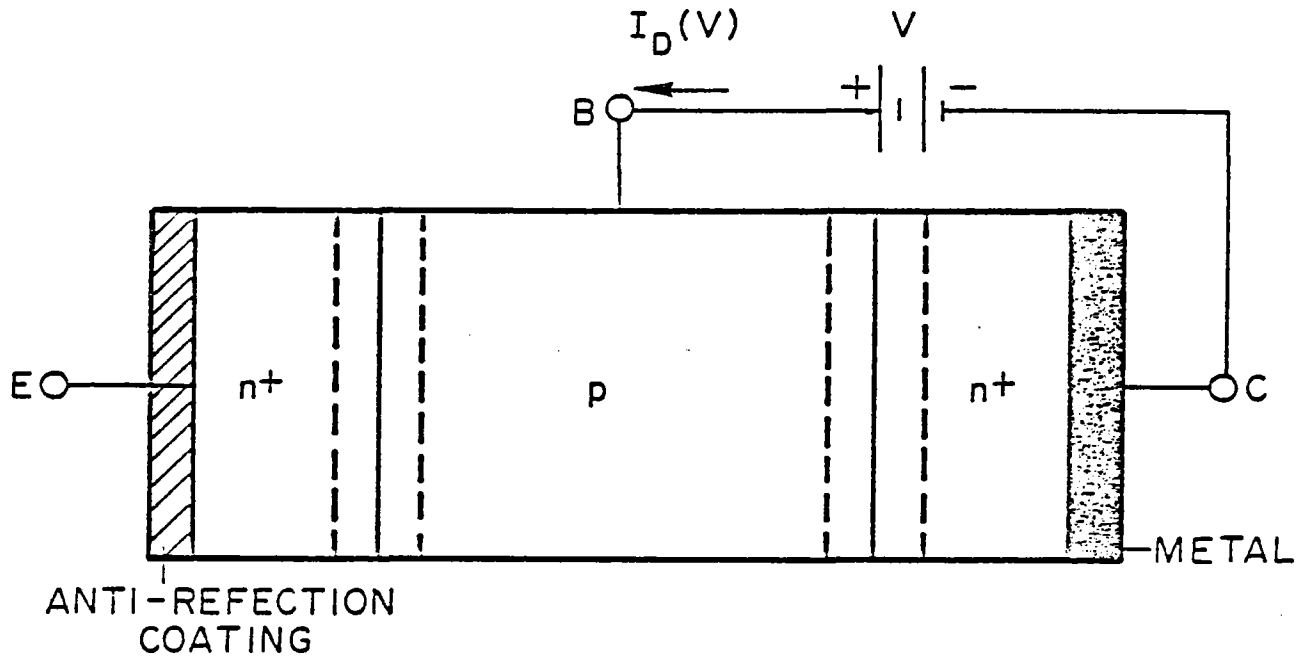


Figure 5

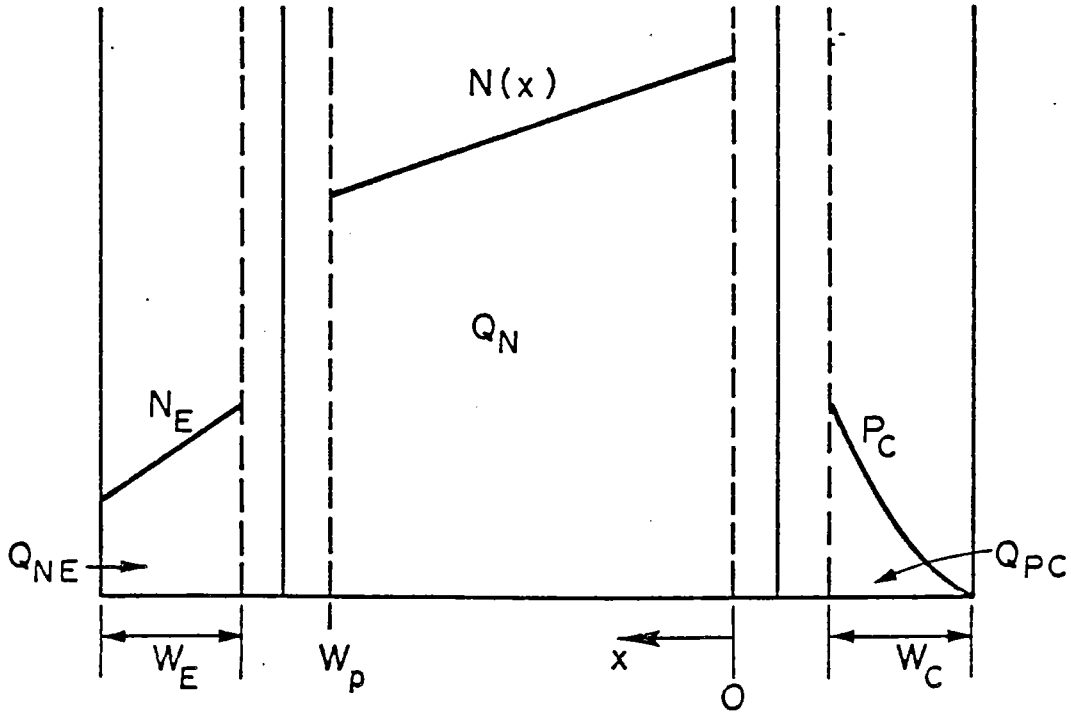
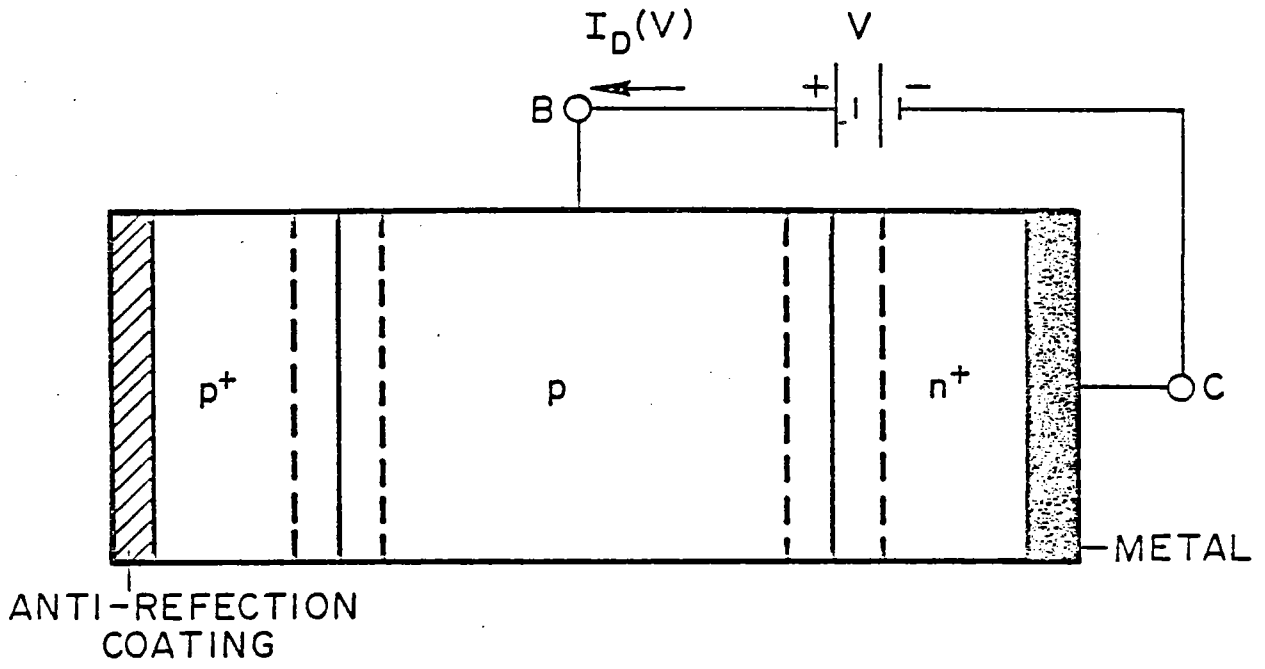
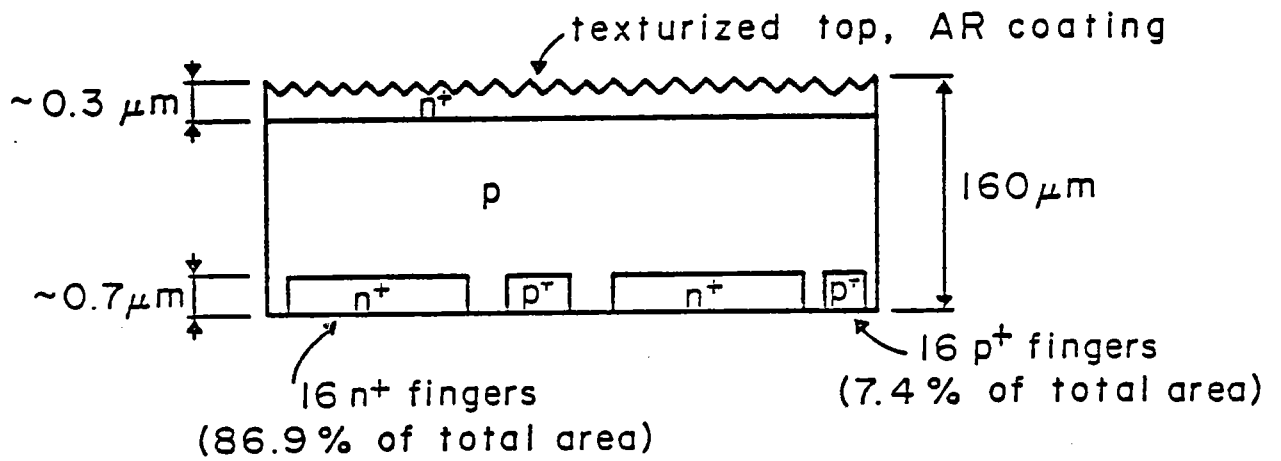


Figure 6

cross-section



top view

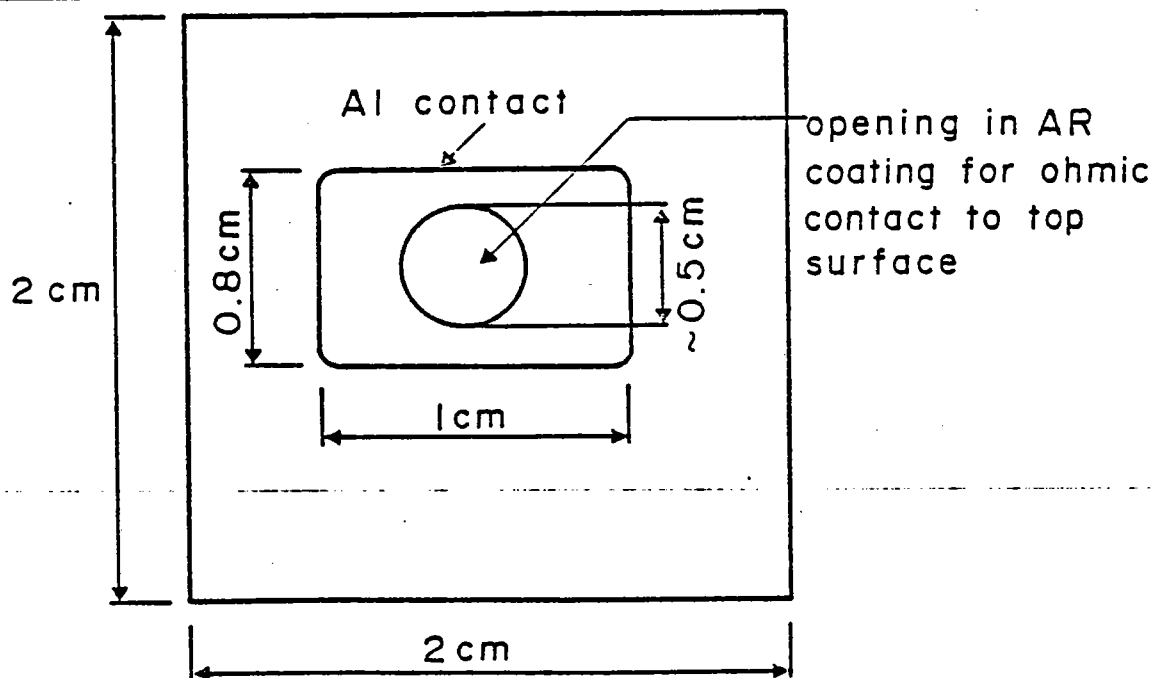


Figure 7

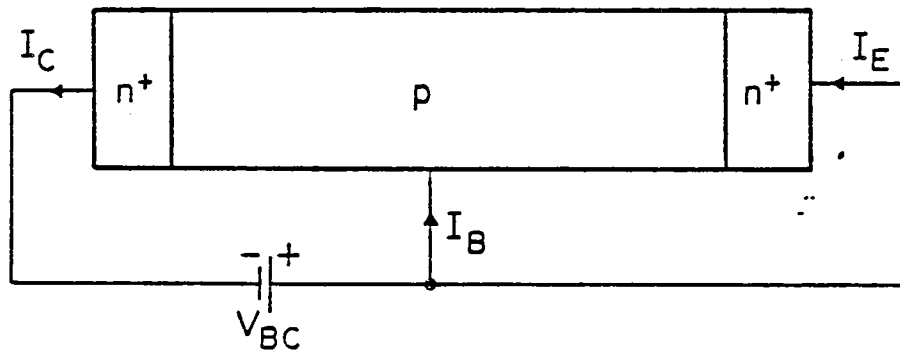


Figure 8

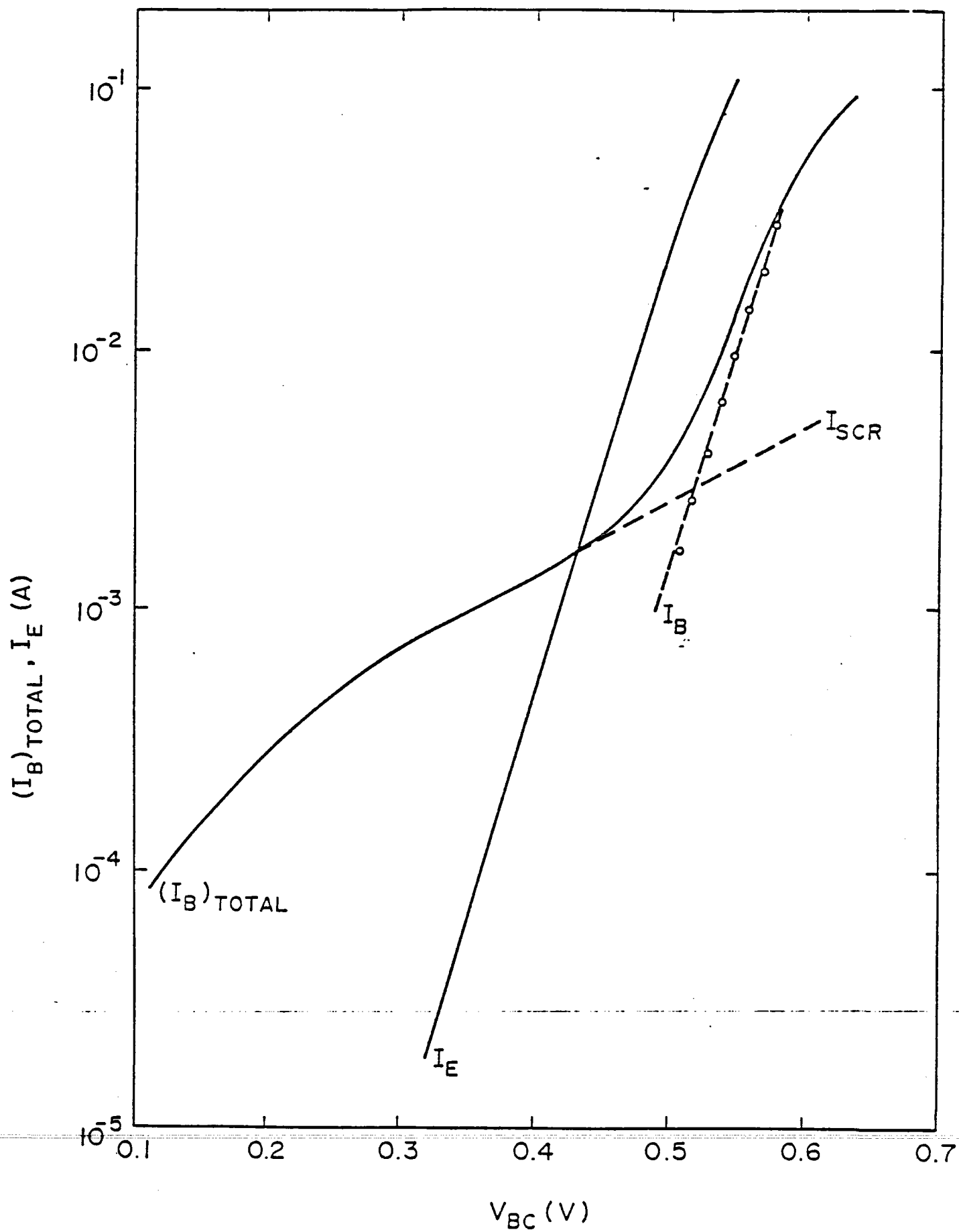


Figure 9

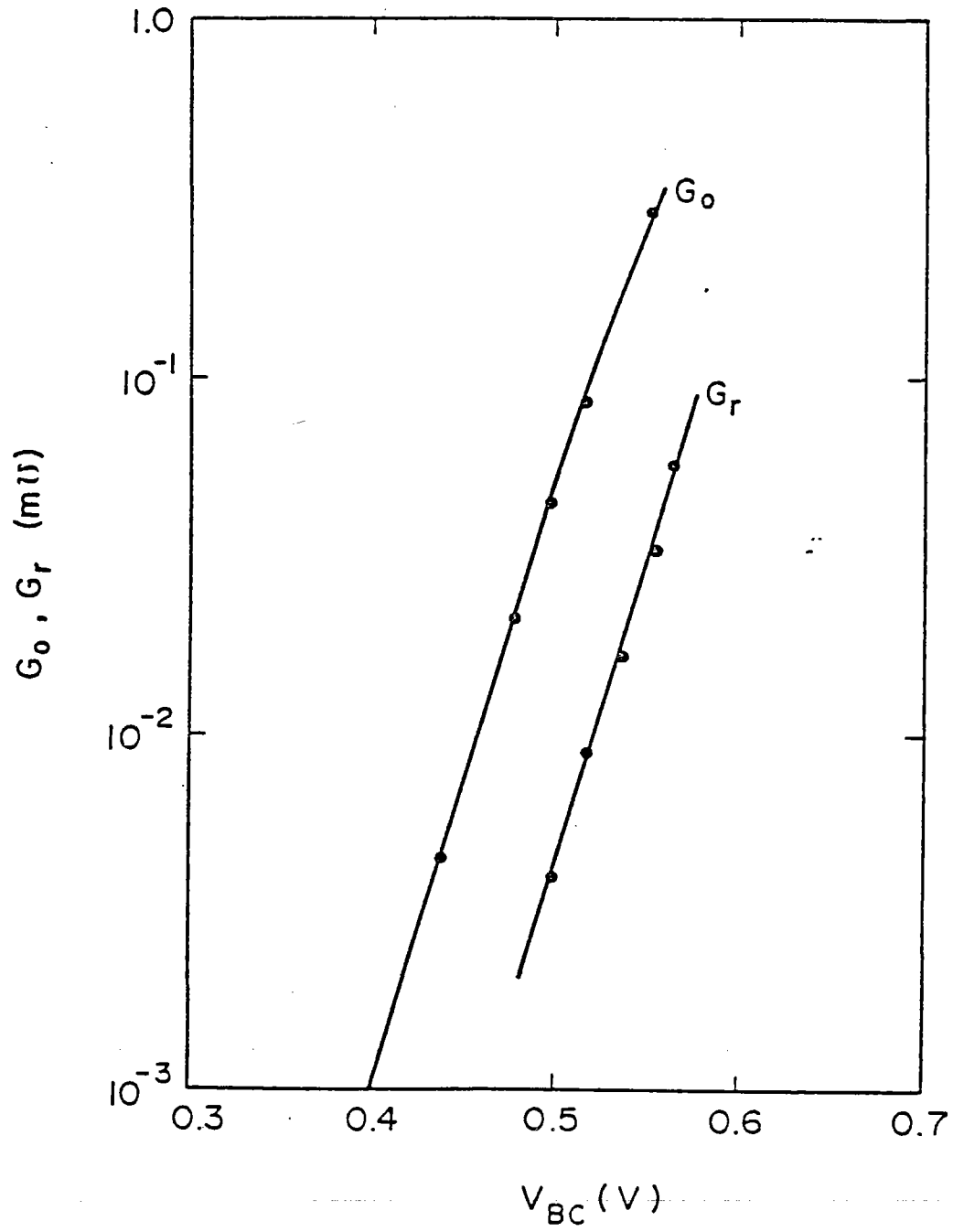


Figure 10

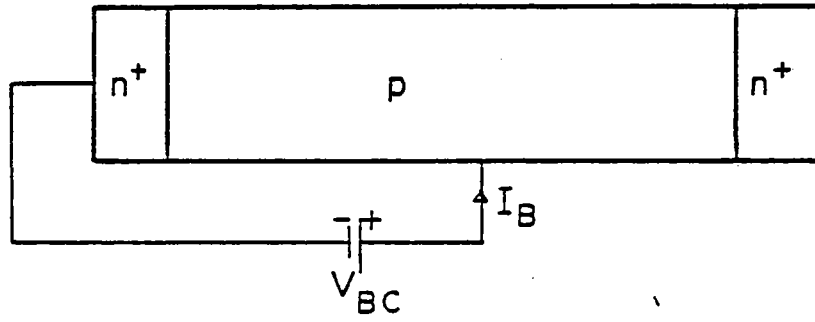


Figure 11

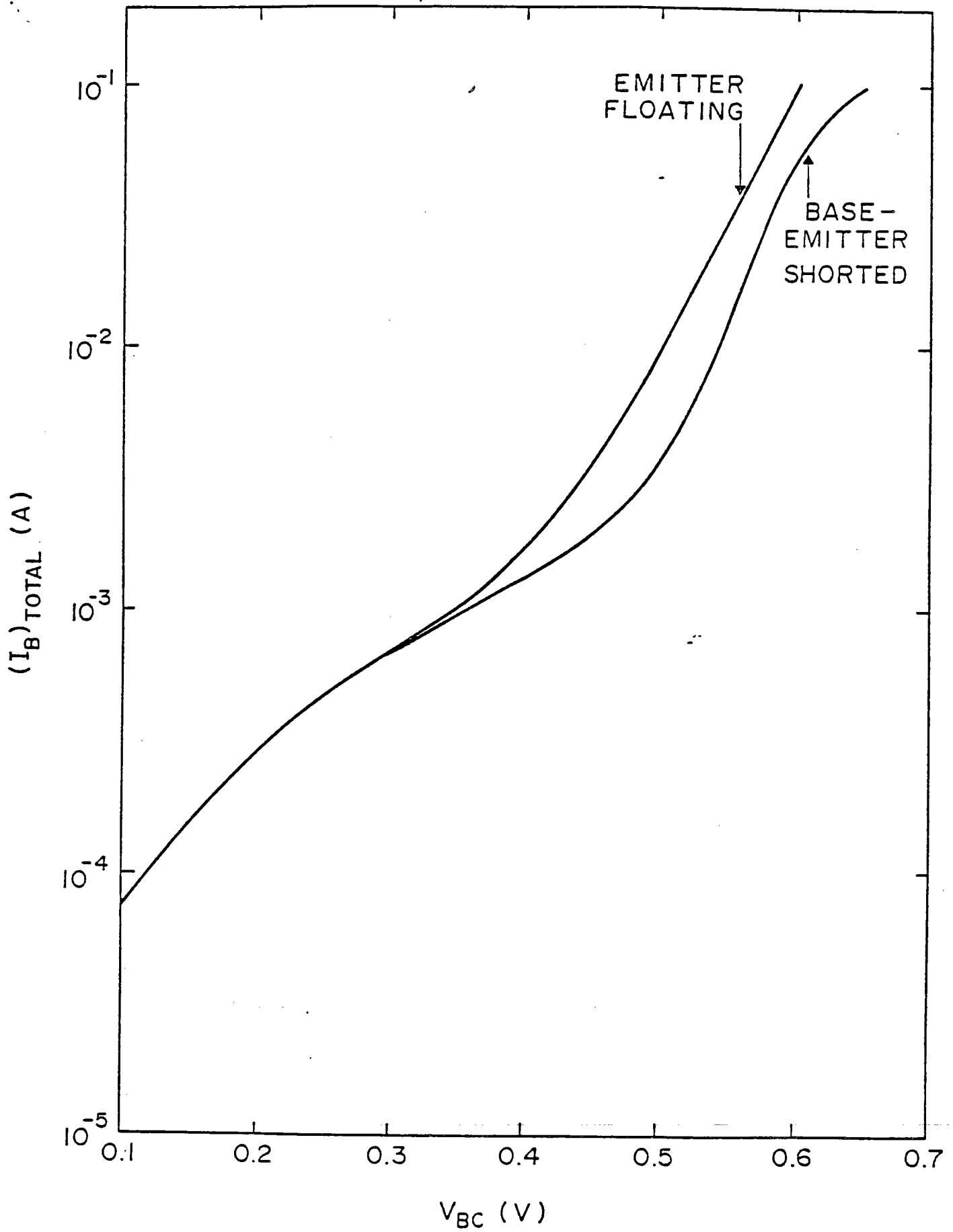


Figure 12

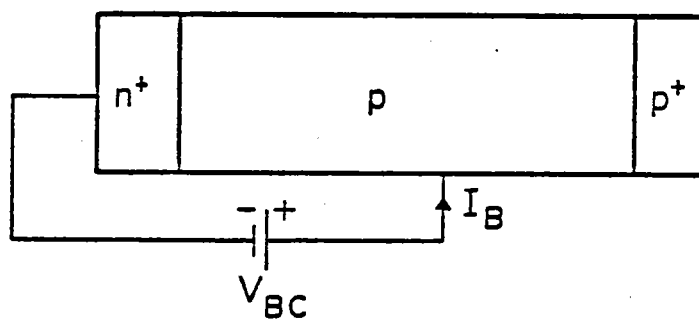


Figure 13

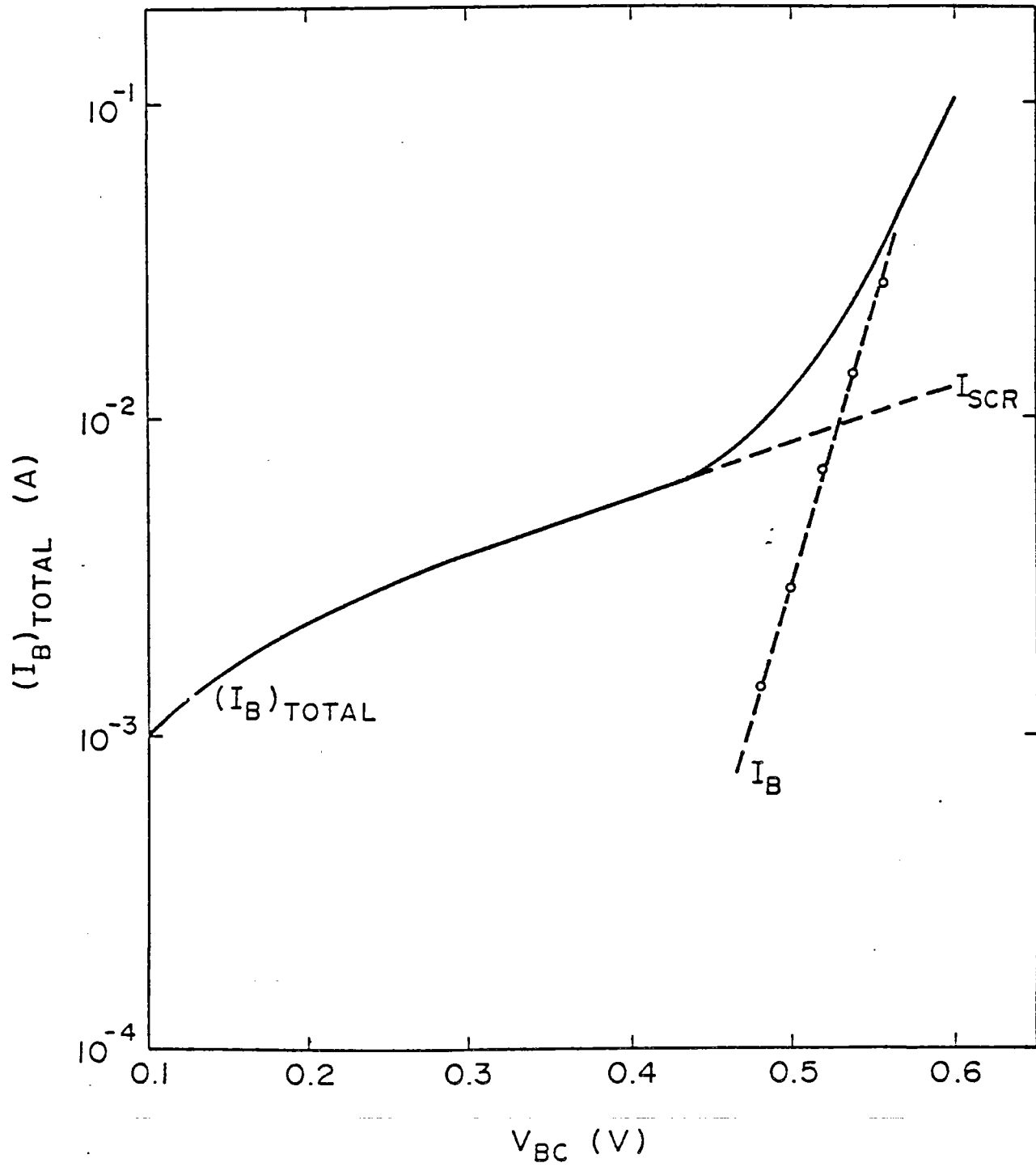


Figure 14

D. EXCHANGE OF TECHNICAL INFORMATION

In addition to mail and telephone communication, the U.S.-Spain technical interaction supported by this program involves visits by the principal investigators to the facilities of one another. Professor Antonio Luque spent six weeks at the University of Florida during the summer of 1979. Technical discussions during this visit benefited work that eventually was presented as "Bifacial Transcells for Luminiscent Solar Concentrators" by A. Cuevas, A. Luque, and J. M. Ruiz, at the 1979 International Electron Devices Meeting in Washington, D.C. in December.

In March 1980, Professor Jerry G. Fossum visited the Universidad Politecnica de Madrid for one week to discuss current topics of interest in this program, including the request for renewal. Professor Fossum presented a seminar to the Instituto de Energia Solar on the work discussed in Section C of this report. Professor Arnost Neugroschel plans to visit the Spanish facility during the summer of 1980.

E. FINANCIAL REPORT

The following is the projected financial status of the U. S. grant as of May 1, 1980.

Salaries and Fringe

Of the total amount of funds budgeted for salaries and fringe benefits (\$5139), approximately \$3100 will have been expended by May 1, 1980. Drs. Fossum, Lindholm, and Neugroschel are currently devoting time to this program and the remaining funds will be expended during May and June 1980.

Consultant

Dr. Alan B. Kuper carries out his functions independently and to date has asked for reimbursement of only \$455.

Equipment

Requisitions in the amount of \$30,000 have been placed for the procurement of equipment, and early delivery is anticipated. The equipment procured consists of a Hewlett-Packard computer and associated instrumentation for automated electrical characterization of solar cells. There are no uncommitted funds in this category.

Operating Expense

Our operating expense budget includes \$3600 for travel. Dr. Fossum recently made a trip to Madrid (cost ~\$1100), and Dr. Neugroschel plans a visit in the near future. The balance in other operating expense funds budgeted for expendables, publications, and computer time is programmed for spending during May and June 1980.

In summary, the \$45,000 granted to support University of Florida personnel and activities will be spent before June 30, 1980, except for a portion of funds budgeted for overseas travel. The \$7000 for Dr. Kuper is being paid as invoiced by him. These consultation funds are principally for support of Dr. Kuper's travel to Spain and payment for his time while in this travel status. His trips have not been scheduled at this time.

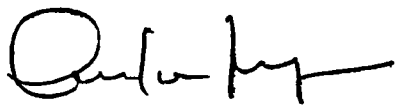
COOPERATIVE RESEARCH GRANT PROJECT

SPAIN- UNITED STATES

UPM/IES/LS/2980

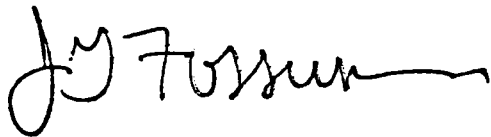
CONTINUATION OF THE REALIZATION AND ANALYSIS OF
SOLAR CELLS WHICH CAN BE ILLUMINATED ON TWO SIDES
REQUEST FOR RENEWAL

SPAIN PRINCIPAL INVESTIGATOR
PROJECT'S HEAD



ANTONIO LUQUE
INSTITUTO DE ENERGIA SOLAR
E.T.S.I. TELECOMUNICACION
CIUDAD UNIVERSITARIA
MADRID 3 (SPAIN)
TEL. (91) 244-1060

U.S. PRINCIPAL INVESTIGATOR
PROJECT'S HEAD



JERRY G. FOSSUM
ELECTRICAL ENGINEERING DEPT.
UNIVERSITY OF FLORIDA
GAINESVILLE, FLORIDA 32611
U.S.A.
TEL. (904) 392-4921

MADRID, APRIL 1980

PREFACE.

The project proposed here is a continuation of the first year of activities conducted within the frame of the Friendship and Cooperation Treaty between the U.S. and the Spanish Governments, and whose management has been assigned to the Joint Spanish-American Committee. The present project was given number III-P-3008 during its first year.

It was foreseen that a second year, as a minimum, would follow to complete the research started the first year.

ABSTRACT.

The objective for the second year is to elaborate a general analysis of surface field bifacial cells, considering high injection effects in the base region, high doping effects in the surface region and surface recombination effects, and bidimensional effects of current transport.

We also intend to develop an economical technology to make the above mentioned cells with at least 12% efficiency.

The task of the Spanish team would be primarily concerned with the development of the technology and study of high injection phenomena. The task of the American team will be mainly, but not exclusively, the analysis of high doping and surface recombination phenomena, giving also priority to providing the Spanish team with U.S. research environment.

1. INTRODUCTION.

The Spanish team at the Polytecnic University of Madrid has developed the bifacial illumination concept as a means to make high concentration levels and static systems compatible. Recently, it has developed the theoretical bases for the concepts involved in bifacial concentration. It has developed, as well, several structures that could be used as bifacial cells. The American team is well recognized for its contributions to the understanding of the physical mechanisms limiting the efficiency of monocrystalline silicon solar cells. This group is also evaluating the technical capabilities of cells (non bifacial) with similar structures to the ones developed by the Spanish group. The global objective of this cooperation is to provide the Spanish team with counseling and assistance about the procedures needed to obtain high efficiency bifacial cells. Conversely, the American team will benefit from the bifacial concentration systems developed by the Spanish team.

In a more detailed way the American team emphasizes research in the analysis of the physical mechanisms involved in the working of bifacial cells, while the Spanish team emphasizes a specific design of bifacial cells, in which all phenomena that limit the efficiency are taken into account, as in the technological development of the cells.

2. FIRST YEAR ACCOMPLISHMENTS OF THE SPANISH TEAM.

2.1. Objectives.

During the first year these proposed primary tasks were accomplished: (1) a theoretical analysis of the n^+pp^+ structure developed by the Spanish team for bifacial illumination, (2) the technological procedure to fabricate at low cost the above cells was developed and (3) the development of some means for simultaneous measurement of surface recombination velocity and diffusion length of minority carriers at the base.

2.2. Theoretical analysis.

With respect to (1) our technical analysis has been directed towards a general treatment of V_{oc} , I_{sc} and the curve factor of the structure in order to be able to appraise the possibilities of the cell. This view is complementary to the view held by the U. of Florida team,

which is centered basically in the analysis of the fundamental recombination mechanisms in the cell, whose main influence is carried into the I_{sc} and V_{oc} values. We have emphasized the bidimensional flow of majority carriers which influences the series resistance of the cell and its curve factor, having used the results of the U. of Florida team, adapted to the aforementioned global analysis for I_{sc} and V_{oc} values.

In this way we were able to design optimized contact masks.

Besides, we developed a formal way to make a general analysis of bifacial structures which can be adapted to back contact interdigitated structures and other related structures that allow us to treat in a unified way pn and pp^+ or nn^+ low-high junctions. This unified analysis has been published [1] and shows as a result that n^+pp^+ or n^+np^+ structures (object of our present research) are potentially superior to any other bifacial structure, among those studied, and that their behaviour could be even superior to that of conventional monofacial cells.

2.3. Measurements of L and S_{eff} .

We have developed a method of simultaneous measurement of the diffusion length L in the base and of the effective recombination velocity at the L-H junction. We made some preliminary measurements with this method. Its basis has been used to evaluate the behaviour of Al-alloy techniques to make pp^+ junctions. This method, which has the advantage of giving simultaneously the diffusion length and the effective recombination velocity, loses precision when both parameters are very high and very small, respectively. Since these are the needed conditions to obtain a good bifacial cell, this method will not be interesting when we improve our technology. In that case we will use in our L measurements the method developed by the Florida team, which is specially valid for these conditions, limiting ourselves to estimate S_{eff} through indirect measurements. For this reason, and in spite of the advantages of this method for other applications (measuring the absorption constant of high wavelengths), we will concentrate our efforts (in relation to the budget that we can reasonably expect) in actions more specifically directed towards obtaining cheap and efficient bifacial cells.

n^+pp^+ and n^+np^+ bifacial cells were obtained using five different technologies, which can be classified in two groups:

- a) technologies with more than one thermic step
- b) technologies with only one thermic step.

In the first ones the n^+ region has been made by phosphorous diffusion and the p^+ region has been made (a) by Al alloy, (b) by ionic implantation of boron or gallium, (c) by conventional diffusion of boron, (d) by pyrolysis and (e) by centrifugation of paints made from silicon organic compounds (Emul-sitone). The second ones, ideally preferable because they maintain a long base lifetime and reduce the cost of fabrication, use simultaneous diffusions to form the p^+ and n^+ regions. The p^+ region was diffused in both cases from boron tribromide in an open tube and the n^+ region was diffused from oxides doped with phosphorous deposits.

The best results have given intrinsic efficiencies of 12% and 10%, with no anti-reflection coating, for n^+p and p^+p junctions, respectively (bifacial efficiency of 11%) using ionic implantation technology (b). At present we have been able to make a conclusive evaluation of alloy technology [2], using, as we have already mentioned, our method of simultaneous measurement of L and S_{eff} . We made a model of the pp^+ junction and we concluded that in order to achieve the best possible results we need to deposit an Al coating (of at least 25 μm) by thick coating techniques and to make the alloy at 800°C. In this way good monofacial cells can be obtained, but not good bifacial ones. To get these it would be necessary to greatly reduce the surface recombination velocity, which does not appear to be easy on the surface resulting after this process. Our experimental results are well interpreted by our model, which also reflects the results of other authors. This work is being prepared for publication.

With respect to other technologies, a full evaluation has not been made yet, but the first results show technologies (b)(ionic implantation) and (d) (pyrolytic deposition) as being very good, but both are rather expensive, at least at the present time. The cheapest is technology (e) (organic silicon compounds) which is also very good ideally, but our results are not yet very positive.

3. FIRST YEAR ACCOMPLISHMENTS OF THE U.S. TEAM.

3.1. Objectives.

During the first year of this U.S.-Spain cooperative research program, the United States (University of Florida) team accomplished three primary tasks.

3.2. Physical bases of B.S.F. cells.

First, a description of the physics of the back-surface-field (BSF) solar cell was developed, in which several key approximations, valid for effective BSF cells, were used to express the results of the analysis in ways that make them useful in understanding the performance of high efficiency BSF cells [3]. This analysis is directly applicable to DSI solar cells. Measured current-voltage characteristics of BSF cells, together with the analysis, were used to describe the important physical mechanisms that control the performance of the BSF solar cell. For example, the analysis enabled the determinations of the carrier lifetimes in the base region and of the effective surface recombination velocity at the low-high (L-H) junction.

3.3. Techniques to measure diffusion lengths.

Second, techniques to measure carrier lifetimes and diffusion lengths in the quasi-neutral base regions, and effective surface recombination velocities at the p-n and L-H junctions of the basic DSI solar cell structures, i.e., n^+pp^+ , p^+nn^+ , n^+pn^+ , and p^+np^+ , were developed [4]. The experimental-theoretical methods enable accurate determinations of the minority-carrier diffusion length in the narrow base region of basic DSI solar cell structures. These methods are unlike more conventional diffusion-length measurements in that they enable the evaluation of diffusion lengths longer than the base width. Once the diffusion length is determined by the new methods, this result can be combined with measured dark I-V characteristics and with small signal admittance characteristics to enable determination of the recombination currents in each quasi-neutral region of the cell, for example, in the emitter, low doped base, and high doped base regions of the BSF cell. For BSF cells, i.e., n^+pp^+ or p^+nn^+ structures, this leads to a value for the effective surface recombination velocity at the L-H junction forming the back-surface field.

3.4. Identification of the physical mechanisms in bifacial cells.

Third, to aid in the identification and characterization of the physical mechanisms occurring in DSI solar cells that limit their conversion efficiencies, a theoretical-experimental study of tandem-junction, front surface field, and interdigitated back contact solar cells was completed [5]. The study provided a unifying view of the physics underlying the performance of these cells, all of which are basic DSI cell structures. The important physical mechanisms that occur in these cells were described, and cell-design trade-offs were defined. Special emphasis was given to qualitative treatments of the important multidimensional transport problems introduced by these cells, treatments which can be applied directly to the study of solar cells being illuminated on both sides.

4. OTHER RECENT RESULTS THAT WIDEN THE INTEREST OF THIS RESEARCH.

The bifacial cell was suggested by the Spanish team in 1977 as the most appropriate photovoltaic structure to work under concentration in systems with great angular aperture. We are developing systems with concentration 6X which are able to "see" the sun the whole year around.

In a recent work [6] we fixed the thermodynamic limits of static concentration for a given angular aperture. The results are extremely promising in that they permit us to achieve concentration values of 17X for direct beam and of 6.29X for isotropic diffuse radiation. A concentrator system with a gain in the 6X range for direct and diffuse radiation is also possible.

This type of concentrators, whose handling and appearance are similar to those of non-concentrating flat panels, has been named by us Flat Panel of Limited Aperture. Such device could be made soon at a cost of about 1/3 of the cost of a conventional flat panel. A projection of the cost of mass producing these devices shows that it would be around 0.5\$/Watt.

In the calculation of these costs we assumed that n^+pp^+ or p^+nn^+ bifacial cells would be used. These cells are being developed with this grant.

5.1. High injection theory.

The fact of having increased from 6X to 17X the possible concentration level in a static concentration system [6], and the possibility of using bifacial cells in high concentration systems imply that these cells are going to work at high concentration not only in open-circuit conditions (which could happen even at 6X) but also under conditions of maximum power extraction and possibly under short-circuit conditions.

As was pointed out by Fossum et al. this working condition reduces the cell recombination, as well as the transit time, which increases the V_{oc} and J_{sc} values.

At the high current density levels implied by the above-mentioned concentration levels there exists a modulation of the cell conductivity which reduces the ohmic drop due to majority-carrier flow. We intend to center our theoretical study in a general treatment of the base phenomena in high injection of the bifacial structure, embracing also the analysis of its contribution to V_{oc} , J_{sc} , the curve factor and the series resistance, studying the effect on the latter ones, not only of the unidimensional effects but of the structure's bidimensional effects as well.

As far as the effect of the highly doped regions not in high injection, we will continue to use theory developed by the U. of Florida team, whose results we plan to employ for our theoretical analysis and also to define the appropriate technology.

The experimental verification of this theory is also part of the present task.

5.2. Technology definition.

During the first year we were able to discard the technology of Al-alloy, which was valid, under certain conditions, for BSF cells, but not for bifacial ones.

For the ionic implantation technology, which has produced excellent experimental results, we do not have in Madrid the necessary equipment (ionic implanter) (present experiments were conducted by J. Eguren during his 45 days stay at the U. of Illinois). On the other hand, and in spite of the fact that with a new concept of ionic implanters they could be promising for low cost solar cell production (research done at Spire Corp., Mass.), they are not yet widely accepted as low cost technology.

As a consequence of all this we will concentrate our efforts in the

double diffusion conventional technology, using solid sources for doping deposited by various techniques.

Together with the diffusion technique we will develop a compatible technique of deposition of anti-reflection coatings and surface passivation. Among the techniques to be analyzed is the deposition of organic silicon compounds charged with titanium oxide or tantalum oxide, the dry oxidation of silicon at low temperatures, the formation of tin oxide at low temperatures with formation of passivating native hydrogen or others.

We have essentially all the equipment we need for our research plans, except some minor items for measurements or special arrangements or connections. There is an exception with respect to pyrolytic deposition of doped oxides, this technique being, after ionic implantation, the one to give best results up to the present. The experiments up to now were done by J. del Alamo in Piher Semiconductors (Barcelona), but an exhaustive research cannot be conducted in this manner. This means that we need to acquire equipment for pyrolytic deposition, and this explains the increase in the budget for the second year.

5.2. Non bifacial structures.

There are several non-bifacial structures which are very similar to our bifacial ones. The theoretical analysis as well as (in a lesser way) the technology that we might develop could be applied to these structures. We refer, particularly, to back-contact interdigitated structures (IBC) of Schwartz and his collaborators, to Texas Instruments tandem-structures and to front surface field structures (FSF).

We shall also apply the high injection theory to conventional cells which, although better studied, have not been thoroughly analyzed under high injection conditions.

6. SECOND YEAR U.S. TASKS.

6.1. Assistance.

With the primary objective of proposing and evaluating design modifications to improve the power-conversion efficiency of DSI solar cells, and in particular the efficiency of DSSF cells, i.e., p^+nn^+ or n^+pp^+ bifacial cells, the U.S. team will provide technical assistance to the Spanish team

by studying the following fundamental problems:

6.2. Transport phenomena in surface regions.

Minority-carrier transport in heavily doped diffused regions of silicon cells. This study should lead to optimal designs of the diffused surface regions, including simple surface passivation techniques, yielding reduced recombination currents in these regions, and hence higher values of open-circuit voltage.

6.3. Physical phenomena in high injection.

Carrier transport in BSF (and DSSF) cells exposed to concentrated sunlight, including the possible condition of high injection in the base region. This study will extend the analysis of [3] to account for finite gradients of the quasi-Fermi levels in the base region and the consequent effect on the fill factor. This extension, together with a proposed study of the fundamental relationship between carrier lifetimes and doping density, should lead to the specification of an optimal base doping density.

6.4. Analysis and design of a IBC cell as bifacial cell.

Analysis and design of the interdigitated-back-contact (IBC) cell as a DSI solar cell. This study will extend the analysis of [5] to account for illumination on both sides of the IBC structure. Since the IBC cell is a planar device, it could possibly yield an effective DSI solar cell whose fabrication is relatively simple.

7. PROGRAM OF TECHNICAL VISITS.

During the second year of the cooperative program we foresee two trips of Spanish investigators to the U.S. where they will visit the University of Florida and other places yet to be determined and will attend professional meetings in their field. Besides, each U.S. investigator will spend one week at the Instituto de Energía Solar in the Universidad Politécnica de Madrid. During these visits, exchanges of information concerning the theory and technology of DSI solar cells will occur.

These activities, together with postal correspondence, will provide a good coordination between the two groups.

8. CURRICULA VITARUM.

8.1. Introduction.

Since in the first year grant application there were included extensive curricula vitarum of all participants in the project, this time only brief resumes will be given, except for Dr. A. Cuevas, who is a new addition and of whom an extended curriculum is included.

8.2. Spanish investigators.

Dr. Antonio Luque. Dr. Luque received the Ingeniero de Telecomunicación degree from the U. Politécnica de Madrid in 1964, the Physics Diploma from the U. of Toulouse in 1965 and his doctorate from the U. Politécnica de Madrid in 1967. He has conducted research in Spain, France, Italy and the U.S. on lasers, physical aspects and semiconductor technology and solar cells and has published over 50 papers and two books. In 1970 he became Full professor at the U. Politécnica de Madrid. In 1969 he founded the Laboratorio de Semiconductores and has since obtained more than \$1,000,000 in research grants. He is Director of the Instituto de Energía Solar and IEEE Senior Member. He received the 1978 García Cabrerizo Prize and the 1980 Master Prize for his work on bifacial cells and his general contributions on photovoltaic effects and their applications to industry.

Dr. J.M. Ruíz. Dr. Ruíz received the Licenciado en Ciencias Físicas degree from the U. Complutense of Madrid in 1966, the doctor degree on Solid State Physics from the U. of Toulouse in 1968 and the doctor degree in Ciencias from the U. Complutense of Madrid in 1977. From 1966 to 1968 he worked on alkaline halides at the Physique des Solides Lab, U. of Toulouse. In 1969 he became a member of the Lab. de Semiconductores, U. Politécnica de Madrid and he is Research Associate and Associate Professor there since 1970. He worked on semiconductor physics with special interest in dynamic bidimensional models. At present his research is centered on solar cells for applications in photovoltaic concentration systems.

Dr. A. Cuevas. Dr. Cuevas was born in Spain in 1953. A detailed curriculum will be found at the end of this application.

J. Eguren. Received his Ingeniero de Telecomunicación degree in 1977 from the U. Politécnica de Madrid. In his second year of studies he became a collaborator at the Lab. de Semiconductores, U. Politécnica de Madrid. Since 1977 is working on surface field bifacial cells, this being his doctor's thesis topic. He published 8 papers and has attended numerous international congresses.

J.A. del Alamo. Ingeniero de Telecomunicacion from the U. Politéc-
ca de Madrid. Student visitor at the U. of Edinbrough (Scanning Electron
Microscopy Dept.) in 1978; his work there received the Antonio Fernandez
Huertas Prize from the Spanish section of IEEE. Visited the Katholieke U.
Leuven in 1979. Also in 1979 he worked in Piher Semiconductores on solar
cell fabrication from oxide deposition by CVD. In 1980 he received First
Prize in the IEEE Undergraduate Student Paper Contest. He was for two years
collaborator in the Lab. de Semiconductores, U. Politécnica de Madrid and
since 1979 is research member at the Instituto de Energía Solar. He published
four papers.

8.3. U.S. investigators.

Dr. Jerry G. Fossum. Dr. Fossum received his doctorate in Electrical
Engineering from the U. of Arizona. He has lectured on electronics for over
a decade and received an associate professorship at the U. of Florida in 1978.
Dr. Fossum has held several consulting and research positions, including a
seven year staff position with Sandia Laboratories where he researched semi-
conductor devices and developed silicon solar cells. Dr. Fossum has published
over 50 papers on semiconductor device physics and technology and on silicon
solar cell development.

Dr. Fredrik A. Lindholm. Dr. Lindholm received his doctorate in Electrical
Engineering from the U. of Arizona. He has lectured on electrical engineering
for nearly two decades and received a professorship at the U. of Florida in
1966. He has consulted for private industry, including four years with Moto-
rola Semiconductor Products, Inc. Dr. Lindholm has been awarded a total of
nearly \$2,000,000 research funding as principal investigator for various pro-
jects, and has published extensively, including three books, four manuals
and dissertations, and over 100 articles on transistors, modelling and solar
cells.

Dr. Arnost Neugroschel. Dr. Neugroschel received his doctorate at the
Technion Israel Institute of Technology. His thesis topic dealt with the
interface properties of doped silicon. He served with Tesla, Inc. in Czechos-
lovakia for two years, doing work in bipolar transistors and microwave diodes,
and spent two years at the U. of Illinois studying semiconductor interface
properties. He has lectured at the U. of Florida for four years and received
an associate professorship in electrical engineering in 1979. He published
more than 20 papers on solid-state electronics and solar cells.

9. BUDGETS.

9.1. Budget for the Spanish team.

Person	Position	Percentage of time worked on this project	Amount \$
A. Luque	Principal investigator	30%	7.337
J.M. Ruiz	Investigator	30%	5.150
A. Cuevas	Investigator	100%	14.220
J. Eguren	Collaborator	100%	12.170
J. del Alamo	Collaborator	63%	6.660
M. Rodrigo	Laborer	50%	4.100
			<u>49.637</u>
			4.963
			<u>54.600</u>
			3.000
			10.000
			1.500
			40.000
			109.100
			<u>10.900</u>
			Indirect costs 10%
			<u>TOTAL: \$120.000</u>

A.	Direct labor (salaries)		\$ 1,841
	J.G. Fossum (J.F.) Principal investigator	5% for 12 months	2,744
	F.A. Lindholm (F.L.) Principal investigator	5% for 12 months	1,444
	A. Neugroschel (AN) Principal investigator	5% for 12 months	
B.	Direct labor (OPS)		7,134
	Graduate student 50% for 12 months		
C.	Fringe benefits 16% of direct labor (salaries) plus \$42/man/month of direct labor (salaries) for State Health Insurance plus 1% of direct labor (OPS) for workman's and unemployment compensation		1,112
D.	Expendable materials Si wafers, gases, etc.		1,000
E.	Travel - 3 one week trips to Spain		4,000
F.	Publications Reports, page charges for journal papers published		1,000
G.	Computer time 1 hour at \$500 per hour		500
H.	Total direct cost less equipment		20,775
I.	Equipment Instruments for electrical characterization of solar cells		15,000
J.	Total direct costs		35,775
K.	Indirect costs each 44.4% of direct cost less equipment		<u>9,224</u>
L.	TOTAL COST		\$ 44,999

References.

1. A. Cuevas, A. Luque, J.M. Ruíz. Bifacial Transcells for Luminiscent Solar Concentration. Records of the I.E.D.M., p. 314, 1979.
2. J. del Alamo, J. Eguren, A. Luque. Operating Limits of Al-alloyed High-Low Junctions for BSF Solar Cells. Sent for publication to Solid State Electronics.
3. J.G.Fossum et al., Physics Underlying the Performance of Back-Surface-Field Solar Cells, IEEE Trans. Electron Devices, vol. ED-27, April 1980.
4. A. Neugroschel, Determination of Lifetimes and Recombination Currents in P-N Junction Solar Cells and Diodes, Annual Progress Report, Spain-U.S.A. Cooperative Research Grant (III-P-3008), April 1980; also submitted to IEEE Trans. Electron Devices, Jan. 1980.
5. J.G. Fossum, A. Neugroschel and F.A. Lindholm, A Unifying Study of Tandem-Junction, Front-Surface-Field, and Interdigitated-Back-Contact Solar Cells, Annual Progress Report, Spain-U.S.A. Cooperative Research Grant (III-P-3008), April 1980; also submitted to Solid-State Electronics, Jan. 1980.
6. A. Luque, Principles of Optimal Photovoltaic Concentration, submitted to Solar Cells, for publication.

CURRICULUM VITAE

Andrés Cuevas

Born: August 23, 1953 in Ponferrada (León). Spain

Address: Manzanares 11, Madrid 5, Spain.

Education:

1969 - High School Diploma, Oviedo, Spain

1975 Ingeniero de Telecomunicación, Universidad Politécnica, Madrid

1980 Doctor Ingeniero de Telecomunicación, Universidad Politécnica, Madrid

Honors:

1976 Awarded Matricula de Honor for his Project for the Ingeniero Degree

1980 Awarded the highest grade on his doctor's thesis: Sobresaliente, cum laude

Experience:

1975-76 Research Associate in the Advanced Semiconductor Technology Project under C.A.I.C.T. In charge of the fabrication of a monolithic integrated circuit R.F.

1976-77 Research Collaborator in the Technical Possibilities of Thin Coated Silicon Solar Cells Project, under C.A.I.C.T.

1977-80 Research Collaborator in the Silicon Solar Cells for Low Cost Bifacial Static Concentration Project, under C.A.I.C.T. In charge of the development of the solar transcell.

Publications:

- Diseño y fabricación de un circuito integrado monolítico amplificador diferencial/cascodo de R.F. Lab. Semiconductores Internal Report, E.T.S.I.T. November 1976, Graduation Project A. Cuevas, C. Dehesa, G. Sala..
- Células solares bifaciales: un nuevo concepto en conversión de energía solar. Records of Meeting on Solar Energy, Madrid, March 1977. UPM/LS/E.T.S.I.T. 0477. A. Luque, A. Cuevas, J. Eguren, J.M. Gomez Agost.
- Conversión directa de energía con concentradores estáticos autorrefrigerados y células bifaciales. Meeting on Solar Energy, Madrid, March 1977. A. Luque, J.M. Gomez Agost, A. Cuevas, J. Eguren.
- Transcell: A Novel Approach for Improving Static Photovoltaic Concentration. Records UPM/ETSIT/LS/0877. A. Luque, A. Cuevas, J. Eguren, J.M. Gomez Agost.
- Double Sided (DS) Solar Cells to Improve Static Concentration. 1977 E.C. Photovoltaic Solar Energy Conference. Luxembourg, Sept. 1977. A. Luque, J.M. Ruiz, A. Cuevas, J. Eguren, J.M. Gomez Agost

Proposal of a novel structure. Solid State Electronics, 21, 755 (1976).
A. Luque, A. Cuevas, J. Eguren.

- Transcell, a Novel Approach to Improve Static Photovoltaic Concentration. ISES International Meeting, New Delhi, 1978. A. Luque, J.M. Ruíz, A. Cuevas, J. Eguren y J.M. Gómez Agost.
- Quasi-Static Concentrator Array for Double Sided Illuminated Solar Cells, ISES Meeting, Atlanta, May 1979. A. Luque, J.M. Ruíz, A. Cuevas, J. Eguren, J. Sangrador, G. Sala, J.M. Gómez Agost, J. del Alamo.
- High Efficiency Transcells and Vertical Multijunction Cells for Double Sided Concentrated Illumination, Proceedings of the 2nd E.C. Photovoltaic Solar Energy Conference, 808, Berlin 1979. A. Cuevas, J. Sangrador, A. Luque, J.M. Ruíz, G. Sala.
- Bifacial Transcells for Luminiscent Solar Concentration. IEDM, Washington, December 1979. A. Cuevas, A. Luque, J.M. Ruíz.
- A n^+pn^+ Cell for Optimal Double-Sided Concentration, 14th IEEE Photovoltaic Spec. Conf., San Diego, January 1980. A. Cuevas, A. Luque y J.M. Ruíz.
- Experimental Behaviour and Performance of the n^+pn^+ Double-Sided Solar Cell. Submitted to the IEEE Transactions on Electron Devices, UPM/ETSIT/LS/1779. A. Cuevas, A. Luque, J.M. Ruíz.
- Double-Sided n^+pn^+ Solar Cells for Bifacial Concentration. Submitted to Solar Cells, UPM/IES/LS/1580. A. Luque, A. Cuevas, J.M. Ruiz.



Inter-office Memorandum

To: M. D. Goldberg
From: Rodger Hardy *RH*
Date: November 21, 1980
Subject: Technical Review of Extension of U.S./Spain Joint Project
on Bifacial Solar Cells

The review of this Request for Renewal has been completed. The proposed research has been deemed to be technically meaningful and the funding level to be reasonable.

In the opinion of this reviewer this program has great relevance to the U.S. Photovoltaics program. Since balance of system costs are so great in the U.S. it has been pointed out by Martin Wolf of the JPL Advisory Group that high cell efficiency is worth some extra cost for material and processing. By the same reasoning a non-tracking concentrator (for which the bifacial cell is being designed) is quite attractive if problems with the dyes can be resolved. Hence this approach is believed to have the potential of meeting long-range cost goals.

In reading reference 1 cited by this proposal it was not at all clear that the unique situation of a bifacial cell immersed in a concentrator was being fully exploited. Usually a crystalline silicon cell must be made fairly thick to absorb the incident light. A trade-off must be made between that effect and minority carrier recombination when the carriers must travel too far through the thick base region. However in this unique situation a photon passing completely through the cell is not lost, but has the possibility of being utilized in another cell in the concentrator. Similarly, the outside of the collecting grid could be made reflective so that instead of "shadowing losses" the light would merely be reflected back into the concentrator.

RH/jms

cc: Don Feucht
Jack Stone
Tom Surek

U.S. - Spain Joint Committee for Scientific and Technical Cooperation
Cooperative Research Project No. 3014
Methane Production from Anaerobic Breakdown
of Urban Solid Wastes

Scientific Report

Methane production from urban solid wastes is but one source of this fuel gas. In order to evaluate the full potential of the nonconventional energy source, an inventory of the quantities of possible feed stock must be made. In addition to urban solid wastes there are many other sources of waste organic material that are potential candidates for this process. One characteristic of the methane fermentation process that makes it an efficient energy producer is the ability to recover energy without first having to dry the material. Consequently, when evaluating the various feed materials, the moisture content becomes an important parameter. Dry material will generally have a higher energy yield when the energy is reclaimed by direct combustion. Conversely, a material with a high moisture content will generally yield more energy if the methane fermentation process is applied. One other factor to consider in methane fermentation is the biodegradability of the material. Certain residues are very resistant to microbiological attack. Consequently, these materials do not provide a suitable substrate for methane fermentation.

An inventory of organic residues of various types was compiled by Adaro. This inventory included all regions of Spain and residues originating from urban areas, including industrial wastes and sewage sludges, residues from agricultural activities including animal wastes and residues from forests and forest related industries. This inventory clearly illustrated that there is a limited number of cities that generate sufficient urban solid waste to justify the installation of this process. A production of at least 100

tonnes per day is required for this system. Consequently additional economic justification is necessary for installation of methane fermentation plants in the small cities. Incorporation of certain industrial solid waste and sewage sludge can significantly alter the economics of methane producing facilities.

The role of the U.S. counterpart in this study was one of technical support. This support was provided in two forms. First, one week was spent in Spain (March 24-30, 1980) working with Adaro engineers in evaluating the data being collected. Second, various technical reports and papers relating to similar studies in the U.S. were obtained for Adaro's staff. This provided supportive data for the evaluations of the residues generated in Spain.

There was a shift in the scope-of-work. This is justified for the following reasons. First, knowledge of the quantity of energy that can be produced by this process must be available in order to properly assess the role of this energy source in the Spanish energy program. Identification of the sources of organics available and their associated quantities is essential to plan for future studies on the use of this process. Secondly, the funds allocated for the first year were totally inadequate to initiate new laboratory research. Had this money been available when Adaro's laboratory facilities were equipped for these studies, they would have been adequate. However, the long delay in awarding these funds resulted in the laboratory activities being changed. Laboratory work has been proposed for the coming year and adequate funds have been allocated for these studies.